

Julius-Maximilians-Universität Würzburg



**Oncolytic virotherapy and modulation of tumor
microenvironment with vaccinia virus strains**

**Onkolytische Virotherapie und Modulation des
Tumormilieus mittels Verschiedener Vaccinia Virus Typen**

Doctoral thesis for a doctoral degree
at the Graduate School of Life Sciences,
Julius-Maximilians-Universität Würzburg,
Section Infection and Immunity

Submitted by

Sandeep S Patil

From

Sangli, India

Würzburg, 2014



Submitted on:

Office stamp

Members of the *Promotionskomitee*:

Chairperson:

Primary Supervisor:

Supervisor (Second):

Supervisor (Third):

Supervisor (Fourth):

(If applicable)

Date of Public Defence:

Date of Receipt of Certificates:

AFFIDAVITY

I hereby confirm that my thesis entitled “**Oncolytic virotherapy and modulation of tumor microenvironment with vaccinia virus strains**” is the result of my own work. I did not receive any help or support from commercial consultants. All sources and / or materials applied are listed and specified in the thesis.

Furthermore, I confirm that this has not yet been submitted as part of another examination process neither in identical nor in similar form.

Place, Date

Signature

Eidesstattliche Erklärung

Hiermit erkläre ich an Eides statt, die Dissertation “**Onkolytische Virotherapie und Modulation des Tumormilieus mittels Verschiedener Vaccinia Virus Typen** ” eigenständig, d.h. insbesondere selbständig und ohne Hilfe eines kommerziellen Promotionsberates, angefertigt und keine anderen als die von mir angegebenen Quellen und Hilfsmittel verwendet zu haben.

Ich erkläre außerdem, dass die Dissertation weder in gleicher noch in ähnlicher Form bereits in einem anderen Prüfungsverfahren vorgelegen hat.

Ort, Datum

Unterschrift

To dad,

Thank you for being my inspiration

Table of Contents

SUMMARY	1
ZUSAMMENFASSUNG	5
CHAPTER 1: INTRODUCTION	9
1.1 Overview of human and canine cancer	9
1.2 Oncolytic virotherapy	9
1.2.1 What are oncolytic viruses?	10
1.2.2 History of oncolytic virotherpay	10
1.2.3 How do oncolytic viruses kill cancer cells?	11
1.2.4 Current status of clinical trials with oncolytic viruses	13
1.3 Oncolytic virotherapy for canine cancer patients	15
1.3.1 Translation of oncolytic virotherapy from dogs to humans and reverse	16
1.4 Oncolytic vaccinia virus	17
1.4.1 History of oncolytic vaccinia virus	18
1.4.2 An overview of vaccinia virus biology.....	18
1.4.3 Preclinical research with vaccinia virus as an oncolytic agent.....	21
1.4.4 Clinical trials with oncolytic vaccinia virus	24
1.5 Tumor microenvironment and oncolytic virotherapy	26
1.5.1 Strategies to manipulate ECM	26
1.5.2 Strategies to target tumor angiogenesis	27
1.5.3 Strategies to modulate the immune response	29
CHAPTER 2: RATINALE AND AIM	34
CHAPTER 3: MATERIAL AND METHODS	36
3.1 Materials	36
3.1.1 Chemicals and enzymes	36
3.1.4 Solutions and buffers	40
3.1.5 Cell lines and culture media	42
3.1.6 Antibodies	43
3.1.7 Recombinant vaccinia virus construct.....	45
3.1.8 Laboratory animals.....	47
3.2 Methods	48
3.2.1 Ethics statement.....	48
3.2.2 Culturing of mammalian cells	48
3.2.3 Virological methods.....	48
3.2.4 Cell viability assay.....	49
3.2.5 Protein analytical methods	50
3.2.6 Mouse experiments.....	52
3.2.7 Detection of β -glucuronidase in mouse serum.....	55
3.2.8 Flow cytometric (FACS) analysis	55
3.2.9 Statistical analysis.....	56

CHAPTER 4: RESULTS	57
4.1 Aim 1: Characterization of oncolytic efficacy of LIVP6.1.1 in canine cancers	57
4.1.1 Characterization of LIVP6.1.1 virus in canine cancer cells under cell culture conditions	57
4.1.2 Oncolytic effects of LIVP6.1.1 on canine cancer xenografts in nude mice	60
4.2 Aim 2: Effect of inhibition of tumor angiogenesis on modulation of VACV therapy	64
4.2.1 GLV-1h109 efficiently replicates in STSA-1 and DT08/40 tumor cells...64	64
4.2.2 GLV-1h109 virus efficiently kills canine cancer cells.....66	66
4.2.3 GLV-1h109 expresses encoded marker proteins in canine cancer cells	67
4.2.4 The GLAF-1 antibody specifically recognizes canine VEGF	68
4.2.5 Canine cancer cells express VEGF under cell culture conditions.....69	69
4.2.6 Systemic administration of GLV-1h109 virus significantly regresses growth of STSA-1 and DT08/40 derived tumors in nude mice.....70	70
4.2.7 Bio-distribution of the virus and presence of GLAF-1 in tumor-bearing nude mice.....72	72
4.2.8 Use of GLV-1h109 as a diagnostic tool for canine cancers	73
4.2.9 GLV-1h109 replication resulted in GLAF-1 protein expression in tumor tissue.....74	74
4.2.10 GLV-1h109 colonization in tumor xenografts significantly inhibited development of tumor vasculature	75
4.2.11 Anti-angiogenesis therapy improved virus replication and distribution in STSA-1 tumor xenografts.....77	77
4.2.12 Combination of VACV with anti-angiogenic therapy improved infiltration of innate immune cells in STSA-1 xenografts	78
4.3 Aim 3: Modulation of immune response by VACV therapy in canine cancer patients	82
4.3.1 Details of canine cancer patients and dose escalation scheme	82
4.3.2 Optimization of canine PBMC staining for flowcytometry analysis	84
4.3.3 V-VET1 treatment induced circulating cytotoxic T cell response in canine cancer patients.....86	86
4.3.4 V-VET1 treatment caused a reduction of circulatory MDSCs in canine cancer patients.....88	88
4.3.5 Tumor type and viral dose did not affect modulation of immune response	92
CHAPTER 5: DISCUSSION	95
5.1 Therapeutic efficacy of the oncolytic VACV LIVP6.1.1 in canine cancer xenografts	97
5.2 The recombinant VACV strain GLV-1h109 encoding the anti-VEGF single-chain antibody was equally efficient in canine cancer xenografts.....99	99

5.3 Anti-angiogenic therapy improved the spread and replication of VACV as well as infiltration of the innate immune response in canine cancer xenografts	102
5.4 VACV injection induced circulatory immune response in canine patients recruited in phase I clinical trial	104
REFERENCES	108
APENDIX.....	121
ACKNOWLEDGMENTS	124
CURRICULUM VITAE.....	126
LIST OF PUBLICATIONS.....	127

SUMMARY

Oncolytic viral therapies have shown great promise pre-clinically and in human clinical trials for the treatment of various cancers. Oncolytic viruses selectively infect and replicate in cancer cells, destroying tumor tissue via cell lysis, while leaving noncancerous tissues unharmed. Vaccinia virus (VACV) is arguably one of the safest viruses, which has been intensively studied in molecular biology and pathogenesis as a vaccine for the eradication of smallpox in more than 200 million people. It has fast and efficient replication, and cytoplasmic replication of the virus lessens the chance of recombination or integration of viral DNA into the genome of host cells. Anti-tumor therapeutic efficacy of VACV has been demonstrated for human cancers in xenograft models with a variety of tumor types. In addition recombinant oncolytic VACVs carrying imaging genes represent an advance in treatment strategy that combines tumor-specific therapeutics as well as diagnostics.

As for other targeted therapies, a number of challenges remain for the clinical translation of oncolytic virotherapy. These challenges include the potential safety risk of replication of oncolytic virus in non-tumor tissue, the relatively poor virus spread throughout solid tumor tissue and the disadvantageous ratio between anti-viral and anti-tumoral immunity. However, manipulation of components of the tumor microenvironment may help oncolytic virus infection in killing the tumor tissue and thereby increasing the anti-tumor efficacy. Furthermore, dogs with natural cancer are considered as one of the best animal models to develop new drugs for cancer therapy. Traditionally, rodent cancer models have been used for development of cancer therapeutics. However, they do not adequately represent several features that define cancer in humans, including biology of initiation of tumor, the complexity of cancer recurrence and metastasis and outcomes to novel therapies. However, the tumor microenvironment, histopathology, molecular and genomics data from dog tumors has significant similarities with corresponding human tumors. These advantages of pet dog cancers provide a unique opportunity to integrate canine cancer patients in the studies designed for the development of new cancer drugs targeted against both human and canine cancers. This dissertation centers on the use of VACV strains in canine cancer xenografts with the aim of understanding the

effects of modulation of tumor microenvironment on VACV-mediated tumor therapy.

In the first studies, wild-type VACV strain LIVP6.1.1 was tested for its oncolytic efficiency in canine soft tissue sarcoma (STSA-1) and canine prostate carcinoma (DT08/40) cells in culture and xenografts models. LIVP6.1.1 infected, replicated within, and killed both STSA-1 and DT08/40 cells in cell culture. The replication of virus was more efficient in STSA-1 cells compared to DT08/40 cells. In xenograft mouse models, LIVP6.1.1 was safe and effective in regressing both STSA-1 and DT08/40 xenografts. However, tumor regression was faster in STSA-1 xenografts compared to DT08/40 xenografts presumably due to more efficient replication of virus in STSA-1 cells. Biodistribution profiles revealed persistence of virus in tumors 5 and 7 weeks post virus injection in STSA-1 and DT08/40 xenografts, respectively, with the virus mainly cleared from all other major organs. Immunofluorescence staining detected successful colonization of VACV in the tumor. Consequently, LIVP6.1.1 colonization in the tumor showed infiltration of innate immune cells mainly granulocytes and macrophages in STSA-1 tumor xenografts. These findings suggest that virotherapy-mediated anti-tumor mechanism in xenografts could be a combination of direct viral oncolysis of tumor cells and virus-dependent infiltration of tumor-associated host immune cells.

In further studies, the effects of modulation of tumor angiogenesis of VACV therapy were analyzed in canine cancer xenografts. GLV-1h109 VACV strain (derived from prototype virus GLV-1h68) encoding the anti-VEGF single chain antibody GLAF-1 was characterized for its oncolytic efficacy in STSA-1 and DT08/40 cancer cells in culture and tumor xenografts. Concomitantly, the effects of locally expressed GLAF-1 in tumors on virus replication, host immune infiltration, tumor vascularization and tumor growth were also evaluated.

GLV-1h109 was shown to be similar to the parental virus GLV-1h68 in expression of the two marker genes that both virus strains have in common (*Ruc-GFP* and *gusA*) in cell cultures. Additionally, the anti-VEGF single-chain antibody GLAF-1 was expressed by GLV-1h109 in both cell cultures and tumor xenografts. The insertion of GLAF-1 did not significantly affect the replication and cytotoxicity of GLV-1h109 in the STSA-1 and DT08/40 cell lines, although at early time points (24-48 hpi), the replication of GLV-1h109 was higher in STSA-1 cells compared to DT08/40 cells. In

addition, STSA-1 cells were more susceptible to lysis with GLV-1h109 than DT08/40 cells. GLV-1h109 achieved a significant inhibition of tumor growth in both STSA-1 and DT08/40 canine xenografts models. Consequently, the significant regression of tumor growth was initiated earlier in STSA-1 tumor xenografts compared to regression in DT08/40 xenografts. The reason for the higher efficacy of GLV-1h109 in STSA-1 xenografts than DT08/40 xenografts was attributed to more efficient replication of virus in STSA-1 cells. In addition, tumor-specific virus infection led to a continued presence of GLAF-1 in peripheral blood, which could be useful as a pharmacokinetic marker to monitor virus colonization and persistence in GLV-1h109-injected xenograft mice. GLAF-1 is a single-chain antibody targeting human and murine VEGF. It was demonstrated that GLAF-1 was functional and recognized both canine and human VEGF with equal efficiency.

Histological analysis of tumor sections 7 days after GLV-1h109 injection confirmed that colonization of VACV and intratumoral expression of GLAF-1 translated into a significant decrease in blood vessel number compared to GLV-1h68 or PBS-treated control tumors. Subsequently, reduction in blood vessel density significantly improved the spread and replication of VACV as observed by FACS analysis and standard plaque assay, respectively. Inhibition of tumor angiogenesis and increased replication of virus further improved the infiltration of innate immune cells mainly granulocytes and macrophages in STSA-1 tumor xenografts. Both the results, i.e. improved virus spread and increased infiltration of innate immune cells in tumor, were explained by a phenomenon called “vascular normalization”, where anti-VEGF therapy normalizes the heterogeneous tumor vasculature thereby improving delivery and spread of VACV. In summary, the effects of inhibition of tumor angiogenesis on virus spread and replication were demonstrated using a vaccinia virus carrying an anti-angiogenic payload targeting vascular endothelial growth factor (VEGF) in canine cancer xenografts.

In the final studies, the effects of VACV therapy on modulation of the immune system were analyzed in canine cancer patients enrolled in a phase I clinical trial. V-VET1 (clinical grade LIVP6.1.1 VACV) injection significantly increased the percentages of CD3+CD8+ T lymphocytes at 21 days after initiation of treatment. CD3+CD8+ T lymphocytes are mainly cytotoxic T lymphocytes that have potential to lyse cancer

cells. Subsequently, the frequency of immune suppressor cells, mainly MDSCs and T_{reg} was also analyzed in peripheral blood of canine cancer patients. Increase in the MDSC population and decreased $CD8/T_{reg}$ ratio is known to have inhibitory effects on the functions of cytotoxic T cells. We demonstrated that injection of V-VET1 in canine cancer patients significantly reduced the percentages of MDSCs at 21 days post initiation of treatment. Additionally, $CD8/T_{reg}$ ratio was increased 21 days after initiation of V-VET1 treatment. We also showed that changes in the frequency of immune cells neither depends on dose of virus nor depends on tumor type according to the data observed from this clinical trial with eleven analyzed patients.

This preclinical and clinical data have important clinical implications of how VACV therapy can be used for the treatment of canine cancers. Moreover, dogs with natural cancers can be used as an ideal animal model to improve the oncolytic virotherapy for human cancers. Furthermore, modulation of tumor microenvironment mainly tumor angiogenesis and tumor immunity has significant impact on the success of oncolytic virotherapy.

ZUSAMMENFASSUNG

Therapien für verschiedenste Krebsarten mittels onkolytischer Viren zeigten sowohl in präklinischen- als auch in humanen klinischen Studien ein erfolgversprechendes Potenzial. Onkolytische Viren infizieren selektiv Krebszellen und replizieren ausschließlich in diesen. In der Folge zerstören sie Tumorgewebe durch Zellyse, während gesundes Gewebe unbeeinträchtigt bleibt. Das Vaccinia-Virus besitzt ein äußerst geringes Risikopotential, und wurde intensiv auf molekularbiologischer Ebene und in Bezug auf seine Pathogenese untersucht. All das qualifizierte es als Vakzin zur Ausrottung der Pocken und seit Markteinführung mehr als 200 Millionen Menschen injiziert. Das Vaccinia-Virus zeigt eine schnelle und effiziente Replikation, welche im Zytoplasma der Zelle stattfindet. Dies verringert die Möglichkeit der Rekombination oder Integration der viralen DNA in das Wirtsgenom. Die therapeutische Wirksamkeit onkolytischer Vaccinia-Viren (VACVs) wurde in humanen Xenograft-Mausmodellen mit unterschiedlichen Tumorarten gezeigt. Rekombinante onkolytische VACVs, welche mit fluoreszierenden Genen ausgestattet sind, kombinieren die Vorteile tumorspezifischer Therapeutika und dienen gleichzeitig als Diagnostika.

Wie auch andere spezifische Therapien, steht auch die onkolytische Virustherapie vor einer Reihe von Herausforderungen. Dazu gehören die Replikation onkolytischer Viren in nicht-kancerogenem Gewebe, relativ schlechte Virusverbreitung durch solides Tumorgewebe und ein unvorteilhaftes Verhältnis zwischen antiviraler und antitumoraler Immunität. Die gezielte Manipulation einzelner Komponenten des Tumormikromilieus kann jedoch zu einer verbesserten Virusinfektion und Lyse des Tumorgewebes führen und somit die Effizienz der antitumoralen Therapie verstärken.

Hunde, welche auf natürlichem Weg eine Krebserkrankung entwickeln, gelten als eines der besten Tiermodelle für die Entwicklung von Medikamenten gegen Krebs. Traditionell wurden Mausmodelle für die Therapieentwicklung von Krebserkrankungen eingesetzt. In Mausmodellen fehlen jedoch verschiedene Eigenschaften, welche eine Krebserkrankung in Menschen definieren. Dazu gehören die Tumorentstehung, die Komplexität des Wiederauftretens des Tumors, die

Metastasierung und Therapievorhersagen für neuartige Medikamente. Daten auf molekularer und genomischer Ebene, das Tumormikromilieu und die Histopathologie von Hundetumoren zeigen jedoch signifikante Ähnlichkeit zu entsprechenden humanen Tumoren.

Die genannten Vorteile von Hundetumoren bieten eine einmalige Chance, Hundekrebspatienten in Studien einzubeziehen, die auf die Entwicklung neuer Krebsmedikamente zur Behandlung von Human- und Hundetumoren abzielen. Im Rahmen dieser Arbeit wurde die Verwendung von VACV-Stämmen zur Therapie von Hundetumoren im Mausmodell und die Auswirkungen der Modulation des Tumormikromilieus auf die VACV-vermittelte Tumorthherapie untersucht.

Im ersten Teil der Studie wurde der wildtypische VACV-Stamm LIVP6.1.1 auf seine onkolytische Effizienz in caninen Weichteilsarkom- (STSA-1) und Prostatakarzinomzellen (DT08/40) sowohl in Zellkultur wie auch im Xenotransplantatmodell getestet. Es konnte gezeigt werden, dass LIVP6.1.1 in Zellkultur erfolgreich in STSA-1- und DT08/40-Zellen replizieren und diese lysieren kann, wobei eine verbesserte Replikation in STSA-1-Zellen verglichen mit DT08/40-Zellen festgestellt werden konnte. Im Mausmodell konnte nachgewiesen werden, dass LIVP6.1.1 sicher ist und sowohl in STSA-1- als auch DT08/40-Xenotransplantaten zur Regression führte. Aufgrund der höheren Replikationsgeschwindigkeit des Virus in STSA-1-Zellen wurde eine schnellere Rückbildung der STSA-1-Xenotransplantate im Vergleich zu DT08/40-Tumoren beobachtet. Weiterhin wurde in Bioverteilungsstudien in beiden Xenotransplantatmodellen jeweils die höchste Virusmenge in den Tumoren nachgewiesen, wohingegen in den Organen nur vereinzelt Virus gefunden wurde. Mittels Immunfluoreszenzfärbung konnte ebenfalls die erfolgreiche Kolonisierung der Tumore durch das Virus veranschaulicht, sowie auch die Einwanderung von Zellen des angeborenen Immunsystems, hauptsächlich Granulozyten und Makrophagen, in STSA-1-Xenotransplantate dargestellt werden. Diese Ergebnisse legen nahe, dass der antitumorale Mechanismus in diesen Xenotransplantaten eine Kombination aus direkter Onkolyse der Tumorzellen und Virus-abhängiger Einwanderung von Tumor-assoziierten Wirtsimmunzellen sein könnte.

In weiteren Studien wurden die Auswirkungen der Veränderung der

Tumorangiogenese im Rahmen der VACV-Therapie im Xenotransplantatmodell von Hundetumoren untersucht. Hierfür wurde die onkolytische Effizienz des VACV-Stammes GLV-1h109 in STSA-1- und DT08/40-Zellen in Zellkultur und im Mausmodell untersucht. GLV-1h109 wurde durch Insertion des Gens für den anti-VEGF-Einzelketten-Antikörper GLAF-1 in das Parentalvirus GLV-1h68 hergestellt. Außerdem wurden die Effekte des in Tumoren lokal exprimierten GLAF-1 auf die Virusreplikation, Einwanderung von Wirtsimmunzellen, Tumolvaskularisierung und Tumorstadium untersucht.

Unter Zellkultur-Bedingungen zeigte GLV-1h109 eine ähnliche Expression der beiden Marker-Gene (*ruc-gfp* und *gusA*) wie sein isogener Stamm GLV-1h68. Die zusätzliche Expression des GLAF-1-Proteins hatte keinen signifikanten Effekt auf die Replikation und Zytotoxizität von GLV-1h109 in den STSA-1- und DT08/40 Zelllinien. Interessanterweise waren STSA -1-Zellen anfälliger für GLV-1h109-Infektion als DT08/40 Zellen. GLV-1h109 wies eine signifikante Hemmung des Tumorstadiums in beiden getesteten STSA-1- und DT08/40-Xenograft-Modellen auf. Die schnellere Regression des Tumorstadiums im STSA-1-Tumor im Vergleich zur Regression von DT08/40-Tumoren, konnte auf die effizientere Kolonisierung und Replikation des Virus in diesen Tumorzellen zurückgeführt werden.

Darüber hinaus führte Tumor-spezifische Virus-Infektion zur dauerhaften Präsenz der GLAF-1 Antikörper im peripheren Blut. Dadurch könnte das Protein als pharmakokinetischer Marker für die Virus Kolonisierung und Persistenz in Mäusen dienen. GLAF-1 ist ein Einzelketten-Antikörper gegen Human-und Maus-VEGF. Wir konnten zeigen, dass das virusproduzierte GLAF-1 Protein funktional ist und sowohl canines wie auch humanes VEGF mit gleicher Effizienz erkennt.

Die histologische Analyse von eingebetteten GLV-1h109-injizierten Tumorschnitten haben bestätigt, dass, die intratumorale Expression von GLAF-1 zu einer signifikanten Abnahme der Blutgefäß-Zahl im Vergleich zu der Zahl der in GLV-1h68 oder PBS-injizierten Kontrolltumoren führte. Interessanterweise führte die Senkung der Blutgefäßdichte zu einer deutlich verbesserten Ausbreitung und Replikation von GLV-1h109, wie durch FACS-Analyse und Standard-Plaque-Test beobachtet wurde. Hemmung der Tumorangiogenese und erhöhte Replikation des Virus bewirkte eine bessere Infiltration von Zellen des angeborenen Immunsystems, hauptsächlich

Granulozyten und Makrophagen in STSA-1-Tumore. Alle diese Vorgänge (verbesserte Virusausbreitung und verstärkte Infiltration der angeborenen Immunzellen im Tumor) könnten durch eine „Gefäß-Normalisierung“ nach der GLAF1–Behandlung erklärt werden.

Zusammenfassend wurde gezeigt, dass im Hunde-Xenograftmodell mittels Virus-vermittelter GLAF-1-Expression die Angiogenese gehemmt wird und dies sich auf die Verteilung und Replikation des Virus auswirkt.

Zuletzt wurde die Wirkung der VACV-Therapie auf die Regulierung des Immunsystems in krebserkrankten Hunden in einer klinischen Studie Phase 1 untersucht. Die Injektion von V-VET1 (klinische Bezeichnung des LIVP6.1.1-Virus) führte 21 Tage nach der Behandlung zu einem signifikanten Anstieg an $CD3^+ CD8^+$ -Lymphozyten. $CD3^+CD8^+$ -T-Lymphozyten gehören zu den zytotoxischen T-Lymphozyten, welche Krebszellen lysieren. Anschließend wurde die Anzahl an Immunsuppressor-Zellen, überwiegend Myeloid-derived Suppressor (MDS)-Zellen und T_{reg} -Zellen im peripheren Blut krebserkrankter Hunde untersucht. Eine funktionale Hemmung der zytotoxischen T-Zellen wird durch eine Zunahme an MDS-Zellen mit gleichzeitiger Abnahme der $CD8^+$ -T-Zellen charakterisiert. Die Daten zeigen, dass der Anteil an MDS-Zellen in krebserkrankten Hunden 21 Tage nach Start der Behandlung mit V-VET1 signifikant gesunken ist. Zusätzlich stieg das Verhältnis von $CD8^+$ -T-Zellen zu T_{reg} -Zellen 21 Tage nach Injektionsstart. Des Weiteren wurde an Hand der erhaltenen Daten von 11 Patienten im klinischen Versuch gezeigt, dass die veränderte Anzahl an Immunzellen weder von der Dosis der Virusinfektion noch von der Art des Tumors abhängig ist.

Unsere präklinischen- und klinischen Studien geben wichtige Informationen für eine klinische Behandlung von krebserkrankten Hunden mittels Virustherapie. Des Weiteren wurde veranschaulicht, dass Hunde sich aufgrund der natürlichen Krebserkrankung als optimales Modell zur Optimierung der onkolytischen Virustherapie in der Humanmedizin eignen. Zusätzlich wurde gezeigt, dass besonders die Regulierung des tumoralen Milieus in Bezug auf Angiogenese und Immunität entscheidend für den Behandlungserfolg sind.

CHAPTER 1: INTRODUCTION

1.1 Overview of human and canine cancer

Cancer is the leading cause of death worldwide, accounting for 7.6 million deaths annually [1]. By 2030, it is projected that there will be ~26 million new cancer cases and 17 million cancer deaths per year [2]. In addition to loss of life, cancer attributes considerable economic loss and drastically reduces quality of life. Furthermore, not only does cancer devastate the lives of humans, it also afflicts animals. Cancer is the most common cause of natural death in dogs. The incidence of cancer is 1 to 2% in the canine population and accounts for about half of the deaths in dogs older than 10 years [3, 4]. Canine cancer has become more prevalent in recent years because of increased life expectancy and greater attention to the health of pets. The range of cancers seen in dogs is as diverse as that in human patients. Because domestic pets share our environment, greater cross-application and study of the protumorigenic and antitumorigenic factors in our shared environment will benefit all species, leading to the development of new families of less toxic antitumorigenic therapies based on novel and established molecular targets [5]. As the standard therapy is usually palliative in canine cancer, there is an excellent opportunity to evaluate alternative approaches.

1.2 Oncolytic virotherapy

While substantial progress has been made in combating cancer, including improved techniques in early diagnosis, advances in surgery, improved chemotherapy, hormonal therapy, immunotherapy, gene therapy, and radiation therapy, treating cancer still remains a considerable challenge. For many cancer types, for which current standard therapies do not provide a cure, new research has led to the development of alternative treatment approaches. One alternate therapeutic approach is oncolytic virotherapy. Oncolytic virotherapy uses viruses that specifically kill cancer cells, while leaving healthy cells unharmed. Conventional chemotherapy is mostly non-targeted, causing general toxicity and severe side effects. Because of the specificity of oncolytic viruses (OVs) for cancer cells, anti-cancer effects may occur in the absence of off-target toxicity.

Cancer virotherapy has progressed into the clinic, with several oncolytic virus platforms currently in or entering phase III human clinical trials. In addition, the

oncolytic adenovirus H101 was approved in China in 2005 for the treatment of head and neck cancer [6]. Additionally, virotherapy has been tested in veterinary medicine. Phase I clinical trials are currently underway in dogs to assess the safety of oncolytic vaccinia virus [7].

1.2.1 What are oncolytic viruses?

Oncolytic viruses are the viruses that selectively infect, replicate in and kill cancer cells, while leaving healthy cells intact. These are multi-mechanistic antitumor agents. OV's not only kill cancer cells by direct infection and oncolysis, but also affect uninfected cells of the tumor by altering the tumor vasculature and by activating antitumor immunity.

Over the last 15 years, antitumor activity of OV's has been demonstrated in different animal models as well as in human and dog cancer patients. Examples include vaccinia virus [8], Newcastle disease virus (NDV) [9], reovirus [10], lentivirus [11], Herpes simplex virus (HSV) [12], enterovirus [13], sindbis virus [14], seneca valley virus [15], adenovirus [16] and raccoonpox virus [17].

1.2.2 History of oncolytic virotherapy

The use of viruses in the treatment of cancer started from the observation that cancer patients who contracted an infectious disease showed brief periods of cancer remission. These patients suffered primarily from hematological malignancies such as leukemia or lymphoma. In 1896, Dock described a 42-year-old woman with "myelogenous leukemia" that went into remission after presumed influenza infection [18]. In another case, chickenpox led to the regression of lymphatic leukemia in a 4-year-old boy [19]. Unfortunately, remission in both these cases lasted only for one month, subsequently progressing rapidly until death. Nonetheless, these observations gave the impression that under the right circumstances certain viruses can destroy tumors.

During the same time, A. Moore, who pioneered the testing of OV's in animal cancer models, teamed up with a clinical oncologist C. Southam. Moore and Southam contributed much to the advancement of OV's in both preclinical trials in animal models and clinical trials in human subjects. They used the Egypt 101 isolate of West Nile virus in more than 150 virus therapy trials against a wide range of cancers [20]. Viremia and intra-tumoral virus replication were confirmed in most patients, but

tumor responses were rare and side effects such as neurotoxicity associated with the viral pathology were observed [20, 21]. Subsequently, other less toxic viruses such as adenovirus and virus strains of poxvirus family entered these investigations. Adenovirus was found to have relatively moderate side effects and consequently, entered clinical trials for the treatment of cervical cancer [22].

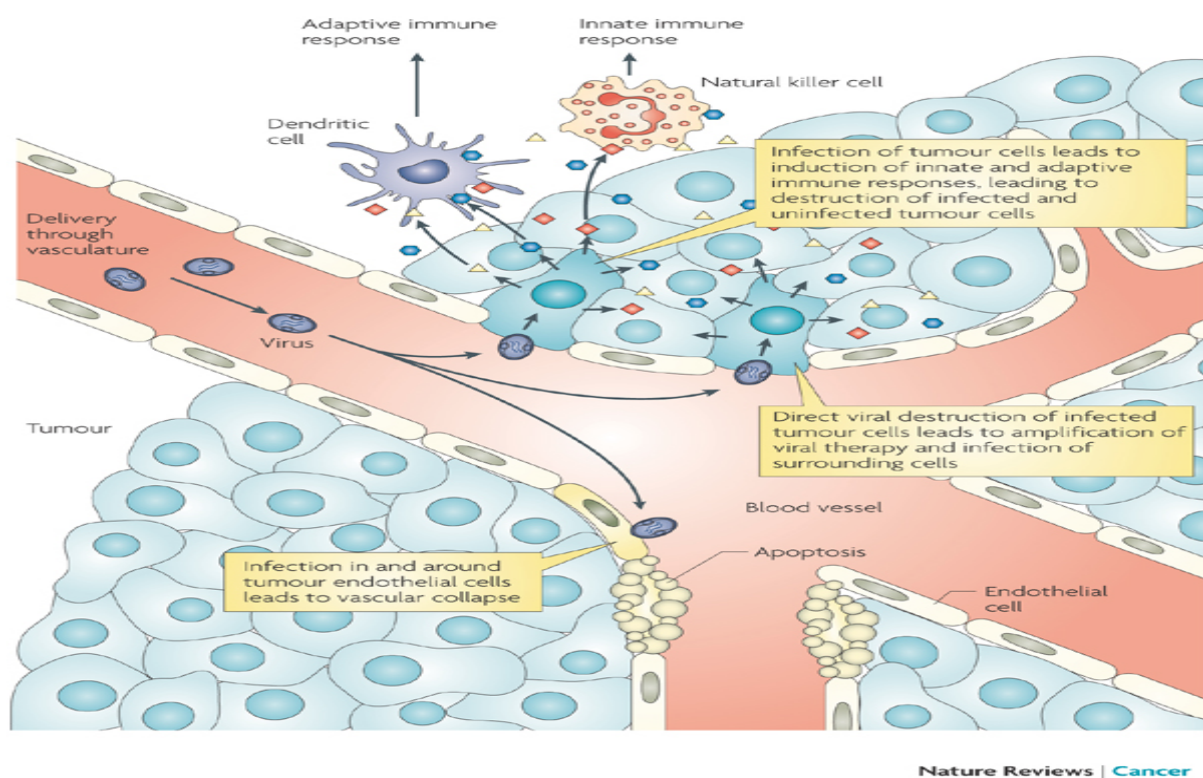
Despite their tremendous anti-cancer potential, it became clear that viruses needed to be more specific to the cancer and less toxic to healthy tissues. Thus began the era of adaptation and genetic engineering of viruses. It was recognized early that viruses were capable of increasing their replication in specific tissues by adaptation on specific cell types. Thus, viruses when continuously passaged in particular cell types were able to replicate only in that cells. Vaccinia virus used as a vaccine against small pox disease is one of such example. Small pox vaccine was continuously passaged from one individual to another, which limited its replication to epithelial cells. In 1922, Levaditi *et al.* showed that a small pox vaccine was able to inhibit the growth of various tumors in rats and mice [23].

The dire need for effective cancer therapy in 1950 drove attempts to reduce virus pathogenicity and increase anti-cancer effects, albeit with limited success. Major advances in virus manipulation were not possible until methods were developed for direct modification of the viral genomes. After it arrived, recombinant DNA technology was applied predominantly to the engineering of adenovirus [24], paramyxovirus [25], Herpes virus [26], and poxviruses [27]. Most viruses can now be adapted or engineered to eliminate their pathogenicity without destroying their oncolytic potency. Yet, even with the newfound ability to engineer viral genomes to produce a new generation of safer, more specific oncolytics, a true therapeutic frontrunner has not emerged.

1.2.3 How do oncolytic viruses kill cancer cells?

Oncolytic viruses destroy malignant cells and display anti-tumor effects through several different mechanisms. Certain viruses like reovirus, vesicular stomatitis virus, measles virus have natural tumor tropism, that is, they infect tumor cells more than they infect healthy cells [28]. Infected tumor cells die either through the direct action of the replicating virus, for example, the overconsumption of cell metabolites, or by secondary effects, such as excessive budding of virus from the cell surface (cell

lysis). The replication cycle repeats, as progeny viruses infect adjacent tumor cells and subsequently kill them. Some OV's synthesize specific proteins during replication that are cytotoxic to cancer cells. For example, adenoviruses led to expression of the death protein E3 and the E4ORF4 protein late in the cell cycle, both of which are toxic to cells [29]. Alternatively, virus replication in endothelial cells of blood vessels may directly or indirectly induce apoptosis in tumor blood vessel endothelium, which further lead to cancer cell death [30]. The third mechanism by which OV's act is by initiating specific and nonspecific anti-tumor immune responses. This may be derived from either the innate immune system, for example, natural killer cells, or the adaptive immune system, via the action of dendritic cells. Induction of specific anti-tumor immunity is thought to provide long-term defense against cancer recurrence [31]. An illustration of the various mechanism of action of oncolytic viruses is provided in Figure 1



Nature Reviews | Cancer

Fig. 1 Mechanism of action of oncolytic Virus [31]

OVs, which are not naturally oncotropic, can also be engineered to replicate in tumor tissue. Better understanding in recent years of molecular events of virus-cell interactions has allowed for the design of genetically engineered viruses that target selected molecules or signaling pathways such as p16, p21, p53, IFN pathway, PTEN, EGFR, VEGFR, STAT3, HSP70, anti-apoptosis or hypoxia [32]. Several OVs including adenoviruses and vaccinia viruses are targeted to human cancer cells by taking advantage of these defective pathways.

1.2.4 Current status of clinical trials with oncolytic viruses

In this modern era, clinical trials of oncolytic virotherapy began using OVs belonging to at least ten different oncolytic virus families. Clinical tolerability of OVs has been excellent, even at the current highest feasible doses. Additionally, recent clinical evidence supporting the efficacy of oncolytic virotherapy comes from several clinical trial reports. The adenovirus ONYX-015 was tested in over 200 patients through Phase I to Phase III clinical trials. Single agent treatment showed limited tumor regression (maximum 14%) with no objective response, however, in combination with chemotherapy 54%-63% patient showed tumor regression. [33]. Meanwhile, randomized, double blind Phase III study of REOLYSIN (Reovirus Type 3 Dearing) in combination with paclitaxel and carboplatin in patients with head and neck carcinoma is currently going on [34]. Reolysin treatment was well tolerated in metastatic melanoma patients in a Phase II study and viral replication was demonstrated in biopsy samples [35]. Likewise, a modified form of the Herpes simplex virus type 1, talimogene laherparepvec (T-Vec), was tested in a Phase III clinical trial in patients with metastatic melanoma. Virus treatment showed 16% durable response rate (DRR) compared to 2% in GM-CSF treated control patients [33]. Similarly, a VACV encoding GM-CSF, JX594, administered by intratumoral injection led to 16% complete response and 10% partial response in metastatic melanoma patients in Phase II trials [36]. In addition to these oncolytic virus strains, various other viruses including measles virus, coxsackie virus and vaccinia virus have completed multiple Phase I trials with promising results. The detailed overview of clinical trials with oncolytic viruses is listed in Table 1.

Table 1: Clinically tested oncolytic viruses in human cancer patient

Virus	Construct	Phase	Cancer type	Response
Adenovirus	CG0070 (Encoding GM-CSF)	Phase II Phase III	Bladder Cancer Papillary Tumors	Recruiting
	ICOVIR-5	Phase I	Melanoma	Recruiting
	CGTG-102	Phase I	Solid tumors	Recruiting
	ColoAd-1	Phase I	Colon cancer	Recruiting
Vaccinia Virus	JX-594	Phase II	Hepatocellular carcinoma	15 % Objective response rate [36]
	GL-ONC1	Phase I	Advanced solid Cancers	Recruiting
Herpes simplex virus (HSV) type 1	HSV1716	Phase I/IIa	Malignant pleural mesothelioma	Recruiting
	G207	Phase Ib/II	Glioma, Glioblastoma	Safe and virus replicated in tumor [37]
	OncoVEX GM-CSF	Phase III	Metastatic melanoma	16 % Durable response rate [38]
Reo virus	REOLYSIN	Phase I/II	Malignant Glioma Soft tissue sarcoma	Safe with Stable Disease [35]
Vesicular stomatitis virus (VSV)	VSV encoding INF- β	Phase I	Hepatocellular carcinoma	Recruiting
Measles virus	Measles encoding CEA	Phase I	Ovarian and Peritoneal cancer	Active
Parvo virus	H-1 PV	Phase I/IIa	Glioblastoma	Recruiting

1.3 Oncolytic virotherapy for canine cancer patients

Despite recent progress in the diagnosis and treatment of advanced canine cancer, overall patient treatment outcome has not been substantially improved. Virotherapy using oncolytic viruses is one promising new strategy for cancer therapy. Oncolytic virotherapy has been tested for the treatment of canine cancer as proof of concept investigations. However, the use of oncolytic virotherapy in veterinary medicine is still far from becoming commercially available as promising laboratory results have yet to be translated into clinical outcomes. So far, canine cancers, such as osteosarcoma, malignant melanoma, lymphoma, soft tissue sarcoma, mammary adenoma and carcinoma, have been tested with only a few oncolytic viruses, mainly the human and canine adenoviruses, canine distemper virus and vaccinia virus strains [32].

Several Ad5-based adenoviral vectors encoding different genetic or molecular factors associated with cancer have been tested with success for treatment of different canine tumors. Adenoviral vector-mediated p53 gene transfer had an anti-tumor effect in canine osteosarcoma xenografts [39]. Moreover, a genetically engineered adenovirus vector targeted to CD40 ligand induced strong cellular and humoral immune response to tumor antigen CEA in dogs [40]. The conditionally replicating canine adenovirus 2 (CAV-2) with the osteocalcin promoter showed significant therapeutic effect in canine osteosarcoma xenograft. In addition, administration of this modified canine adenovirus to normal dogs showed only moderate virus-associated toxicity [32]. A very recent study demonstrated that canine mast cell tumors (MCT) were highly susceptible to reovirus infection *in vitro* and a single intratumoral reovirus injection significantly regressed canine mast cell tumor xenografts. However, reovirus also infected normal canine mast cells raising safety concerns [41].

Like adenovirus and reovirus, VACV has demonstrated promising oncolytic potential against canine cancer xenografts in mouse model. GLV-1h68 (Genelux Corporation, USA), a VACV strain that has shown promising preclinical data and is now undergoing clinical trials in humans, was tested for the treatment of canine cancers. GLV-1h68 (named GL-ONC1 as produced for clinical investigation) was developed from the Lister strain by inserting three expression cassettes encoding *Renilla*

luciferase–*Aequorea* green fluorescent protein fusion (*Ruc*-GFP), *lacZ*, and β -glucuronidase into the *F14.5L*, *J2R* (thymidine kinase) and *A56R* (hemagglutinin) loci of the viral genome, respectively [8]. The effect of the virus was studied in xenograft models with the canine mammary carcinoma cell line MTH52c, the canine soft tissue sarcoma and the canine mammary adenoma cell line ZMTH3 in nude mice. GLV-1h68 efficiently infected, replicated in and destroyed all three types of cells in culture [42]. In all three models, significant inhibition of tumor growth was observed after a single systemic administration of GLV-1h68. Additionally, GLV-1h68 enabled the detection of metastases via optical imaging. Another oncolytic vaccinia virus strain LIVP1.1.1, a new variant isolated from the wild-type LIVP strain, efficiently killed the canine soft tissue sarcoma cells. Systemic administration of LIVP1.1.1 led to significant growth inhibition of canine soft tissue sarcoma xenografts in nude mice. The LIVP1.1.1 mediated therapy significantly improved survival of sarcoma bearing mice and resulted in almost complete tumor regression [42]. Considering the promising results in several canine cancer xenografts, the VACV derived from LIVP strain called V-VET1 is being analyzed in phase I study for safety and dose escalation in dogs with different cancers [7].

1.3.1 Translation of oncolytic virotherapy from dogs to humans and reverse

The preclinical development of anticancer drugs has been based primarily on the implantation of murine or human cancer cells into mice. Naturally occurring cancers in pet dogs that share many features with human cancers are prominent and alternative models for development of anticancer drugs [43]. Studying dogs with cancer is likely to provide valuable information that is distinct from that generated in studies of rodent cancers alone. Canine cancers show significant similarity with human cancers including histological appearance, tumor genetics, molecular targets, biological behavior and response to conventional therapy [44, 45]. In both species, tumor initiation and progression is influenced by similar factors like age, nutrition, sex and environmental exposure. Dogs show as diverse cancers as seen in humans. Many of the treatment options used in veterinary medicine resemble protocols used to treat human cancer patients. In addition, public release of nearly 99% canine genome sequences provided a window of opportunity to expand the scope of comparative oncology [46]. Comparison of canine genome sequences with the human genome suggests that around 19,000 genes identified in the dog match to

similar or orthologous genes in the human genome. The genetic and biological similarities between two species have been utilized for the development of various anticancer drugs for canine as well as human cancers patients and oncolytic virotherapy is not an exception [47].

It is well known that despite evidence of oncolytic virus efficacy in mouse cancer models, many viruses fail in human trials due to unacceptable toxicity or lack of efficacy [48]. Some strains of oncolytic viruses such as the human adenovirus and the vaccinia virus in general do not productively replicate in mouse cells [49]. Thus, certain permissive cancer cells are grown in immunocompetent animals to study virus replication. Although these cancer models provide certain degree of understanding of oncolytic activity of virus, artificial establishment of these tumors as subcutaneous xenografts raises concern as to how well this model mimics their natural human counterparts. Hence, pet dogs with tumors are necessary models to demonstrate efficacy of OVs for both canine and human cancers. In addition, an alternative approach may be the use of species-specific viruses in their natural hosts. For example, application of canine adenovirus 2 in osteosarcoma of dog has shown to address the issue of tumor setting, efficient virus replication and oncolysis [50]. Canine osteosarcoma resembles human osteosarcoma at several levels including histopathology and metastatic behavior. In addition, canine adenovirus 2 shares similarities with human adenoviruses that are used as oncolytic agents for human osteosarcoma. Thus, considering vast similarities between osteosarcoma and adenovirus strains from both the species, the data from these studies are more reliable and helpful in designing human clinical trials.

Development of oncolytic virotherapy for treatment of canine cancer patients is of prime importance. Taking into consideration the value of comparative oncology, data obtained from human clinical trials can be effectively transferred to canines and vice versa.

1.4 Oncolytic vaccinia virus

Vaccinia virus (VACV) is arguably the most successful live biotherapeutic agent in medical history. It was the active agent of the smallpox vaccine that successfully eradicated smallpox, one of the most deadly diseases in human history [51]. VACV has also been exploited as a therapeutic agent against cancer since 1922. This virus selectively infects and destroys tumor cells, while sparing normal cells, both in cell

culture and in animal models. Anti-tumor therapeutic efficacy also has been demonstrated in human patients and in canine patients with a variety of tumor types [8, 42]. In addition recombinant oncolytic VACVs carrying imaging genes represent an advance in treatment strategy that combines tumor specific therapeutics as well as diagnostics (theranostics) [52]. This chapter briefly describes previous and current vaccinia viruses as oncolytic agents in cancer therapy.

1.4.1 History of oncolytic vaccinia virus

The true origin of VACV is not known. In the 18th century, Edward Jenner used as a vaccine for smallpox a virus that he isolated from a milkmaid, presumably a cowpox virus [53]. The virus was passaged from one individual to another over the next 130 years. In the 1930s, when small pox vaccination commenced with this virus, it became clear that the strain was distinct from the cowpox virus. This new strain, subsequently named “vaccinia virus”, is speculated to have either derived from the cowpox virus through serial passages under laboratory conditions or represented a laboratory survivor of a virus that is extinct in nature [54].

Even before VACV gained popularity in the medical community as the choice for smallpox vaccination, it was used as a therapeutic agent for the treatment of cancer. In 1922, Salmon and Baix observed that VACV successfully infected and produced characteristic lesions in a large breast carcinoma of a female patient after intratumoral inoculation [23]. In 1960, Burdick reported that malignant melanoma of a female patient went into remission after VACV treatment [55]. In 1987, Arakawa reported for the first time, that intravenous injection of VACV was effective in treating patients with lung, renal adenocarcinomas or multiple myeloma [56]. Subsequently, with the advances in recombinant DNA technology, VACV strains have been engineered to encode foreign genes in cancer cells that can kill the cancer cells or help the activation of the immune system [57].

1.4.2 An overview of vaccinia virus biology

VACV is a double-stranded DNA virus that replicates entirely in the cytoplasm of host cells. It produces three forms of infectious particles: intracellular mature virus (IMV), cell-associated enveloped virus (CEV) and extracellular enveloped virus (EEV). Vaccinia IMV particles are brick-shaped, approximately 300 X 240 X 120 nm in size, with a lipoprotein shell surrounding a complex core structure. The core structure contains a linear, double-stranded DNA genome of approximately 192 kb.

The VACV genome encodes around 200 genes that are largely non-overlapping. The process of cell entry by VACV is not well understood. For instance, it is presumed that VACV gains entry into cells via a cellular receptor, yet that receptor has not been unequivocally identified. Moreover, VACV can enter many different cell lines, suggesting that either it uses many different receptors or it uses a single receptor ubiquitous to all cells. IMVs enter cells by fusion with the plasma membrane [58]. In contrast, EEVs enter cells by endocytosis followed by low pH disruption of the EEV outer membrane and fusion of the released IMV with endosomal membranes [59].

Unlike other DNA viruses, vaccinia virus remains in the cell cytoplasm for the entire duration of the infectious cycle [60]. Vaccinia encodes its own proteins required for replication, especially those essential for DNA replication and mRNA synthesis. Because of its lack of dependency on host proteins, VACV replicates well in many different cell types.

After entry into the cytoplasm while the viral cores are only partially uncoated, the virus transcribes early class genes encoding viral proteins required for synthesis and maturation of viral RNA. The encoded early proteins include RNA polymerase, transcription factors, mRNA capping and methylating enzymes, and poly (A) polymerase. Subsequently, the viral cores undergo a second uncoating in preparation for viral DNA replication. Replication of the viral DNA occurs very efficiently within the infected cell. The time of onset of DNA synthesis varies to some extent with multiplicity of infection (m.o.i.) and cell type. It typically begins 1–2 h after infection and within several hours results in the generation of about 10,000 genome copies per cell, of which half are ultimately packaged into infectious virions [27]. DNA replication occurs at sites in the cytoplasm termed “viral factories”. DNA synthesis begins with the introduction of a nick in one DNA strand near one or both ends of the viral genome [57]. Viral DNA replication is followed by expression of intermediate class genes, which encode late class viral proteins. Late viral proteins encode enzymes and structural proteins that are assembled into the final viral particles. Promoters for early, intermediate, and late viral genes contain distinctive sequence elements that regulate the timing and the extent of viral gene transcription and translation [61]. Upon synthesis of the late structural proteins, infectious virus particles are assembled, a process that eventually leads to lysis of the infected cell.

Assembly of viral particles takes place in the so-called “virus factories”. The newly synthesized viral genomes are wrapped in a complex scaffold of proteins and lipids to form the first infectious viral particles called IMVs [62]. The majority of the IMVs remain within the cell until lysis. However, a small subset of IMVs leaves the factory in a microtubule-dependent manner and these particles become wrapped by a double-layer of membrane derived either from the early endosomes or from the trans-Golgi network to form intracellular enveloped viruses (IEVs), an intermediate between the IMVs and the CEVs/EEVs [63]. IEVs then move along microtubules to the cell surface [64], where the outer envelopes of the IEVs fuse with the plasma membrane, exposing enveloped virions on the cell surface. Some of them are retained on the cell surface to become CEVs, while others dissociate from the cell as EEVs. The different forms of virus particles produced by VACV replication have different properties relating to the promotion of cell-to-cell virus spread and evasion of circulating antibodies and complement in the blood stream. The replication cycle of VACV is represented diagrammatically in Fig. 2.

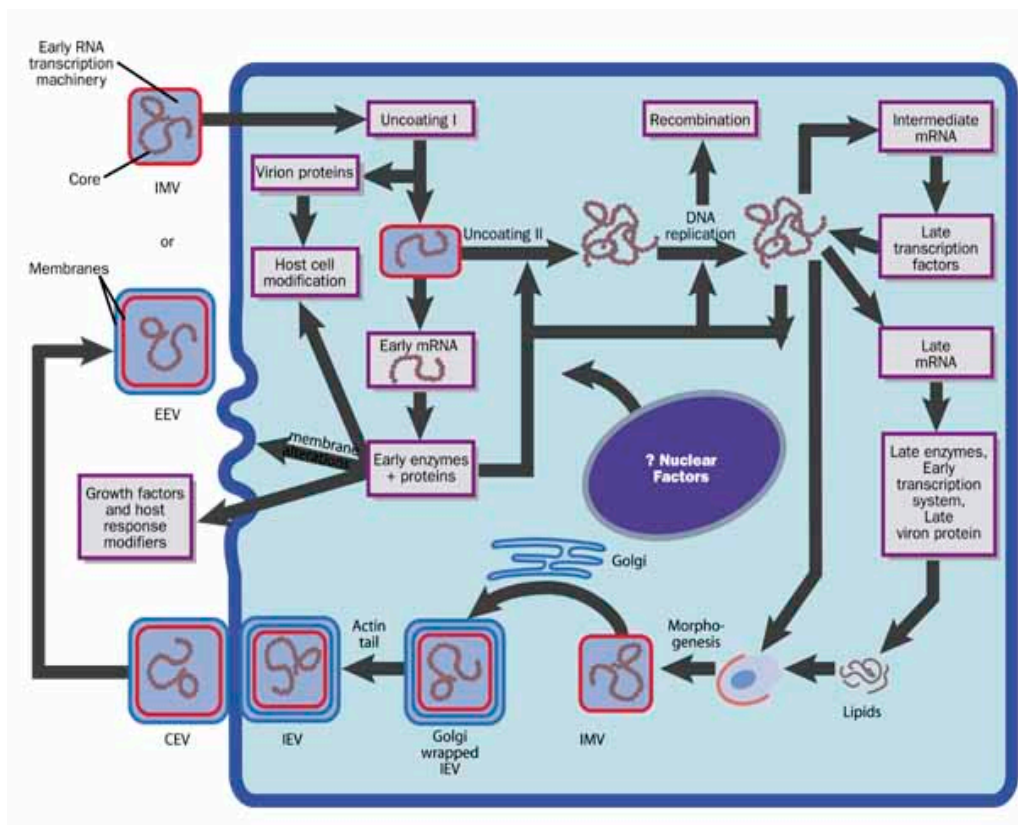


Fig 2. The cytoplasmic replication of vaccinia virus

Abbreviations: IMV, intracellular mature virus; IEV, intracellular enveloped virus; CEV, cell-associated enveloped virus; EEV, extracellular enveloped virus. [65]

1.4.3 Preclinical research with vaccinia virus as an oncolytic agent

VACV exhibits a broad host range, allowing its use in many experimental animal models. This broad host range makes it possible that a VACV strain characterized in preclinical studies may also be used in human and canine cancer patients. VACV is used for cancer therapy mainly via three approaches:

- i) As a replication competent (oncolytic) virus to directly lyse tumor cells,
- ii) As a gene delivery vector to express therapeutic and diagnostic genes with added therapeutic benefit and
- iii) Combination of VACV with other anti-cancer therapies.

1.4.3.1 Replication-competent oncolytic vaccinia virus in preclinical research

VACV has a natural tropism for tumors. Studies have shown that after intravenous administration of VACV into tumor-bearing animals, the highest amounts of virus were recovered from tumors with little virus detected in other organs [8]. The oncolytic potential of VACV varies depending on the strain of the virus. Lister, Copenhagen, Wyeth and Western Reserve strains have demonstrated oncolytic potency [66]. In contrast, strains such as MVA and NYVAC do not replicate in mammalian cells and, therefore, have no oncolytic potential. The antitumor efficacy of each strain is predominantly based on its infectivity to cancer cells, its replication potential, its cell-to-cell spreading and its cell lysis potential. LIVP1.1.1 virus derived from the lister strain; exhibit significant oncolytic potency in various human and canine cancer xenograft models[42, 67]. Interestingly, the virus thymidine kinase (tk) gene, important for VACV replication, was found to be naturally inactivated in both these Lister-derived strains, making them dependent on host-derived thymidine kinase activity, found mostly in cancer cells [42].

Replication competent viruses also kill cancer cells by modulating host immunity. VACV infection results in cell destruction and release of cellular danger signals (danger-associated molecular pattern molecules) and viral danger signals (pathogen-associated molecular pattern molecules) as well as tumor associated antigens. These antigens activate immune responses against the tumor tissues. LIVP6.1.1 infection in mouse tumor xenografts enhances Infiltration of innate immune cells into mouse xenograft tumors by infection with LIVP6.1.1 and, resulting in an overall improvement in oncolytic efficacy [42]. Additionally, oncolytic VACV

infection of tumors induces blood vessel collapse within the infected tumors contributing to tumor regression [68].

1.4.3.2 Development of vaccinia virus as a delivery vehicle for therapeutic and diagnostic genes

Oncolytic VACV, with its ability to replicate exclusively in tumor tissue, may be an ideal gene transfer agent for therapeutic proteins to cancer cells. VACV infection enables the localized expression of transgene-encoded proteins at high concentration in a large proportion of the tumor cells. Because of its large genome, VACV can easily contain and simultaneously lead to expression of multiple transgenes. Different promoters can regulate the timing and extent of expression of these transgenes. Transgene products can either be produced intracellularly or can be efficiently secreted from the infected cells. Indeed, many recombinant VACV constructs containing transgenes have been made and tested preclinically for expression and activity of the heterologous products and their benefit in antitumor efficacy and/or in imaging.

VACV has been engineered to express tumor-associated antigens to elicit antigen-specific immune responses. Recombinant VACV vectors carrying carcinoembryonic antigen (CEA) were constructed and examined in numerous preclinical studies [69]. Clinical trials have been conducted with these vectors to examine their toxicity, immune activities, and tumor responses in patients with advanced or metastatic CEA-expressing adenocarcinomas [70]. The vaccines were well tolerated and effective at inducing CEA-specific cytotoxic T cell responses [71]. In another example, use of VACV as a vehicle for delivery of anti-angiogenic factors to tumor sites has been well established. Destruction of tumoral vasculature using anti-angiogenic agents is emerging as a promising therapeutic modality for treatment of solid tumors. VACV encoding single-chain antibody against VEGF (GLV-1h109) improved the therapeutic response in mice with human tumor xenografts [72]. The VACV platform has been used also to express other immunomodulatory molecules like interleukins (IL-4, IL-24, hyper IL-6), interferons (IFN- γ) and several immune activating antibodies (CTLA-4, PD-1 and PDL-1), each of which regulate the immune response and exert potent antitumor immunity to various extents [27, 73]. In addition, VACVs express prodrug-converting enzymes that kill tumor cells by

localized conversion of a prodrug to a cytotoxic agent. Two prodrug-converting enzymes/prodrug systems (i.e. cytosine deaminase/5-fluorocytosine (CD/5-FC) system and purine nucleoside phosphorylase/6-methylpurine deoxyriboside (PNP/6-MPDR) system) have been analyzed using replication selective VACV platforms. In both cases, the prodrug-converting enzymes were expressed by the recombinant VACV. Virus-mediated oncolysis and concomitant expression of cytosine deaminase enzymes significantly improved tumor cell death after addition of 5-FC. Furthermore, oncolytic VACVs containing imaging genes represent a new treatment strategy that combines tumor site-specific therapeutics and diagnostics, also called “therognostics” [51]. The genes encoding green fluorescent protein (GFP), luciferase and luciferase-GFP fusion protein have been incorporated in many oncolytic VACV constructs to detect and monitor therapy and virus distribution in live animal. The oncolytic VACV GLV-1h68 containing the gene encoding the fusion protein, *Renilla* luciferase- *Aequorea* GFP, enabled accurate, non-invasive detection and optical imaging of tumor regression in real time in a xenograft mouse model, as well as microscopic imaging of tumor biopsies at the tissue and cellular levels. In addition, the VACV platform has been used for gene-directed production of melanin specifically in tumor tissue [52]. Intratumoral production of melanin has the potential for use in several clinical diagnostic (e.g. marker during surgery, for endoscopy, in optoacoustic and MR imaging) and therapeutic procedures (near IR light induced thermotherapy).

1.4.3.3 Combination of VACV and other therapeutic modalities

Since the modes of tumor destruction of oncolytic virotherapy and other therapeutic modalities (e.g. chemotherapy, radiotherapy and immunotherapy) are different, the potential exists for synergy in combination treatments. In preclinical studies, oncolytic VACV GLV-1h68 was used in combination with cisplatin or gemcitabine, and the combination therapy resulted in a significantly faster decrease in tumor size [74]. In combination with radiation therapy, VACV showed improved virus replication and therapeutic response in several tumor models. Preferential replication of systemically delivered oncolytic VACVs GLV-1h68 and LIPV1.1.1 was seen in glioma xenografts that had been focally irradiated. The increased virus replication correlated with increased tumor regression and improved overall mouse survival [75]. Thus, tumor targeted ionizing radiation can be combined with systemically delivered oncolytic

VACV with synergistic results [76]. Other complementary therapeutic combinations of VACV with immunotherapy, surgery, hyperthermia and therapeutic monoclonal antibodies have also been evaluated with evidence of compatibility and/or improved efficacy.

1.4.4 Clinical trials with oncolytic vaccinia virus

Following a century of preclinical and clinical work, oncolytic viruses are now proving themselves in advanced phases of clinical trials. Oncolytic VACV strains (attenuated and genetically modified) are in various phases of clinical trials for treatment of a wide variety of cancers in both human and canine. VV-IL-2 a recombinant VACV leading to expression of the human IL-2 gene was the first cytokine-encoding VACV studied clinically in human patients with solid tumors [77]. Neither toxicity nor virus shedding was detected with VV-IL-2 in these patients. However, no significant tumor regression was observed. Another recombinant VACV strain, JX-594 that leads to expression of human GM-CSF, was evaluated in Phase I and Phase II clinical trials for treatment of human patients with malignant mesothelioma and liver carcinoma. The virus was administered either intravenously or intratumorally and it was well tolerated with only infrequent, mild adverse effects. The virally encoded GM-CSF was detected at the injection sites in the tumors explaining capacity of virus to successfully expressing the transgene in tumor tissue. In addition, injection lesions were heavily infiltrated with CD4+ and CD8+ T lymphocytes, B lymphocytes, macrophages and eosinophils in patients with malignant mesothelioma. A second randomized Phase II trial with JX-594 virus in hepatocellular carcinoma patients showed anti-tumor efficacy, effects on tumor vasculature, and a dose dependent improved overall survival [78].

Oncolytic VACV GLV-1h68 (GL-ONC1) has also been tested for its safety in Phase I clinical trials in human patients with solid tumors. This recombinant VACV is systemically delivered either as a single agent for treatment of advanced solid tumors or in combination with cisplatin and radiotherapy in head and neck cancer patients. GL-ONC1 is also in a Phase I/II clinical study in human patients with peritoneal carcinomatosis in which virus is delivered intraperitoneally [34]. The clinical trials with GL-ONC1 are currently ongoing and results are pending. Several additional VACV platforms are currently under trial for treatment of various human malignancies. The detailed overview of clinical trials with VACV is listed in table 2.

Table 2: Clinically tested oncolytic viruses in human and canine cancer patient

Virus	Phase/ (Route)	Modification	Cancer type	Response
GL-ONC1	I/II (i/p)	TK deletion +GFP, B-gal, B-gluc	Peritoneal Carcinoma	Active trial
GL-ONC 1	I (i/v)	TK deletion +GFP, B-gal, B-gluc	Solid tumors	Active trial [79]
GL-ONC1 + cisplatin and radiation therapy	I (i/v)	TK deletion +GFP, B-gal, B-gluc	Head and neck cancer	Active trial
GL-ONC1	I (i/pl)	TK deletion +GFP, B-gal, B-gluc	Lung cancer, mesothelioma	Active trial
JX-594	I (t/d)	TK deletion + GM- CSF	Hepatic carcinoma	30% PR, 60% SD, 10% PD [78]
JX-594	II (i/t)	TK deletion + GM- CSF	Hepato- Cellular carcinoma	16% CR [36]
JX-594	I (i/v)	TK deletion + GM- CSF	Solid tumors	Active trial
JX-594 + Irinotecan	I/IIb (i/v)	TK deletion + GM- CSF	Colorectal carcinoma	Active trial
JX-594	I/II (i/t)	TK deletion + GM- CSF	Malignant Melanoma	Safe and SD
V-VET1	I (i/v)	TK deleted lister strain	Canine solid tumors	Active trial [7]
VV-IL-2	I (i/t)	TK deleted + P7.5-hIL-2	Malignant mesothelioma	No significant tumor regression
Wild type Vaccinia Virus	I (i/ves)	Not applicable	Advanced bladder cancer	75 % patients showed 4-year survival.
rV-B7.1	I (i/t)	Human B7.1	Malignant melanoma	10% patient showed PR

i/p: Intra-peritoneal, i/v: Intravenous, t/d: Transdermal, i/t: Intra-tumoral, i/ves: Intra-vesicle, i/pl: Intra-plural, TK: thymidine kinase, GM-CSF: Granulocyte-macrophage-colony stimulating factor, GFP: Green fluorescent, β -Gluc: β -glucuronidase,

In contrast to the clinical progress of human oncolytic virotherapy, there are very few clinical trials using OV for canine cancer patients. Currently, a Phase I clinical study is underway to evaluate the safety of intravenous administration of VACV strain LVP6.1.1 (V-VET1) in canine cancer patients at Angel Care Cancer Center,

Carlsbad, California, USA. Results from this dose escalation study in dogs are positive and LIVP virus was found in biopsies weeks after treatment [7].

Despite the continuing results of VACV clinical studies showing acceptable safety and promising efficacy, the mechanisms of action of VACV in cancer therapy are still ill defined. The relative contributions of “pure” oncolysis, modulation of tumor microenvironment post-oncolysis, and the benefit of adding a transgene are not clearly understood. For example, while much is known about how OVVs initially infect tumors, very little attention is placed on the multiple barriers that inhibit optimal virus spread throughout the tumor. Understanding the complex nature of the tumor microenvironment and its effects on oncolytic virotherapy could be of significant importance for improving the overall therapeutic activity and clinical utility of OVVs.

1.5 Tumor microenvironment and oncolytic virotherapy

Systemic infection of oncolytic VACV specifically infects tumor cells and subsequently virus spreads throughout the tumor. While only a very small fraction of the intravenously administered virus reaches the tumor site and the virus that does infect the tumor rapidly amplifies within the tumor cells. For efficient intratumoral amplification, virus must overcome several obstacles within the tumor microenvironment. For example, VACV must travel through heterogeneous and perfused tumor vasculature, avoid entrapment in the extracellular matrix (ECM) and evade various immune cells. However, the poorly arranged and chaotic nature of the tumor microenvironment may constitute weaknesses in the anti-virus defenses that improve effectiveness of oncolytic VACV-mediated tumor therapy. Numerous strategies are employed to manipulate the components of tumor microenvironment to improve virus infection and spread within the tumor tissue as well as the killing of tumor cells by the immune system.

1.5.1 Strategies to manipulate ECM

The extracellular matrix in solid tumors is composed of complex secretions of proteins and proteoglycans produced by both neoplastic and normal stromal cells. Slight changes in the tumor ECM organization can have tremendous impact on cancer cell biology and its response to therapy. ECM of most tumors includes mesenchymal proteins that are absent in normal tissue and render the matrix of these tumors very distinct from normal tissue. Increased ECM secretion in tumors

also results in increased water retention that increases interstitial fluid pressure. Apart from increased pressure, the interlocked meshwork of secreted proteins presents a physical barrier that interferes with efficient dispersal of therapeutics within the solid tumor [80]. Inefficient dispersal of OV through the solid tumor has been previously noted and is considered to be one of the major limitations of Oncolytic virotherapy. This has been evidenced by discrete focal viral localization in tumor xenografts treated with VACV in mice [81]. Viral presence has also been shown to localize only in small discrete areas in clinical tissues harvested from human patients treated with HSV [82]. These observations indicate that approaches used to modulate the complex extracellular matrix should enhance oncolytic VACV efficacy. Several innovative strategies to enhance VACV spread within the tumor microenvironment have been investigated in recent years. A naturally occurring form of poxvirus, an extracellular enveloped virus (EEV) that possesses host cell derived lipid bilayer has been evolved for rapid spread within the tumors. Kirn *et al.* compared the oncolytic potential of low versus high-EEV producing VACV strains. VACV strains that produced high amount of EEV particles displayed improved spread within the tumor after systemic delivery, resulting in significantly improved therapeutic response [83]. Another approach to manipulate ECM is to arm oncolytic viruses with the enzymes that degrade the ECM. Oncolytic vaccinia virus GLV-1h255 containing the matrix metalloproteinase-9 gene was constructed and used to treat PC-3 tumor-bearing mice. VACV-mediated intra-tumoral over-expression of matrix metalloproteinase-9 lead to a degradation of collagen IV, facilitating intra-tumoral viral dissemination and resulting in accelerated tumor regression [84].

1.5.2 Strategies to target tumor angiogenesis

Angiogenesis is the process of formation of new blood vessels that involves the migration, growth, and differentiation of vascular endothelial cells. Folkman in 1971 proposed that primary solid tumors could attain a size of around 1-2 mm diameter even in an avascular state. When tumors attains a size of 1-2 mm diameter, surrounding mature host blood vessels begin formation of new blood capillaries, which grow towards and infiltrate the tumor mass [85]. A variety of growth factors families and their related receptor; collectively called as tumor angiogenic factors (TAFs), trigger the angiogenic switch in tumors. TAFs mainly include fibroblast growth factor (FGF), vascular endothelial growth factor (VEGF), VEGF tyrosine

kinase receptors, platelet derived growth factors (PDGFs), angiopoietin and angiopoietin tyrosine kinase receptors. Tumor cells and surrounding normal cells release TAFs, which regulate the formation of new blood vessels. The newly formed blood vessels provide oxygen and nutrients to the growing tumor and allow the tumor to invade nearby tissue and to proliferate. However, the newly formed blood vessels are highly permeable because of immature endothelial cells and fewer intracellular junction complexes than in the normal vasculature. These abnormal blood vessels allow escape of tumor cells from the primary tumor to distant organs leading to metastasis. Therefore targeting tumor vasculature remains a very significant area of preclinical and clinical cancer research.

Obstructions of blood flow to the tumor by treatments that target tumor vasculature induces ischemia or cytostasis thereby preventing oxygen and nutrient supply to cancer cells in the center of solid tumors. Further lack of oxygen and nutrients leads to death of the cancer cells. Moreover, Jain *et al.* showed that use of anti-angiogenic agents that were originally targeted to inhibit formation of new blood vessels, could transiently “normalize” the tumor vasculature. Normalization of tumor vasculature alleviates hypoxia, increases delivery of drugs and anti-tumor immune cells, and improves the outcome of various therapies [86].

Inhibiting tumor angiogenesis by blocking TAFs can potentially affect tumor growth. Most of the anti-angiogenic agents that entered the drug development pipeline targeted VEGF ligands or receptors. VEGF has a key role in the signaling pathways that mediate angiogenesis, tumor growth, and metastasis. Monoclonal antibodies against VEGF are now in widespread clinical use in oncology. Bevacizumab (Avastin, Genentech, USA), a humanized anti-VEGF-A monoclonal antibody was the first anti-angiogenic drug approved by FDA of USA. However, efforts to develop other anti-angiogenic targets such as angiopoietin and PDGFs are ongoing [87]. Various anti-angiogenic molecules e.g. Aflibercept (Zeltrap, Sanofi Aventis, USA), Sorafenib (Nexavar, Bayer Healthcare, USA), Sunitinib (Sutent, Pfizer inc, USA) are approved for the treatment of one or more tumor types. In addition, clinical trials are ongoing with new anti-angiogenic agents that mainly target TAFs [34]. Despite these efforts, the clinical outcomes in cancer patients treated with anti-angiogenic therapies have been less than anticipated. However, anti-angiogenic therapy alone was not expected to be curative but can only prevent any new expansion and tumor

when reach the size of 1-2 mm diameter can regrow without vasculature. Therefore, combining anti-angiogenic approaches with additional anti-cancer approaches, like oncolytic virotherapy would provide combined benefits. Viral oncolysis would kill the tumor cells and anti-angiogenic therapy would inhibit the tumor spread and metastasis.

Oncolytic VACVs are the leading viral vectors that are targeted against tumor angiogenesis. VACV engineered to target cells with activated of Ras/MAPK signaling pathway (JX-549) specifically infected tumor-associated vascular endothelial cells in hepatocellular carcinoma patients hence, and caused disruption of tumor perfusion. This virus has shown natural ability to infect vascular endothelial cells [68]. In addition, VACVs have been able to deliver angiogenesis inhibitors to the tumor site, providing local expression of these proteins on a continual basis consequently maximizing efficacy and limiting side effects. Since VEGF is highly expressed in many cancers, this pathway has been targeted by many VACV encoding anti-angiogenic inhibitors. More recently, Guse *et al.* showed that VACV armed with soluble VEGF receptor 1 protein enhanced antitumor efficacy in a renal cell cancer model [88]. VACV has also been used to deliver a single chain antibody directed at VEGF. The VACV strain GLV-1h109 that expresses anti-VEGF single-chain antibody has significantly improved therapeutic efficacy in human tumor xenografts compared to parental virus GLV-1h68 [72]. In addition, VACV armed with other endogenous inhibitors of, for example, angiostatin and FGF was shown to be more efficient than its unarmed counterpart [89].

1.5.3 Strategies to modulate the immune response

Apart from tumor vasculature and ECM, infiltrating host immune cells are another significant component of the tumor microenvironment. While host immune cells have the potential to initiate and activate a potent anti-tumor immune response, they are often utilized by the tumor to produce pro-angiogenic, pro-invasive and pro-tumorigenic signaling. Classically, the immune system is thought to limit efficacy of oncolytic virotherapy, leading to viral clearance. However, preclinical and clinical data suggest that in some cases virotherapy may in fact act as a cancer immunotherapy. Oncolytic viruses induce tumor cell death by inducing apoptotic or necrotic pathways. During the cell death process, dying cells release tumor-associated antigens (TAAs). These TAAs coupled with danger signal associated with

virus infection could create a favorable environment that would elicit a specific immune response. Considering the dual role of immune system in tumor biology, it is important to understand the immune response to viruses and virus-colonized tumors in order to develop successful strategies to combat cancer with OVs.

1.5.3.1 Innate immune response and oncolytic virotherapy

The ability of the innate immune response to limit viral replication has been demonstrated in several experimental models [90] and in clinical studies [91]. The manipulation of the innate immune response in favor of antitumor activity represents a critical target for achieving successful tumor immunotherapy. Innate immune response may be directly cytotoxic to tumors, while it can also help to induce an adaptive immune response [92]. Among innate immune cells, the strongest anticancer response exists for Natural Killer (NK) cells [93]. In addition, dendritic cells (DCs) play a role in priming the adaptive T cells as well as recruit and interact with NK cells [94]. Macrophages constitute a dominant fraction of the innate immune cells that infiltrate developing tumors. Although macrophages are key orchestrators of the microenvironment that supports tumor progression, certain phenotype macrophages can mediate antitumor functions [95]. The impact of macrophages on tumor biology is largely influenced by cytokine signals within the tumor microenvironment. These signals produce a heterogeneous population of macrophages, which are commonly described based on their similarity to an M1 (classically activated) or M2 (alternatively activated) phenotype. M1 macrophages, following exposure to interferon- γ (IFN- γ), have tumoricidal activity and elicit destruction of tumor tissue [96]. However, another type of innate immune cells categorized as myeloid derived suppressor cells (MDSCs) are potent immunosuppressive cells. In malignant states, MDSCs are induced by growth factors secreted by tumor cells. MDSCs play an important part in suppression of host innate and adaptive immune responses through several mechanisms such as production of arginase 1, release of reactive oxygen species and nitric oxide and secretion of immune-suppressive cytokines. This leads to a permissive immune environment enabling the growth of malignant cells. MDSCs may also contribute to angiogenesis and tumor invasion [97]. These findings highlight two extreme views of the immune system in relation to the efficacy of oncolytic virotherapy. On one hand, innate immune system promotes tumor progression; on other hand, experimental data

indicate that it has significant anti-tumor activity. Attempts have been made to modulate the innate immune response, aiming either to limit the innate response in order to enhance viral replication, or to enhance innate antitumor activity. The outcomes of these conflicting strategies provide insight into the role of the innate response to oncolytic virotherapy.

Expression of IFN- β has been hypothesized to limit viral replication in normal tissue while allowing replication in tumor tissue, as tumor cells are commonly resistant to antiviral effects of type I IFNs. A VACV encoding INF- β (JX-594) significantly improved tumor selectivity and efficacy, in association with generation of anti-tumor immunity compared to a control VACV without IFN- β [98]. In addition, genetically engineered VACV (Vvdd) when combined with an agonist antibody specific for co-stimulatory molecule CD137 induced an antitumor response. In an immune competent mouse model this combination treatment significantly reduced tumor growth relative to either treatment alone. Tumor growth inhibition was associated with greater infiltration of CD8+ T cells and NK cells, and more sustained presence of neutrophils at the tumor site. Depletion of T or NK cells or neutrophils reduced efficacy, confirming their contribution to an effective therapeutic response [99]. Furthermore, inhibition of MDSCs has improved the efficacy of oncolytic virotherapy. Oncolytic herpes simplex virus 1 (HSV-1) viruses armed with 15-prostaglandin dehydrogenase effectively reduced primary tumor growth and inhibited secondary metastasis in BALB/c mice with 4T1 breast cancer xenografts. Mice treated with HSV-1 encoding 15-prostaglandin dehydrogenase showed statistically significant decrease in splenic MDSCs compared to parental virus [100].

1.5.3.2 Adaptive immune response and oncolytic virotherapy

Cytotoxic T cells (CTL) and helper T cells are major contributors of the adaptive immune system that have significant antitumor effects. Oncolytic virus mediated tumor cell lysis release TAAs in tumor microenvironment and interacts with DCs via Pattern recognition receptors (PRRs) or Toll like receptors (TLRs). DCs and macrophages are classical antigen presenting cells (APCs) that present TAAs and induce adaptive immune response. A tumor-directed immune response involving cytotoxic CD8+ T-cells, T helper 1 (Th1) cells, and natural killer (NK) cells appear to protect against tumor development and progression. On the contrary, the immune response that involves B-cells, the activation of chronic humoral immunity and/or a T

helper 2 (Th2) polarized response can promote tumor development and progression [101]. CD8+ cytotoxic T cells recognize TAAs presented by MHC class I molecules on tumor cells and kill cancer cells using the perforin / granzyme system. Another type of T cells i.e. CD4+ T-cells are an important factor of the tumor microenvironment, which modulate the anti-tumor immune response. CD4+ T cells are activated in response to cytokines that are classified into two categories, Th1 and Th2. After stimulation, the Th1 cells secrete interferon gamma (IFN- γ), transforming growth factor-beta (TGF- β), tumor necrosis factor alpha (TNF- α), and interleukin 2 (IL-2). These cytokines cooperate with the functions of cytotoxic CD8+ T-cells, producing a tumoricidal activity. In contrast, Th2 cells express interleukin (IL) 4, 5, 6, 10, and 13 induce anergy of T-cells and loss of cytotoxicity, while increasing the humoral immunity (lymphocyte B function). Thus, Th1 cell responses benefit antitumor immunity, whereas Th2 cell responses produce a down-regulation of antitumor cell mediated immunity and increase the humoral pro-tumorigenic responses [101]. However, regulatory T-cells (T_{reg}) and immature myeloid cells suppress antitumor immunity. T_{reg} cells are a distinct group of lymphocytes with immunosuppressive properties that usually maintain immune tolerance. T_{reg} cell suppressive activity is beneficial by restricting T cell response against self-antigens and preventing inflammatory and autoimmune diseases. In cancer, their inhibitory role in limiting immune response against “pseudo-self antigens” from tumor origin avoids an effective anti-tumoral immune response and often culminates into negative outcomes for the patient. These cells may play an important deleterious role in cancer immunopathology due to their potent suppressive activity of both T-cell activation and effector functions [102]. Furthermore, immature myeloid cells induce cytotoxic T-cells anergy by binding to T-cell receptor (TCR) complex in absence of co-stimulatory signals, which suppresses the anti-tumor activity of T cells.

Considering the anti-tumor role of the adaptive immune system, the range of oncolytic viruses that have been reported to facilitate the generation of adaptive antitumor immunity reflects the broad applicability of the principle. Sequential administration of adenovirus and VACV in Syrian hamster with pancreatic cancer xenografts induced anti-tumor CTL and further significantly improved tumor regression [103]. In murine models, tumor delivery of oncolytic VACV by cytokine-induced killer (CIK) cells induced antitumor immunity [104]. Attempts have been

made to enhance the immunotherapeutic potential of oncolytic viruses by incorporating immunostimulatory transgenes. Cytotoxic T cells were induced in human liver cancer patients treated with VACV encoding GM-CSF (JX-594) [36]. Granulocyte-monocyte colony-stimulating factor (GM-CSF) promotes the differentiation of progenitor cells into dendritic cells, and has been successfully used in strategies to generate tumor-reactive cytotoxic lymphocytes. Chemokines have also been inserted into oncolytic viral vectors in order to promote the recruitment of immune effectors to the tumor microenvironment. Oncolytic adenovirus encoding the chemokine RANTES recruited DCs to the tumor microenvironment, eliciting antigen-specific CTL and NK cell responses, and promoted tumor regression [105]. These observations provide important insights into future strategies for optimizing the immunotherapeutic potential of oncolytic viruses. However, in many of these experiments it is difficult to decide the relative importance of direct viral oncolysis and immune mediated bystander killing of uninfected tumor cells. In conclusion, certain components of the immune system work in concert with, rather than at odds with oncolytic virotherapy. Thus, designing of oncolytic virus should consider immune activation as a part of solution, rather than a problem.

CHAPTER 2: RATINALE AND AIM

Oncolytic virotherapy is one of the promising approaches to treat cancer. Use of oncolytic VACV has shown promising results in both preclinical and clinical studies against various human cancers. However, oncolytic virotherapy using vaccinia virus against canine cancers is relatively new and the role of oncolytic VACV in treating canine cancers is not well understood. Preclinical studies of oncolytic virus efficacy and its mechanism of action were traditionally conducted in rodents. However, dogs have a long history of use in cancer research based on their strong anatomical and physiological similarities to humans. Therefore, the canine model provides opportunity for investigating treatment strategies both experimentally and clinically. Human and dog tumors show extensive similarities in histological appearance, tumor genetics, biological behavior and response to conventional therapy. The tumor microenvironment of both species shows enormous similarities. Thus, studying oncolytic virus and tumor microenvironment interaction in dogs with cancer could provide valuable information related to human cancer. Moreover, clinical investigation in dogs is possible based on the large proportion of pet dogs that are diagnosed and treated for cancer. Therefore, advancing the development of oncolytic viruses for treatment of cancer in canines could serve both to provide additional safe and effective treatments for dogs, contributing to veterinary medicine, but also as an additional model to translate the information gained to the treatment of cancer in humans.

As for other targeted therapies, a number of challenges remain for oncolytic virotherapy. These challenges mainly include replication of OV in non-tumor tissue, poor delivery of OV to the tumor site, relatively poor virus-spread throughout the solid tumor tissue, inefficient viral replication in immune-competent hosts and disadvantageous ratio between anti-viral and anti-tumoral immunity. Limited delivery of OV to the tumor site is mainly attributed to virus neutralization by blood components. However, components of tumor microenvironment that include heterogeneous tumor vasculature, premature extracellular matrix and an army of innate immune cells, affect the spread and replication of OV in the tumor tissue. Despite this limitation, it has been shown that OV are also able to take advantage of certain features of tumor microenvironment. OV are modified or armed to inhibit the heterogeneous tumor vasculature density, which further improves tumor response. Alteration of extracellular matrix showed improved virus spread within the tumor

tissue. In addition, manipulation of the innate immune response helped the OV infection in killing the tumor tissue and thereby enhanced the anti-tumor efficacy. Thus, to understand the role of oncolytic VACV and its modulation by the tumor microenvironment, the current studies were designed with following aims.

- 1) To characterize the efficacy of oncolytic VACV strains in canine cancer xenografts in nude mice.
- 2) To analyze the role of tumor angiogenesis on modulation of oncolytic VACV in canine cancer xenografts in nude mice.
- 3) To analyze the role of the immune response on modulation of oncolytic VACV therapy in canine cancer xenografts in nude mice as well as in canine cancer patients.

CHAPTER 3: MATERIAL AND METHODS

3.1 Materials

3.1.1 Chemicals and enzymes

Chemical	Manufacturer
1x PBS	Sigma
3X FLAG peptide	Sigma
Acetic acid (C ₂ H ₄ O ₂)	Fisher
Acrylamide / bisacrylamide	BioRad
Ammonium persulfate (APS)	Merck
Benzonase	Merck
Bovine serum albumine (BSA)	Omega Scientific
Bradford reagent	BioRad
Bromophenol blue	Sigma
Carboxymethylcellulose (CMC)	Sigma
Crystal Violet	Sigma
Comassie Brilliant Blue G-250	Fisher
Collagenase I	Sigma
OneComp eBeads (Compensation beads)	eBioscience
Diaminoethanetetraacetic acid (EDTA)	Fisher
Dimethylsulfoxide (DMSO)	Sigma
Dithiothreitol (DTT)	Bio-Rad
DMEM medium	Cellgro
DNase I	Calbiochem
ECL	GE healthcare
Ethanol (p.a.)	Sigma
Fetal bovine serum (FBS)	Cellgro

Ficoll - paque plus	Sigma
Hanks balanced salt solution (HBSS)	Cellgro
Hoechst 3342	Sigma
Hydrochloric acid (HCl) 12 M	VWR
Hydrogen Peroxide (H ₂ O ₂)	Sigma
Isoflurane	VetEquip
Laemmli sample buffer 4x	BioRad
Magnetic beads	Sigma
Mowiol 4-88	Sigma
N', N', N', N'-Tetramethylethylenediamine (TEMED)	Fluka
Non-essential amino acids (NEAA)	Cellgro
Paraformaldehyde	EMS
Penicillin / Streptomycin	Mediatech
Powdered milk	DB
Potassium chloride (KCl)	Fisher
Potassium ferricyanide (K ₃ Fe(CN) ₆)	Sigma
Potassium ferrocyanide (K ₄ Fe(CN) ₆ ·3H ₂ O)	Sigma
Prestained protein marker	BioRad
Protease inhibitors mix	Invitrogen
Roswell Park Memorial Institute medium (RPMI-1640)	Cellgro
Recovery cell culture freezing medium	Cellgro
Sodium bicarbonate (NaHCO ₃)	Cellgro
Sodium chloride (NaCl)	VWR
Sodium dodecyl sulfate (SDS)	Fisher
Sodium hydroxide (NaOH) 2N	Fisher
Sucrose	Sigma
β-Mercaptoethanol	Sigma

Tissue Tek O.C.T.	Sakura Finetek
Trichloroacetic acid	BDH
Tris-HCl	Fisher
Tris-Base	Fisher
Triton X-100	Sigma
Trypan blue	Cellgro
Trypsin-EDTA	Cellgro
Tween 20	BioRad

3.1.2 Kits

Kits	Manufacturer
Cell proliferation Kit II (XTT assay)	Roche
Canine VEGF Quantikine ELISA kit	Quantikine
Protein purification kit	Sigma
DC protein assay kit	BioRad
Foxp3 / transcription factor staining buffer set	eBioscience

3.1.3 Equipments

Equipments	Manufacturer
Accuri C6 Cytometer	BD Bioscience
Anesthetic devices	VetEquip
Amicon Ultra-15 Centrifugal Filter Unit 10 kDa NMWL	Millipore
BD Conto RUO FACS machine	BD Bioscience
Biological safety cabinet, class II	Thermo electron
Blotting paper 3MM	Whatman
Cell counting chamber	VWR
Cell culture dishes (96, 24,12, 6-well)	Corning Inc

Cell culturing flasks	Corning inc
Centrifuge Centra CL2	Thermo Scientific
Centrifuge Micro CL21	Thermo Scientific
Centrifuge Sorvall RC 6 Plus	Thermo Scientific
CO ₂ incubator	Sanyo
Cryostat 2800	Leica Microsystem
Digital caliper	VWR
EDTA tube	DB
Electrophoretic vertical system	Hoefer DALT
Embedding Mold Tissue-Tek	IMEB Inc
Film cassette	Fisher
Film developer AGFA CP1000	Superior Radiographic
Fluorescence microscope IX71	Olympus
Imaging system	Carestream
Insulin syringe-100 29G1/2	DB
Inversed microscope CK30	Olympus
Leica TCS SP2 AOBS confocal laser microscope	Leica microsystem
MagNA beads	Roche
MagNA Lyser Mastercycler	Roche
Micro-Hematocrit Capillary Tubes	Global scientific
Mini-electrophoresis system	BioRad
Nitrocellulose membrane	Fisher
Orbital shaking	VWR
Pro Microplate Reader	Tecan Crailsheim
PVDF membrane	Invitrogen
Semi-Dry Blot apparatus	Peqlab
Sonifier 450	Branson

Spectrophotometer	Thermo Scientific
Stirrer	VWR
Surgeon scissors	E.A. Beck
Tweezers	E.A. Beck
Vortex VX100	Labnet
Water bath	Fisher

3.1.4 Solutions and buffers

1 mM Tris-HCl (pH 9.0)	0.158 g	Tris-HCl
	1 L	HyPure Cell Culture dH ₂ O
10 mM Tris-HCl (pH 9.0)	1.576 g	Tris-HCl
	1L	HyPure Cell Culture dH ₂ O
3.7% PFA	3.7 g	PFA in 37°C H ₂ O
	ad NaOH	until solution clears
	10 ml	10x PBS (pH7.4)
	ad 100 ml	dH ₂ O
Histology blocking buffer	0.3%	Triton X-100
	5%	FBS
		1X PBS (pH 7.2)
CMC overlay medium	7.5g	CMC
	50 ml	FBS
	11 ml	Penicillin / Streptomycin
	500 ml	DMEM

Crystal violet staining solution	1.3 g	Crystal Violet
	50 ml	ethanol
	300 ml	formaldehyde (37%)
	ad 1L	dH ₂ O
Lysis buffer / tumor PFU determination	1 tab	Protease inhibitor comp
	10 ml	1X PBS (pH 7.2)
Lysis buffer / tumor lysate	1 tab	Protease inhibitor comp
	50 mM	Tris-HCl (pH 7.4)
	2 mM	EDTA (pH 7.4)
	2 mM	PMSF
	10 ml	1X PBS (pH 7.2)
PBS Tween-20	0.05 %	Tween-20
		1X PBS (pH 7.2)
RIPA lysis buffer	50 mM	Tris-HCl (pH 7.8)
	150 mM	NaCl
	0.1 %	SDS
	0.5 %	sodium deoxycholate
	1 %	NP-40 / Triton X-100
	1 mM	PMSF
	1 tab	Protease inhibitor comp

3.1.5 Cell lines and culture media

3.1.5.1 Cell lines

CV-1	African green monkey kidney fibroblast cell line (ATCC, catalogue number CCL-70TM)
DT08/40	Canine prostate carcinoma cell line (Kind gift from Dr. Nolte School of vet. medicine Hannover)
STSA-1	Canine soft tissue sarcoma cell line (Kind gift from Dr. Nolte School of vet. medicine Hannover)

3.1.5.2 Culture media used for propagation of cell lines

CV-1	500 ml	DMEM High glucose
	50 ml	FBS
	5.5 ml	Penicillin / Streptomycin
DT08/40	500 ml	DMEM High glucose
	100 ml	FBS
	5.5 ml	Penicillin / Streptomycin
STSA-1	500 ml	MEM with Earle's salt
	50 ml	FBS
	5.5 ml	Penicillin / Streptomycin
	2 mM	Glutamine
	1 mM	Sodium pyruvate
	0.1 mM	Non-essential amino acids

3.1.6 Antibodies

3.1.6.1 Antibodies for staining of tumor sections

Primary antibodies

Primary antibody	Origin	Manufacturer
Anti-vaccinia	Rabbit	Abcam
Anti-CD31	Hamster	Chemicon
Anti-mouse Ly6G	Rat	eBioscience
Anti-mouse F4/80	Rat	eBioscience
Anti-DDDDK	Rabbit	Abcam
Anti- β -glucuronidase	Rabbit	Sigma
Anti- β -actin	Mouse	Abcam

Secondary antibodies

Secondary antibody	Origin	Manufacturer
Anti-rabbit HRP	Goat	Abcam
Anti-mouse HRP	Rabbit	Abcam
Anti-rat Cy3	Donkey	Jackson ImmunoResearch
Anti-rat Cy5	Donkey	Jackson ImmunoResearch
Anti-hamster Cy5	Donkey	Jackson ImmunoResearch
Anti-rabbit Cy3	Donkey	Jackson ImmunoResearch

3.1.6.2 Antibodies for flowcytometry

3.1.6.2.1 Antibodies for staining of mice immune cells

Antibody	Clone	Origin	Manufacturer
Anti-mouse CD16/32	93	Rat	Biolegend
Anti-mouse MHCII-PE	M5	Rat	eBioscience
Anti-mouse CD11b-PerCP Cy5.5	M1/70	Rat	eBioscience
Anti-mouse F4/80-APC	BM8	Rat	eBioscience
Anti-mouse Ly6G-APC	RB6-8C5	Rat	eBioscience
Anti-mouse CD45-FITC	30-F11	Rat	eBioscience

3.1.6.2.2 Antibodies for staining of canine immune cells

Antibody	Clone	Origin	Manufacturer
Anti-Canine CD45-FITC	YKIX716.13	Rat	eBioscience
Anti-canine CD3-Pacific blue	CD3-12	Rat	Serotec
Anti-canine CD4-APC	YKIX302.9	Rat	eBioscience
Anti-canine CD8a-eFlour710	YCATE55.9	Rat	eBioscience
Anti-canine CD25-PE	P4A10	Mouse	eBioscience
Anti-mouse Foxp3-PECy7	FJK16s	Rat	eBioscience
Anti-canine MHCII-FITC	YKIX334.2	Rat	eBioscience
Anti-canine CD11b	CA16.3E10	Mouse	Serotec
Anti-human CD14-PerCPCy5.5	M5E2	Mouse	BD Bioscience
Anti-canine CD11c-APC	BU15	Mouse	eBioscience
Dog T lymphocyte cocktail	NA	Mix	BD Bioscience
Dog activated T lymphocyte	NA	Mix	BD Bioscience
Anti-mouse IgG-PE	NA	Goat	Abcam

3.1.7 Recombinant vaccinia virus construct

The replication-competent recombinant vaccinia viruses used in this work have been constructed and engineered at the Genelux Corporation facility in San Diego, USA. Vaccinia virus strain LIVP6.1.1 was derived from LIVP (Lister strain, Institute of Viral Preparations, Moscow, Russia), a European vaccine strain (Fig. 3a). GLV-1h68 is a genetically stable oncolytic virus strain designed to locate in, enter, colonize and destroy cancer cells without harming healthy tissues or organs. The GLV-1h68 virus is a derivative of the vaccinia virus Lister strain (LIVP wild type). It was constructed by insertion of three expression cassettes [*Renilla* luciferase-*Aequorea* green fluorescent protein (*Ruc*-GFP), β -galactosidase (*lacZ*) and β -glucuronidase (*gusA*)] into the *F14.5L*, J2R, and *A56R* loci of the viral genome, respectively (Fig. 3b). The gene for the *Ruc*-GFP fusion protein located in the *F14.5L* locus is under control of a synthetic early/late promoter whereas the marker gene β -galactosidase in the TK/J2R locus is under control of the p7.5 promoter. The third genetic insertion, β -glucuronidase was inserted into the *A56R* locus and is under control of the p11 promoter [8].

Another virus used in this work is GLV-1h109, which is a direct derivative of the parental GLV-1h68. GLV-1h109 contains the gene encoding anti-VEGF single-chain antibody under the control of vaccinia synthetic late promoter. The *lacZ* marker gene in the J2R locus of GLV-1h68 was replaced with GLAF-1 in GLV-1h109 (Fig. 3c). Anti-VEGF single-chain antibody GLAF-1, comprising an Igk light chain leader sequence, the V_H chain sequence of the G6 Fab, a $(G_4S)_3$ linker sequence, the V_L chain sequence of the G6 Fab, and a C-terminal DDDDK sequence (Fig. 3d). The GLAF-1 protein has shown to bind both murine and human VEGF with high affinity [72].

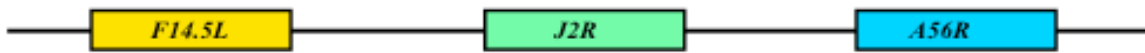


Fig. 3a LVP6.1.1



Fig. 3b GLV-1h68

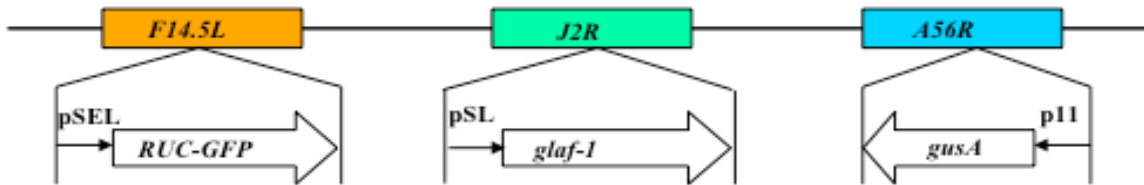


Fig. 3c GLV-1h109

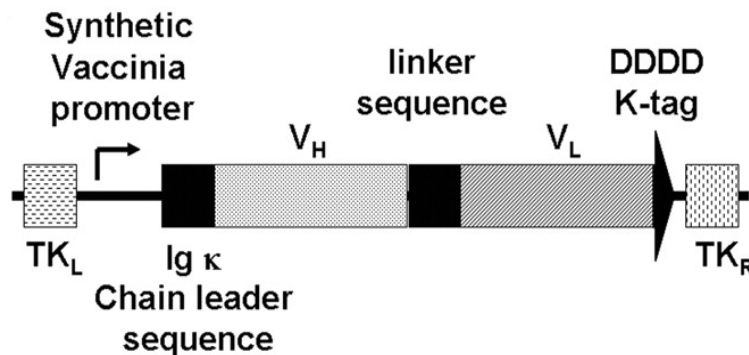


Fig.3d Schematic presentation of GLAF-1

Fig 3. Schematic representation of vaccinia virus constructs and marker genes

The LVP6.1.1 virus strain construct with predominant genes is represented in fig. 3a. The LVP wild type virus strain was used for the generation of modified GLV-1h68 according to Zhang et al. (Fig. 3b) and the GLV-1h68 virus was used for the construction of GLV-1h109 (Fig. 3c). GLAF-1 is a single-chain anti-VEGF antibody with two variable loops joined by linker (Fig. 3d). Abberations: p11: VACV p11 late promoter; pSEL: VACV SEL promoter; pSE, VACV SE promoter; pSL, VACV SL promoter; p7.5, VACV 7.5 K early/late promoter.

3.1.8 Laboratory animals

For *in vivo* experiments, athymic nude FoxN1 mice were used. The animals were purchased from Harlan. The FoxN1 mice are characterized by an autosomal recessive mutation in the *nu* locus on chromosome 11. This leads to a completely hairless phenotype in the mice. Additionally, these animals feature a dysfunctional and rudimentary thymus, which manifests in a T cell deficiency. Due to the defects in the immune system of the mouse, athymic nude FoxN1 mice are well suited as adequate laboratory animals in oncology, immunology and additional fields of biomedical research. Another advantage of this mouse model is that these animals will not reject xenografts. Antibody production is possible in athymic nude FoxN1 mice as well. Animals were kept in a circadian rhythm of twelve hours of day following twelve hours of night. In addition, light intensity was alleviated to account for the albinism of the mice. All the mice experiments were performed in accordance with protocols approved by the Institutional Animal Care and Use Committee (IACUC) of Explora Biolabs (San Diego, CA, USA; protocol number: EB11-025) and/or the government of Unterfranken, Germany (permit number: 55.2- 2531.01-17/08 and 55.2-2531.01-24/12).



Fig.4. Phenotype of an athymic nude FoxN1 mouse (<http://www.harlan.com>)

3.2 Methods

3.2.1 Ethics statement

The institutional review board / animal care and use committee approved the canine clinical trial protocol and all patient owners gave written informed consent to participation and provision of study samples.

3.2.2 Culturing of mammalian cells

CV-1 cells and canine cancer cells (STSA-1 and DT08/40) were cultured in well plates, dishes, or flasks, depending on the purpose. To get enough cells, the stock cells were normally scaled up in 225T flasks (40 ml medium volume). A proper ratio of stock cells was pipetted into a tissue culture flask containing the respective fresh culture medium (Material). Cells were grown in a humidified 5% CO₂ incubator at 37°C. To maintain appropriate growth of those cells, they were closely observed and their medium was changed regularly to ensure that the cells were in a good condition. At 80-90% confluence, cells were washed with PBS and treated with 5 ml EDTA-trypsin. After 5 to 8 minutes (cells should become detached), the flask was shaken to completely detach the cells. Then, 10 ml medium containing Mg²⁺ and Ca²⁺ (growth medium with FBS) was added to stop the EDTA-trypsin reaction. Cells were re-suspended by being pipetted up and down several times to disrupt the cell clumps. Cell counting was performed by using a hemocytometer under an inverted light microscope. The cells were then ready for passage with a designated ratio into suitable plates, dishes, or flasks.

3.2.3 Virological methods

3.2.3.1 Infection of cell cultures

Cancer cells were seeded into the desired well plate format. After 24 h in culture, when cells reached a confluence of 95-100%, cells were infected with recombinant vaccinia virus with the desired multiplicities of infection (MOIs). Cells were incubated for 1 h at 37°C after which the infection medium (2% FBS) was removed and cells were cultured in fresh growth medium.

3.2.3.2 Viral replication assay

For the viral replication assay, different canine cancer cells were infected with VACV strains at an MOI of 0.1. After 1 h incubation at 37°C with gentle agitation every 20

min, the infection medium (2% FBS) was removed and replaced by a fresh growth medium. After 1, 12, 24, 48, 72 and 96 h, the cells and supernatants were harvested. Following three freeze-thaw cycles, serial dilutions of the supernatants and lysates were tittered by standard plaque assays on CV-1 cells. All samples were measured in triplicate.

3.2.3.3 Standard plaque assay

For standard plaque assay, ten-fold serial dilutions of the virus stock were prepared. Confluent CV-1 cells in 24-well plates were infected with 200 μ L in triplicates with the respective virus dilution. Carboxy methylcellulose (CMC) overlay medium was added after 1 h of infection and the CV-1 cells were incubated for 2 days at 37°C. Well plates were then stained with 250 μ L of crystal violet solution per well and incubated for several hours at room temperature. Well plates were then washed, dried, and virus plaques can be counted. Virus titers were calculated using the following formula:

$$\frac{\text{Average plaque forming units (pfu)} \times \text{dilution factor}}{\text{Infection volume}} = \text{pfu / well}$$

3.2.4 Cell viability assay

The amount of viable cells after VACV infection was measured using 2,3-bis [2-methoxy-4-nitro-5-sulfophenyl]-2H-tetrazolium-5-carboxanilide inner salt (XTT) assay. 1×10^4 cells/well were seeded in 96-well plates (Nunc). After 24 h in culture, cells were infected with vaccinia virus strains using multiplicities of infection (MOI) of 0.1 and 1.0. The cells were incubated at 37°C for 1 h, then the infection medium (2% FBS) was removed and subsequently the cells were incubated in fresh growth medium.

Viability of cells was measured using XTT assay kit (Cell Proliferation Kit II, Roche Diagnostics), according to the manufacturer's protocol at 24, 48, 72 or 96 h after virus infection. Quantification of cell viability was performed in an ELISA plate reader (Tecan Sunrise, Tecan Trading AG) at 490 nm with a reference wavelength of 690 nm. The relative number of viable cells was expressed as percent cell viability. Uninfected cells were used as reference and were considered as 100% viable.

3.2.5 Protein analytical methods

3.2.5.1 Protein isolation

3.2.5.1.1 From cultured cells

RIPA lysis buffer supplemented with complete protease inhibitor cocktail was used to isolate total proteins. Cells cultured in 6- or 12-well plates were washed with 1x PBS and a proper amount of lysis buffer (300 μ l of lysis buffer for 10^6 cells) was added. Adherent cells were scraped off the wells using sterile cell scrapers, and then transferred to 1.5 ml microcentrifuge tubes. Membranes from cells were disrupted by 2 cycles of sonication for 1 min at 4°C. Supernatants were collected after 10 min of centrifugation at 10,000 rpm. Protein concentration was determined by DC protein assay kit (Bio-rad) or Bradford protein assay.

3.2.5.1.2 From animal tissue

Tissues were weighted, cut into small pieces and transferred to MagnaBead tubes containing cold RBM lysis buffer supplemented with complete protease inhibitor cocktail (0.8 g tissue in 500 μ l RBM buffer, tumors in 1 ml RBM buffer). Tissues were homogenized using MagNA lyser (Roche Diagnostics) at 6,500 rpm for 30 sec. Sample went through 3 freeze-thaw cycles and 3 rounds of sonification at maximum level for 30 sec at 4°C. The tissue lysates were centrifuged at 10,000 rpm for 10 min at 4°C. Proteins in supernatants were collected, quantified and stored at -80°C.

3.2.5.2 Protein Quantification

A straight calibration line was established using definite amounts of protein (0, 0.2, 0.4, 0.6, 0.8, 1.0 mg/ml bovine plasma gamma globulin) to analyze the amount of total protein in a sample. The BioRad DCTM Protein Assay kit was used and samples were incubated in the dark for 15 min at room temperature. Absorption at a wavelength of 750 nm was measured using a plate reader. A standard curve was established and exact protein amounts of the samples were calculated by plotting the absorbance against the equation of the trend line of the standard curve.

3.2.5.3 SDS-PAGE

SDS-PAGE is used to separate proteins according to their molecular weight. Sodium dodecyl sulfate (SDS) is an anionic detergent that is used to denature proteins by wrapping around the protein backbone by binding to positively charged side chains of amino acids. This process charges the proteins homogenously negative. Protein

separation is based on the molecular weight of the proteins. Generally, bigger proteins need wide meshed gels to quickly migrate during gel electrophoresis and therefore, smaller proteins migrate faster than bigger proteins. Protein samples were prepared with a total protein concentration of 20 µg and heat inactivation and the reducing agent β-mercaptoethanol was used to reduce disulfide bonds within the three-dimensional protein structure prior to Bis-Tris gel loading.

3.2.5.4 Protein transfer by Western blot

During the electrophoretic migration, the negatively charged proteins bind to the membrane through hydrophobic interaction. The secondary and tertiary structure of the polypeptides is partially restored during this process and allows antibody binding to specific epitopes. For protein transfer, a vertical wet blotting chamber was used. The applied amperage is dependent on the size of the polyacrylamide gel and was calculated using the following equation:

$$\text{Amperage [mA]} = \text{gel size [cm}^2\text{]} \times 0.8$$

3.2.5.5 Immunodetection

For immunodetection, blotted proteins are incubated with primary antibodies that bind to epitopes of the protein of interest. Subsequently, the proteins are incubated with a secondary antibody that was raised against the primary antibody. Prior to immunodetection, blots are blocked to avoid unspecific antibody binding. Tween-20 in intermediate wash steps is used as a detergent that separates unspecific bindings. Blots were incubated with the primary antibodies of according dilutions (1:1,000 – 1:10,000) at 4°C overnight, while accordingly diluted secondary antibodies (1:5,000, 1:10,000) were incubated at room temperature for 2 h. The secondary antibody binds to species-specific sites and is horseradish peroxidase- (HRP) labeled. In alkaline conditions HRP acts as a catalyst for the oxidation of luminol to 3-aminophthalic acid. To exhibit its luminescence, luminol must first be activated with an oxidant like hydrogen peroxide (H₂O₂). Oxidation of luminol triggers light emission that can be detected using an X-ray film developer.

3.2.5.6 ELISA

ELISA quantitatively determined the expression of the recombinant GLAF-1 proteins in sera. For the standard curve, 6 two-fold serial dilutions of purified GLAF-1 protein ranging from 625 ng/ml to 19.5 ng/ml were prepared in PBS/2% FBS. Purified GLAF-

1 protein required to obtain the standard curve was produced as described in the section 3.2.5.7. Ninety-six well plates pre-coated with recombinant human VEGF (Sigma) were blocked and incubated with standards or 1:25 dilutions of sera samples in triplicates. Following 1.5 h incubation at room temperature, the wells were washed with PBS/0.05% Tween and incubated with a rabbit anti-DDDDK antibody for 1 h at room temperature. All wells were washed and incubated with a secondary HRP-conjugated anti-rabbit IgG. Color was developed using 3,3',5,5'-tetramethylbenzidine (TMB), and the reaction was stopped with 2N HCl. Absorbance was read in an Infinite 200 Pro Microplate Reader at 450 nm.

3.2.5.7 Purification of GLAF-1 from VACV infected cells

Two flasks of confluent CV-1 cells were infected at an MOI of 1 with GLV-1h109 encoding GLAF-1 under the synthetic late promoter in 15 ml of CV-1 media containing 2% FBS. Two days after infection the virus and GLAF-1 containing medium was filtered (0.2 μm) to remove all viral particles. To concentrate the media from 15 ml to 1 ml, the suspension was loaded on Amicon Ultra-15 columns with a molecular mass cut off of 10 kDa. The samples were centrifuged using a rotating swing bucket 4000 rounds per minute (rpm) for 15 min. Functional GLAF-1 was purified from the concentrate with a FLAG Immunoprecipitation kit which allows immunoprecipitation and elution of an active FLAG-tagged protein. Purified GLAF-1 was analyzed for the correct molecular weight on a Coomassie stained gel and protein concentration was determined using BioRad DCTM Protein Assay kit using a protein standard created from bovine plasma gamma globulin.

3.2.6 Mouse experiments

3.2.6.1 Subcutaneous xenografts

All animal experiments were carried out in accordance with protocols approved by the Institutional Animal Care and Use Committee (IACUC) of Explora Biolabs (San Diego, CA, USA; protocol number: EB11-025) and/or the government of Unterfranken, Germany (permit number: 55.2-2531.01-17/08). Five to six week old male Hsd:athymic Nude-Foxn1nu mice (Harlan) were implanted subcutaneously (s.c.) with 1×10^6 STSA-1 or 5×10^6 DT08/40 (in 100 μl PBS) cells into the right hind leg. Treatment started when tumors reached a volume of 200-300 mm^3 (DT08/40) or STSA-1 600-1000 mm^3 . Recombinant vaccinia virus was administered systemically

by intravenous (i/v) injection into the lateral tail vein of 5×10^6 plaque-forming units (pfu) in 100 μ l PBS at day 0. Control animals were inoculated with 100 μ l PBS only. Tumor growth was measured using a digital caliper and tumor volume was calculated as $0.5 \times \text{length} \times \text{width}^2$ (mm^3). Average tumor volume was plotted against at each time point to monitor therapeutic efficacy. Blood (50-100 μ l) was collected from retro-orbital vein at regular interval for further analysis. Body weight was measured as net body weight ($\text{body weight} - \text{tumor volume}/1000 \text{ mm}^3$) to exclude tumor mass. Mice were sacrificed when the body weight dropped by 20% of their original body weight or the tumor volume exceeded 3000 mm^3 . The experiments were terminated 42 or 49 days post injection (dpi). The significance of the results was calculated by Student's t-test. Results are displayed as means \pm standard deviation (SD). P values of <0.05 were considered significant. Mice were also monitored for change in body weight and signs of toxicity.

3.2.6.2 Anesthesia

Laboratory mice were solely anesthetized using isoflurane, which is a highly volatile anesthetic with hypnotic and muscle-relaxing effects. Mice were put in a knockout box and a mixture of isoflurane and oxygen was administered to the mice. Isoflurane has a very low distribution coefficient and therefore mice react rapidly on increasing or decreasing concentrations.

3.2.6.3 Determination of vaccinia viral titers in tumor tissue and body organ

Tumors and body organs (spleen, kidney, liver, testes, lungs) of virus-treated animals were surgically excised at different time points post inoculation and placed in two volumes of homogenization buffer [50 mM Tris-HCl (pH 7.4), 2 mM EDTA (pH 7.4)] supplemented with Complete Protease Inhibitor Cocktail. Tumors were homogenized using a MagNA Lyser at a speed of 6,000 rpm for 30 sec (three times). After three freeze-thaw cycles, supernatants were collected by centrifugation (6,000 rpm, 5 min, 4°C). Viral titers were measured by standard plaque assay on CV-1 cells.

3.2.6.4 Histological and microscopic analysis of tumors

For histological studies, tumors were surgically excised and snap-frozen in liquid nitrogen, followed by fixation in 4% paraformaldehyde/PBS at pH 7.4 for 16 h at 4°C . After dehydration in 10% and 30% sucrose (Carl Roth) specimens were embedded

in Tissue-Tek® O.C.T. (Sakura Finetek Europe B.V.). Tissue samples were sectioned (10 µm thickness) with the cryostat 2800 Frigocut (Leica Microsystems GmbH). Sections were incubated with 200µl permeabilization buffer (0.2% Triton-X 100, 5% FBS in 1 x PBS), and subsequently with a primary antibody (1:100 to 1:1000 dilution) for overnight at 4°C on shaker. After washing away the unbound primary antibodies, tumor sections were incubated with secondary antibodies for 1 h at RT. Sections were then embedded onto microscope slides with Mowiol 4-88. Endothelial blood vessel cells were stained with a hamster monoclonal anti-CD31 antibody. Anti-Mouse Ly-6G, anti-Mouse F4/80 or rabbit anti-DDDDK antibody were used to stain granulocytes (mainly neutrophils), macrophages or GLAF-1 protein respectively. LIVP6.1.1 was labeled using polyclonal rabbit anti vaccinia virus (anti-VACV) antibody. Cy3- and Cy5-conjugated secondary antibodies (donkey) were obtained from Jackson ImmunoResearch (Pennsylvania, USA). Hoechst 33342 was used to label nuclei in tissue sections. The fluorescence-labeled preparations were examined using the Leica TCS SP2 AOBS confocal laser microscope equipped with argon, helium-neon and UV laser and the LCS 2.16 soft-ware (1024 × 1024 pixel RGB-color images). Digital images were processed with Photoshop 7.0.

3.2.6.5 Measurement of blood vessel density and fluorescence intensity of the CD31 signal in the tumor tissue

Blood vessel density was measured in digital images (100× magnification) of CD31-labelled 10-µm-thick tumor cross-sections using Leica TCS SP2 AOBS confocal laser microscope. Eighteen images per tumor were analyzed per staining (3 tumors per group, 3 sections of each tumor and 6 images per section). Exposure time for individual images was adjusted to ensure clear visibility of all detectable blood vessels and decorated with 8 equidistant horizontal lines using Photoshop 7.0. All blood vessels crossing these lines were counted to obtain the vessel density per section. Fluorescence intensity of the CD31-labelling in 10-µm-thick sections of control tumors and infected and non-infected areas of virus-colonized tumors was measured on digital images (100× magnification) of specimens stained for CD31 immunoreactivity. On the fluorescence microscope, the background fluorescence was set to a barely detectable level by adjusting the gain of the CCD camera before all the images were captured with identical settings. RGB-images were converted into 8-bit gray scale images (intensity range 0–255) using Photoshop 7.0. The

fluorescence intensity of the CD31-labeling represented the average brightness of all vessel related pixels and was measured using Image J software <http://rsbweb.nih.gov/ij>.

3.2.7 Detection of β -glucuronidase in mouse serum

The lyophilized fluorogenic probe FDGlcU (Invitrogen, Karlsruhe, Germany) was dissolved in DMSO (36.5 mM). The collected mouse serum was diluted 1:15 with PBS and 80 μ l of each sample were mixed with 2.5 μ g FDGlcU. After incubation for 1 h at 37°C, fluorescence was read in Lumox 384-well plates (Sarstedt, Nümbrecht, Germany) using an Infinite 200 Pro Microplate Reader (Tecan, Crailsheim, Germany).

3.2.8 Flow cytometric (FACS) analysis

3.2.8.1 Analysis of tumor immune cells from mouse

Single cell suspensions of tumors were prepared at 7 days post virus injection from three untreated and VACV treated mice. Tumors were surgically excised, weighed, and minced into small (1–2 mm³) pieces with a scalpel, and immersed in 10 ml of digestion mixture [5% FBS in RPMI 1640, 0.5 mg/ml collagenase D (Roche), 0.2 mg/ml hyaluronidase, type V (Sigma), and 0.02 mg/ml DNase I (Sigma)] per 0.25 g of tumor tissue. The suspension was incubated with agitation at 37°C for 45 min. The suspension was then filtered sequentially through 70- and 40- μ m cell strainers (BD Falcon) and washed with 5% FBS in RPMI 1640 and resuspended in 2% PBS. Cells were counted and 100,000 cells/test were taken for further staining. To block non-specific staining, single cells were pre-incubated with 0.5 μ g of anti-mouse CD16/32 antibody (clone 93) per one million cells for 20 min on ice. After that, the cells were incubated at 4°C for 15 min in PBS with 2% FBS in the presence of appropriate dilutions of labeled monoclonal antibodies: anti-mouse MHCII-PE (Clone M5 114.15.2), anti-CD11b-PerCPCy5.5 (Clone M1/70), anti-F4/80-APC (Clone BM8), anti-Gr-1-APC (Ly-6G, Clone RB6–8C5). The Anti-Gr-1 mAb (RB6–8C5) has long been used to stain MDSCs and allows the distinction of at least two subsets of granulocytes (Gr-1^{high}CD11b⁺) and monocytic cells (Gr-1^{int}CD11b⁺). Stained cells were subsequently analyzed, using Accuri C6 Cytometer and FACS analysis software CFlow Version 1.0.227.4 (Accuri Cytometers, Inc.).

3.2.8.2 Analysis of peripheral blood mononuclear cells (PBMC) from canine cancer patients

Canine PBMC were prepared by centrifugation of fresh canine peripheral blood over Ficoll-paque plus (Sigma-Aldrich). Initially the plasma was decanted and stored at -70°C for subsequent cytokine assay. PBMC were divided into 1×10^6 aliquots and stored in Recovery cell culture freezing medium freezing and stored in liquid nitrogen until analysis. On the day of staining, PBMC aliquots were thawed at 37°C and washed with 5% RPMI media. For each staining 100,000 cells were taken. For external staining, the cells were washed with FACS buffer (PBS plus 2% PBS) and then stained in combinations of monoclonal antibodies. The following monoclonal antibodies that binds canine immune cell marker were used for staining (plus the appropriate compensation beads): Canine CD45-FITC (clone YKIX716.13), Human CD3-Pacific blue (clone CD3-12), Canine CD4-APC (clone YKIX302.9), Canine CD8a-eFlour710 (clone YCATE55.9), Canine CD25-PE (clone P4A10), Mouse Foxp3-PECy7 (clone FJK16s), Canine MHCII-FITC (clone YKIX334.2), Human CD14-PerCP Cy5.5 (clone M5E2), Canine CD11c-APC (clone BU15), Canine CD11b-PE (clone CA16.3E10), Dog T lymphocyte cocktail (BD Bioscience) and Dog activated T lymphocyte cocktail (BD Bioscience). For internal staining (Foxp3), a Foxp3 / transcription factor staining buffer kit was used. Cells and antibodies were incubated on ice for 30 min and then washed twice in FACS buffer before being re-suspended in 200 μl BD fixative. For controls, compensation beads (OneComp ebeads- eBioscience) were used. Compensation beads were stained with equal concentrations of antibody that was used for staining PBMCs and incubated for 30 min and then washed twice with FACS buffer and re-suspended in 200 μl 2% PBS. The cells were either stored in the dark at 4°C before analysis or analyzed immediately on a Beckman-Coulter EPICS XL flow cytometer.

3.2.9 Statistical analysis

Statistical analysis of data generated from animal experiments was performed with SPSS, version 11 (SPSS, Inc.). To determine significance between two treatment groups a two-tailed unpaired t-test was used (Excel 2007 for Windows).

CHAPTER 4: RESULTS

4.1 Aim 1: Characterization of oncolytic efficacy of LIVP6.1.1 in canine cancers

VCAV-mediated therapy of canine cancer is of a great importance considering its use in veterinary medicine as well as for the development of oncolytic virotherapy for human cancers. In initial experiments, the efficacy of the oncolytic VACV strain LIVP6.1.1 in canine cancer xenografts was evaluated. Establishment of canine soft tissue sarcoma and canine prostate carcinoma xenografts using newly isolated STSA-1 and DT08/40 cell lines respectively in nude mice is described. Furthermore, the infiltration of innate immune cells in LIVP6.1.1-infected canine tumor xenografts is analyzed.

4.1.1 Characterization of LIVP6.1.1 virus in canine cancer cells under cell culture conditions

LIVP6.1.1 was isolated from a wild-type stock of the Lister strain of vaccinia virus (Lister strain, Institute of Viral Preparations, Moscow, Russia) and represents a “native” virus (without genetic manipulations). The replication efficiency and oncolytic potential of LIVP6.1.1 was analyzed in canine soft tissue sarcoma (STSA-1) and canine prostate carcinoma (DT08/40) cells.

4.1.1.1 LIVP6.1.1 virus efficiently replicates in canine cancer cells

The oncolytic potential of OV is dependent on their ability to efficiently infect and replicate in cancer cells. In order to test the efficiency of virus replication, STSA-1 and DT08/40 cells were infected with LIVP6.1.1 at an MOI of 0.1. Standard plaque assays were performed for all samples to determine the viral titers at different time points during the course of infection (Fig. 5). Efficient LIVP6.1.1 viral replication (>100-fold titer increase at 48 or 96 hpi) was observed in both cell lines. The maximum viral titers were observed (5.34×10^6 pfu/well) in STSA-1 at 48 hpi. The highest virus titers in virus infected DT08/40 cells were observed (8.24×10^6 pfu/well) at 96 hpi (Fig. 5). LIVP6.1.1 virus replication efficiency was dependent on the infection time point and tumor type. However, LIVP6.1.1 virus did replicate exponentially in both canine cancer cell lines.

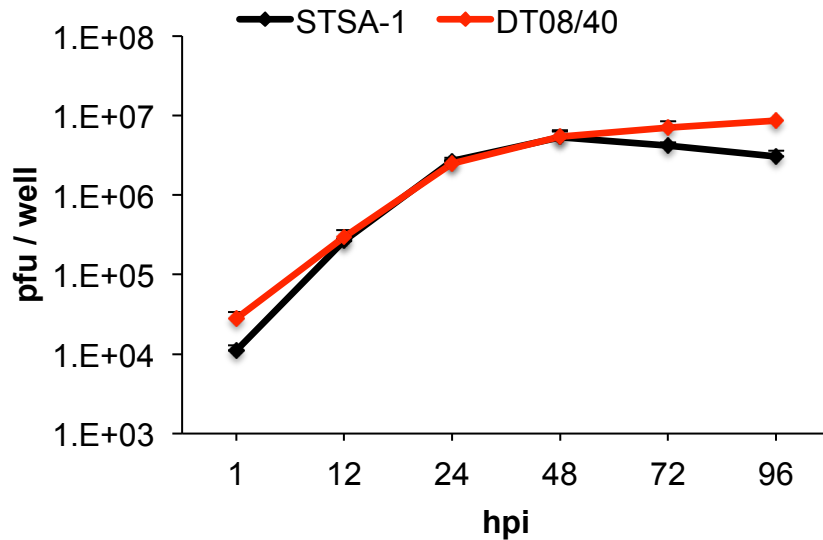


Fig. 5 Replication of LVP6.1.1 in canine cancer cell line

STSA-1 and DT08/40 cells were grown in 24-well plates and infected with LVP6.1.1 at an MOI of 0.01. Supernatant and cells were collected at different time points. Viral titers were determined on CV-1 monolayer by standard plaque assay. Total viral titers (supernatant and cells) are shown here.

4.1.1.2 LVP6.1.1 virus efficiently kills canine cancer cells

An essential feature of oncolytic viruses is their ability to efficiently infect, replicate in and lyse cancer cells. The ability of LVP6.1.1 to lyse cancer cells was analyzed in STSA-1 and DT08/40 cells. The cancer cells were seeded three days prior to infection in 24-well plates and then infected with LVP6.1.1 at MOIs of 1.0 and 0.1. The cell viability was analyzed at 24, 48, 72 and 96 hpi, respectively by XTT assays (Fig. 6). At MOI of 1.0, the LVP6.1.1 virus was highly cytotoxic to STSA-1 (Fig. 6A) resulting in 83% cytotoxicity over 3 days. One day later similar cytotoxicity was observed in DT08/40 cells (Fig. 6B). Thus, LVP6.1.1 virus infection efficiently killed both canine cancer cell types.

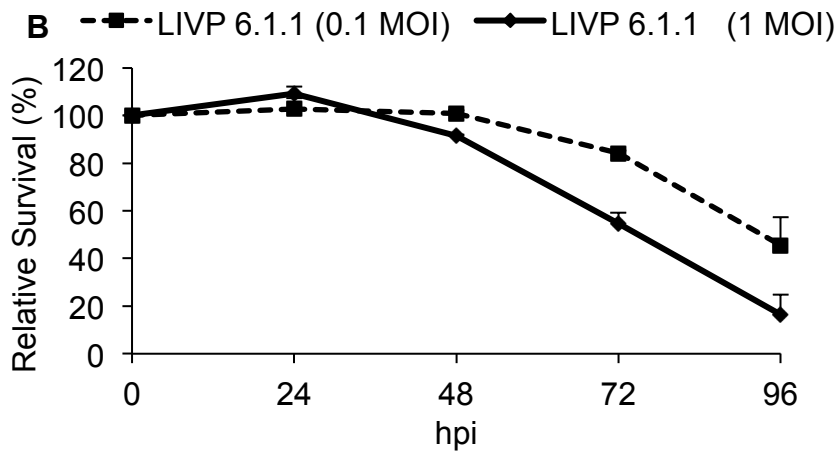
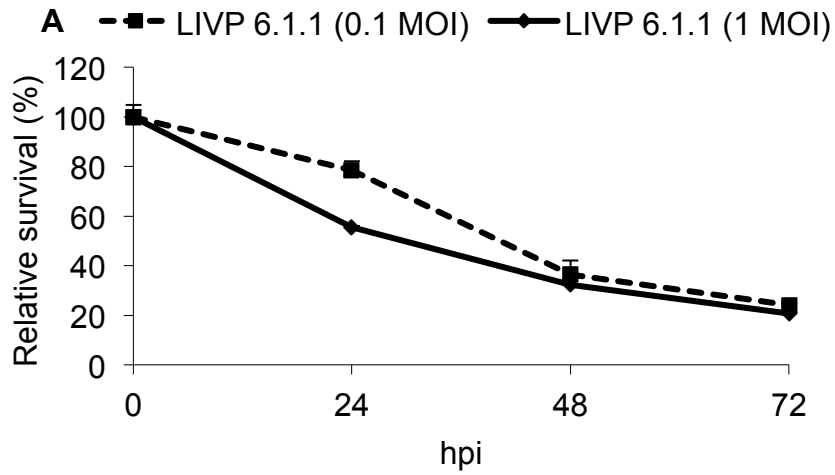


Fig. 6. Viability of soft tissue sarcoma STSA-1 (A) and prostate carcinoma DT08/40 (B) cells after LIVP6.1.1 infection at MOIs of 1.0 and 0.1.

Viable cells after infection with LIVP6.1.1 virus at MOIs of 0.1 and 1.0 were detected using a XTT assay. Mean values and standard deviations (n=3) are shown as percentages of respective controls.

4.1.2 Oncolytic effects of LIVP6.1.1 on canine cancer xenografts in nude mice

After characterization of LIVP6.1.1 in canine cancer cells, the effects of the LIVP6.1.1 virus on growth of tumor xenografts was evaluated. The therapeutic efficacy of LIVP6.1.1 in the soft tissue sarcoma STSA-1 and prostate carcinoma DT08/40 subcutaneous xenograft models was evaluated in nude mice.

4.1.2.1 Therapeutic efficacy and toxicity of LIVP6.1.1 in STSA-1 and DT08/40 xenografts

Tumors were generated by implanting 1×10^6 STSA-1 cells subcutaneously into the right hind leg of 6- to 8-week-old female nude mice (NCI/Hsd/Athymic Nude-Foxn1nu). Five weeks post implantation, all mice developed tumors with volumes of 600 to 1000 mm³. Mice with larger tumors were selected for virus injection since the late stage of the tumor development is more representative of human clinical practice. Animals were separated into two groups (n = 6/ group) and were injected either with a single dose of LIVP6.1.1 (5×10^6 pfu) or PBS intravenously into the lateral tail vein. The single intravenous virus administration led to a significant decrease in STSA-1 tumor growth in all virus-treated mice compared with PBS control mice (Fig. 7A). Due to excessive tumor burden (>3000 mm³), all animals in the control PBS group were euthanized after 14 dpi. The therapeutic effect of LIVP6.1.1 was also evaluated on the progression of the slow growing canine prostate carcinoma DT08/40 tumors in nude mice by measuring the tumor volume at various time points. Data demonstrated again that a single injection with LIVP6.1.1 vaccinia virus led to significant inhibition of the tumor growth (*p <0.05) of all virus-treated mice compared with the control PBS animals on 35, 42 and 49 dpi (Fig. 7B). To monitor the general well being of animals, mice were weighed once a week. The net bodyweight was calculated in exclusion of the tumor mass. A drop in body weight is often indicative of a decrease in health due to viral toxicity, other infections, increasing tumor burden or development of metastases. As can be observed in Fig. 7C and 7D, all LIVP6.1.1-treated mice showed relatively stable mean net body weight over the course of the studies. There were no other signs of virus-mediated toxicity. In summary, treatment with the vaccinia strain LIVP6.1.1 demonstrated anti-tumor activity in canine soft tissue sarcoma and canine prostate xenograft models without signs of virus-mediated toxicity.

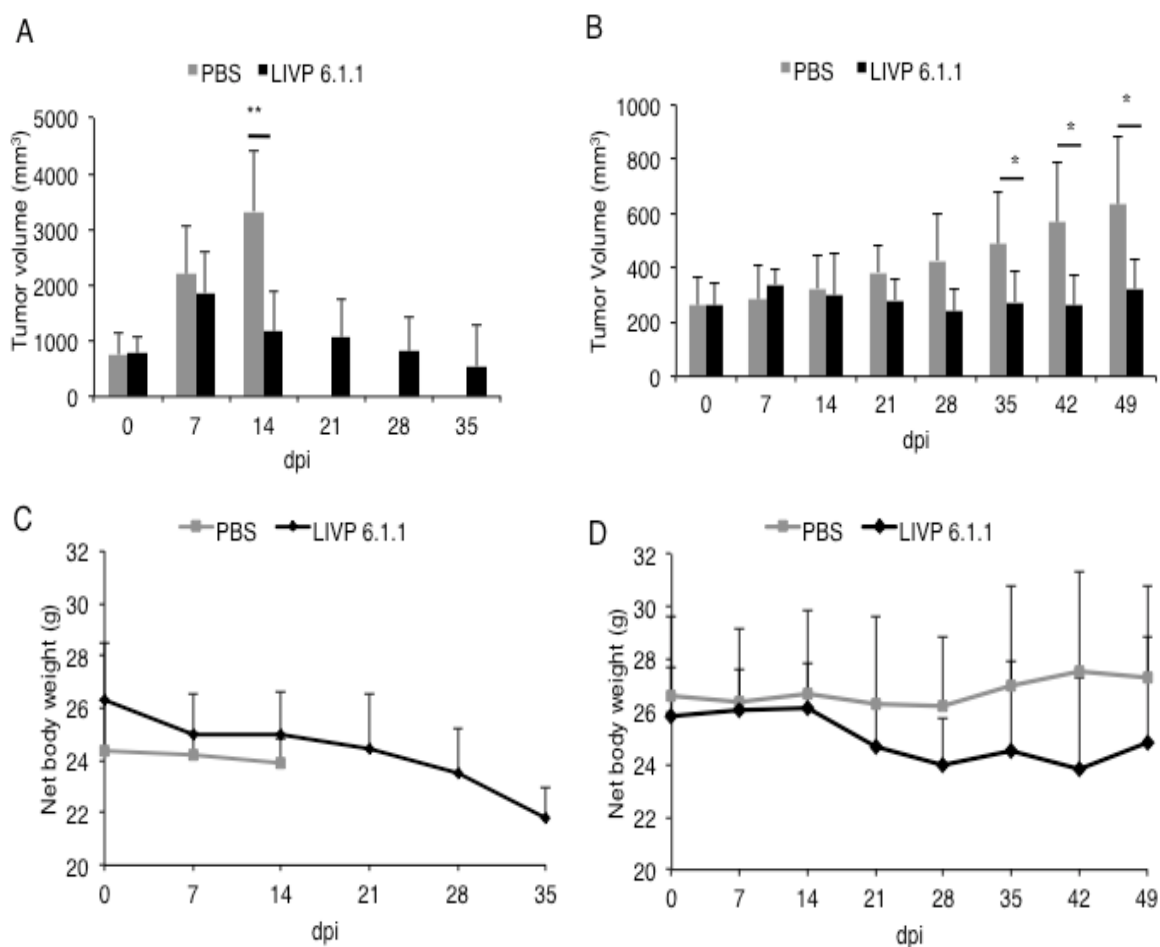


Fig. 7. Effects of intravenous LIVP6.1.1 virus injection on tumor growth (A, B) and the body weight (C, D) of mice with STSA-1 or DT08/40 xenografts

STSA-1 (A, C) and DT08/40 (B, D) tumor-bearing mice (n = 6 per group) were either treated intravenously (i/v) with a single dose of 5×10^6 pfu LIVP6.1.1 or with PBS (control). The statistical significance was confirmed by Student's t-test where * and ** indicate $P < 0.05$ and < 0.01 , respectively.

4.1.2.2 Bio-distribution and persistence of LIVP6.1.1 in STSA-1 tumor-bearing nude mice

The virus distribution and persistence of LIVP6.1.1 in virus-treated mice with STSA-1 xenografts was determined using standard plaque assay. Table 3 summarizes the virus distribution data at 35 dpi. In all virus-treated mice the highest viral titers were observed in the primary tumors. In addition, low numbers of LIVP6.1.1 pfu were also detected in liver, lung, spleen and kidney of the treated animals (Table 3). However, LIVP6.1.1 was highly tumor-selective, as 10^4 – 10^5 fold more virus particles were found in the solid tumors compared to the healthy tissues of the treated animals.

Table 3: Bio-distribution of LIVP6.1.1 in virus-treated STSA-1 xenografts at 35 days post injection (dpi)

pfu/g of tissue	STSA-1 xenografts treated with 5×10^6 pfu LIVP6.1.1				
	Mouse # 301	Mouse # 302	Mouse # 304	Mean 35 dpi	STDEV 35 dpi
Tumor	2.75E+07	3.58E+07	3.76E+07	3.36E+07	5.38E+06
Lung	1.14E+02	4.40E+02	1.42E+02	2.32E+02	1.80E+02
Liver	4.00E+01	5.33E+01	1.00E+02	6.40E+01	3.10E+01
Spleen	7.00E+01	3.33E+01	1.25E+02	7.60E+01	4.60E+01
Kidney	2.50E+02	1.46E+02	1.06E+03	4.85E+02	4.99E+02

The virus titres were determined by standard plaque assays on CV-1 cells using aliquots of the homogenized organs and are presented as mean pfu/g of organ or tissue. For each organ, two aliquots of 0.1 ml were measured in triplicates (estimate of assay sensitivity >10 pfu/organ).

The virus distribution in the primary STSA-1 tumors was also evaluated by immunohistochemical staining at 35 dpi (Fig. 8). Since LIVP6.1.1 does not encode any reporter genes, we analyzed viral spread within STSA-1 xenografts by antibody staining to VACV protein A27L. The staining pattern of VACV protein demonstrated that STSA-1 tumors in all treated mice were significantly infected with vaccinia virus, which led to oncolysis and destruction of tumor tissues.

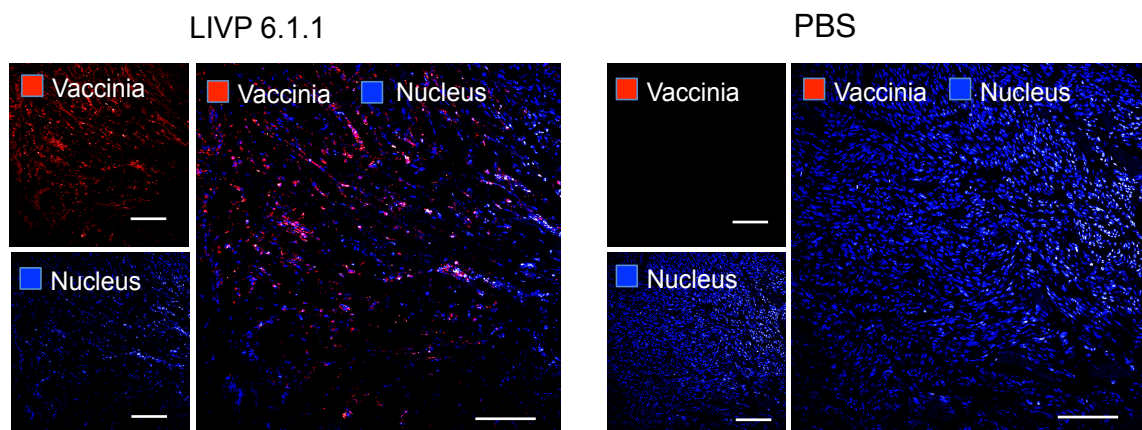


Fig. 8. Immunohistochemical staining of infected and uninfected STSA-1 xenograft tumors at 35 dpi.

Tumor-bearing mice were either mock-treated (PBS) or injected with LIVP6.1.1. Tumor sections were labeled with anti-vaccinia virus antibodies (red). Blue color represented nuclear staining (Scale: 200 μ m)

4.1.2.3 LIVP6.1.1 colonization induces infiltration of innate immune cells in STSA-1 tumor xenografts

To evaluate the role of the host immune system in virus clearance and the involvement in tumor growth inhibition, mice bearing STSA-1 tumors were either treated with a single intravenous injection of LIVP6.1.1 or PBS. Mice were sacrificed 7 days post injection. Single-cell suspensions prepared from tumors were stained for immune cell antigen markers, which were further analyzed by flow cytometry. LIVP6.1.1 infection and colonization significantly increased infiltration of Gr-1^{high}CD11b⁺ (granulocytes), Gr-1^{int}CD11b⁺ (monocyte), F4/80⁺CD45⁺ (macrophages) and MHCII⁺CD45⁺ cells in virus infected tumors compared with PBS-treated tumors (table 4).

Table 4. Percentages of immune cells in STSA-1 xenografts 7 days after LIVP6.1.1 or PBS treatments

Immune cells	PBS / tumor Mean ± SE	LIVP6.1.1 / tumor Mean ± SE	PBS vs LIVP6.1.1 (p value)
CD45 ⁺ MHCII ⁺	0.66% ± 0.23%	2.67% ± 0.35%	** (p=0.002)
CD45 ⁺ F4/80 ⁺	0.77% ± 0.47%	4.61% ± 0.25%	*** (p=0.001)
CD11b ⁺ Gr-1 ^{int}	0.2 % ± 0.08%	3% ± 0.69%	* (p=0.018)
CD11b ⁺ Gr-1 ^{hi}	0.27% ± 0.08%	2.48% ± 0.70%	* (p=0.03)

Immune cells are defined as follows: MHCII⁺CD45⁺ (mainly B cells, macrophages and dendritic cells), F4/80⁺CD45⁺; (macrophages), Gr-1^{high}CD11b⁺ (granulocytes) and Gr-1^{int}CD11b⁺ (monocytes). Experiments were done twice with at least 3 mice per group. The data are presented as % of CD45⁺ cells. The statistical significance was analyzed using two-tailed unpaired Student's test (** P <0.01, **P <0.01 and *P <0.05).

4.2 Aim 2: Effect of inhibition of tumor angiogenesis on modulation of VACV therapy

In initial experiments, oncolytic VACV colonization of tumors and infiltration of innate immune cells was shown to significantly inhibit growth of canine cancer xenografts. However, components of the tumor microenvironment may potentially influence the success of oncolytic virotherapy. Among numerous factors, tumor angiogenesis and tumor immunity appear to be critical in influencing the efficacy of virus-mediated tumor therapy [72]. In the following series of experiments, VACV strain GLV-1h109 encoding a single-chain antibody against VEGF was utilized to augment the anti-tumor effects of virotherapy. VEGF is a potent regulator of tumor angiogenesis and several anti-VEGF antibodies have been developed for the treatment of human and canine tumors [72, 106]. Further, as presented in the previous section, VACV colonization in tumor tissue induced infiltration of innate immune cells. Thus, GLV-1h109 virus was designed to target two important components of the tumor microenvironment i.e. tumor angiogenesis and tumor immunity.

GLV-1h109 was derived from the prototype oncolytic vaccinia virus GLV-1h68 by replacing the *lacZ* gene (β -galactocidase) by the GLAF-1 gene (Fig 3c). GLV-1h68 was derived from L1VP (lister) strain by inserting three expression cassettes (encoding *Renilla* luciferase–*Aequorea* green fluorescent protein, β -galactosidase, and β -glucuronidase) into the *F14.5L*, *J2R* (encoding thymidine kinase) and *A56R* (encoding hemagglutinin) loci of the viral genome, respectively (Fig 3b). GLV-1h68 has been used as a simultaneous diagnostic and therapeutic agent [8]. Likewise, the GLV-1h109 virus retains two of the three marker proteins of GLV-1h68 (*Renilla* luciferase–*Aequorea* green fluorescent protein, GLAF-1 and β -glucuronidase) and the expression of these marker proteins was utilized to monitor virus colonization. A recombinant VACV strain GLV-1h109 was characterized in STSA-1 and DT08/40 canine cancer cells.

4.2.1 GLV-1h109 efficiently replicates in STSA-1 and DT08/40 tumor cells

One of the factors that regulate the oncolytic potential of OVs is their ability to infect and/or efficiently replicate in cancer cells. The replication ability of GLV-1h68 in canine cancer cell lines is well known [42]. However, it was important to find out whether replacing the *lacZ* gene in GLV-1h68 by the GLAF-1 might have affected the infectivity and replication of GLV-1h109 in canine cancer cells. STSA-1 and DT08/40

cells were infected with either GLV-1h109 or GLV-1h68 at an MOI of 0.1. The maximum viral titers were observed at 48 hpi in STSA-1 cells for both GLV-1h68 (2.98×10^6 pfu/well) and GLV-1h109 (3.01×10^6 pfu/well) (Fig. 9A). In addition, GLV-1h68 and GLV-1h109 viruses efficiently infected and replicated in DT08/40 cells with a maximum titer of 1.23×10^6 pfu/well and 1.56×10^6 pfu/well at 72 hpi respectively (Fig. 9B). The maximum titer of GLV-1h109 in STSA-1 cells at 48 hpi was nearly twice the maximum titer of GLV-1h109 in DT08/40 cells at 72 hpi, indicating that GLV-1h109 replicates better and faster in STSA-1 cells (**P = 0.00004; Student's t-test). Overall, the replication efficiency of GLAF-1 encoding VACV strain, GLV-1h109 was similar to that of the parental GLV-1h68 virus in both the canine cancer cell lines.

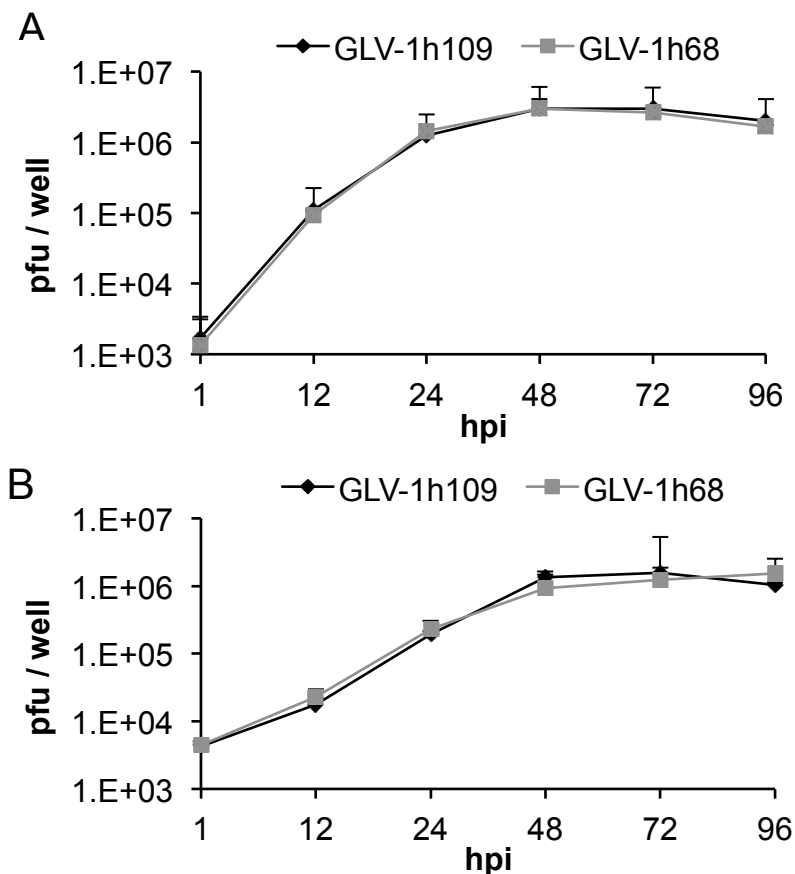


Fig. 9. Comparison of the replication efficiency of the vaccinia virus strains GLV-1h109 and GLV-1h68 in canine cancer cells

STSA-1 (A) or DT08/40 (B) cells grown in 24-well plates were infected with either GLV-1h109 or GLV-1h68 at a MOI of 0.1. Supernatants and cells were collected for the determination of virus titres at various time points. Viral titres expressed as total pfu per well (supernatants and cells) were determined from triplicate measurements by standard plaque assay in CV-1 cells. Averages plus standard deviation are plotted.

4.2.2 GLV-1h109 virus efficiently kills canine cancer cells

It is well known that manipulation of the viral genome as occurs in recombinant viruses reduces their replication efficiency and oncolytic potential. Thus, the characterization of the newly generated oncolytic vaccinia virus strain GLV-1h109 especially in canine cancer cells was of a prime importance. GLV-1h68 was used in comparison. STSA-1 cells were seeded three days prior to infection in 24-well plates and were then infected with either GLV-1h109 or GLV-1h68 at MOIs of 1.0 or 0.1. Cell viability was analyzed at 24, 48, 72 and 96 hpi respectively, by XTT-assays (Fig 10A). Ninety-six hours after GLV-1h109-infection, only 17.8% and 17.5% STSA-1 cells survived the treatment at MOIs of 0.1 and 1.0, respectively. At the same time point and MOIs, 18.6% and 18.2% of STSA-1 cells remained viable after GLV-1h68 infection.

The oncolytic potential of GLV-1h109 was also compared to GLV-1h68 in DT08/40 cells (Fig. 10B). In these experiments, GLV-1h109 and GLV-1h68 virus infections resulted in similar oncolytic efficacy at 96 hpi and at MOIs of 0.1 and 1.0. Thus, GLV-1h109 showed a similar oncolytic potential to that of parental virus GLV-1h68 in both canine cancer cell lines, however, the rate of oncolysis was greater in STSA-1 cells than in DT08/40 cells.

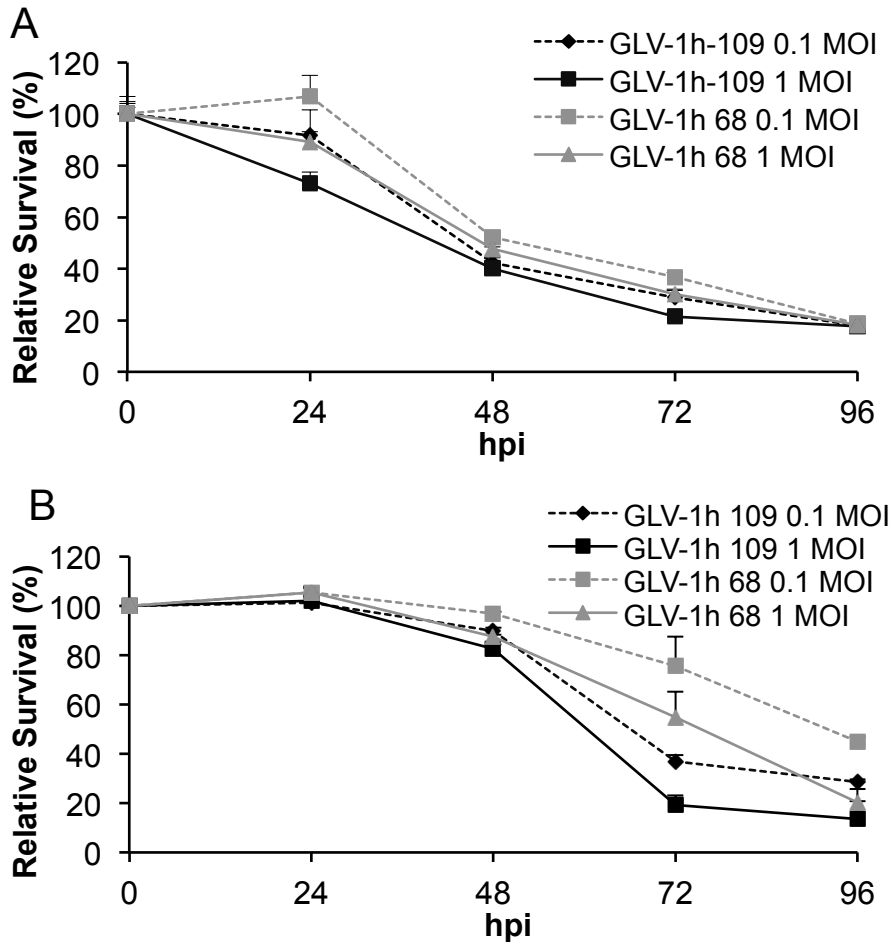


Fig. 10. Viability of canine soft tissue sarcoma (STSA-1) (A) and prostate carcinoma (DT08/40) (B) cells after GLV-1h109 or GLV-1h68 infection.

Viable cells after infection with each virus was detected using a XTT assay. Mean values and standard deviations (n=3) are shown as percentages of respective controls. The data from one of the three independent experiments is presented here. There were no significant differences between groups at 72 and 96 hpi (P >0.05).

4.2.3 GLV-1h109 expresses encoded marker proteins in canine cancer cells

Expression of anti-VEGF single chain antibody GLAF-1 and β -glucuronidase (*GusA*) proteins in GLV-1h109-infected STSA-1 or DT08/40 cells could be used as important indicators in the diagnosis and treatment of canine cancers. For this purpose, 10^6 STSA-1 or DT08/40 cells were infected either with GLV-1h109 or GLV-1h68 (control) at an MOI of 1.0 in 6-well plates. Supernatants and lysates were harvested at 24, 48 and 72 hpi respectively, and analyzed by Western blot using anti-GLAF-1, anti-*GusA* and anti- β -actin antibodies. The β -actin was used as a loading control.

Expression of these marker proteins in virus-infected STSA-1 cells is shown in Figure 8. GLAF-1 protein of expected size (30 kDa) was detected in both lysates and

supernatants of GLV-1h109-infected STSA-1 cells (Fig 11A). Similar expression of GLAF-1 protein was detected in GLV-1h109 infected DT08/40 (Figure 11B). No protein of similar size was detected in GLV-1h68 infected or uninfected cells of both cancer types. Additionally, *GusA* was detected in the cells infected with the GLV-1h68 as well as GLV-1h109.

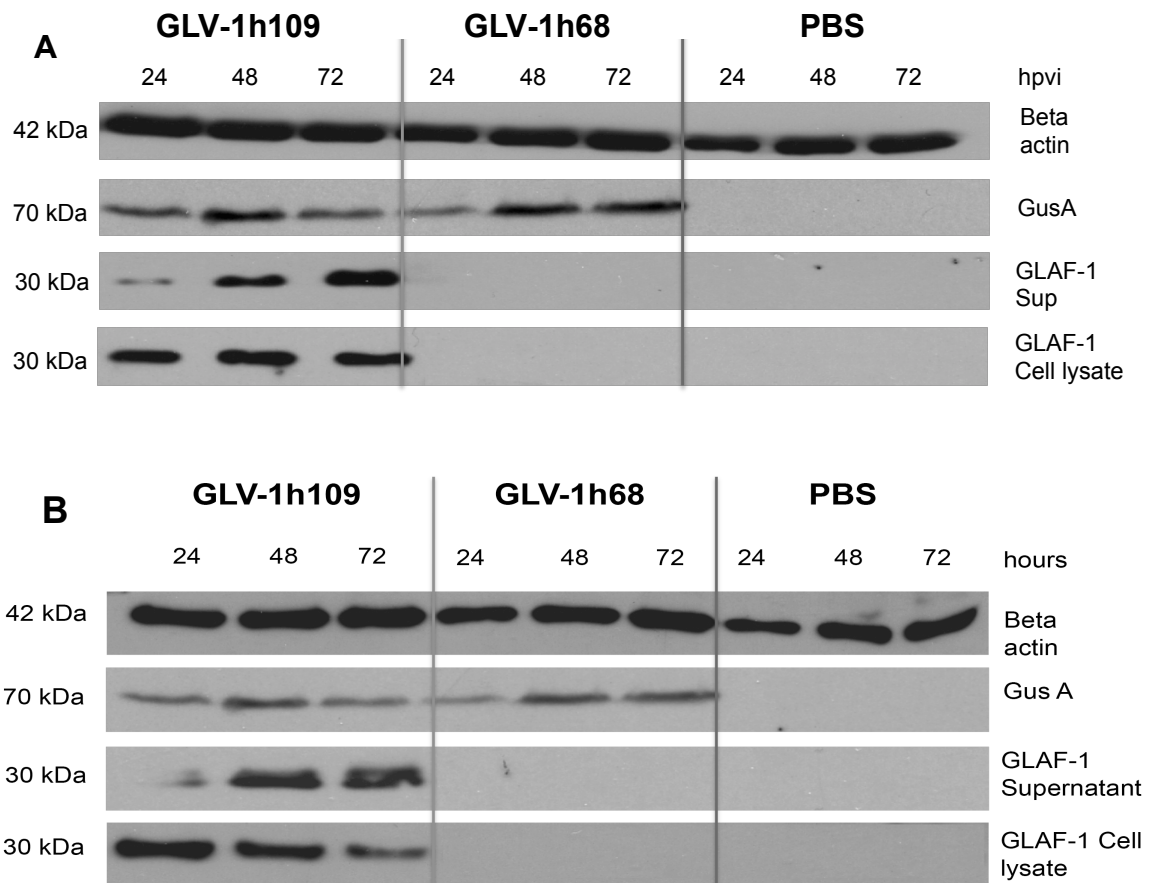


Fig. 11. Expression of virus encoded proteins GLAF-1 and *GusA* in canine cancer cells

Western blot analysis of STSA-1 (A) and DT08/40 (B) cells infected with either GLV-1h109, GLV1h 68 virus at an MOI of 1 or PBS. Protein fractions from cell lysate and culture supernatant were isolated at different time points and analyzed by Western blot.

4.2.4 The GLAF-1 antibody specifically recognizes canine VEGF

GLV-1h109 significantly enhanced the therapeutic efficacy and inhibited tumor angiogenesis in human tumor xenografts as compared to the parental virus, GLV-1h68 [72]. GLAF-1 was directed against human and murine VEGF and showed

efficient binding affinity with VEGF from both the species [72]. However, the use of GLV-1h109 for canine cancer therapy and effects of GLAF-1 on canine tumor angiogenesis was only possible, provided GLAF-1 binds to canine VEGF. Thus, the ability of purified GLAF-1 antibody to bind recombinant canine VEGF (R&D System, Minneapolis, MN, USA) was tested by standard ELISA. Binding affinity of GLAF-1 with human VEGF was taken as positive control and relative binding with canine VEGF was plotted. As seen in Fig. 12, GLAF-1 was functional and recognized both canine and human VEGF with substantial comparability.

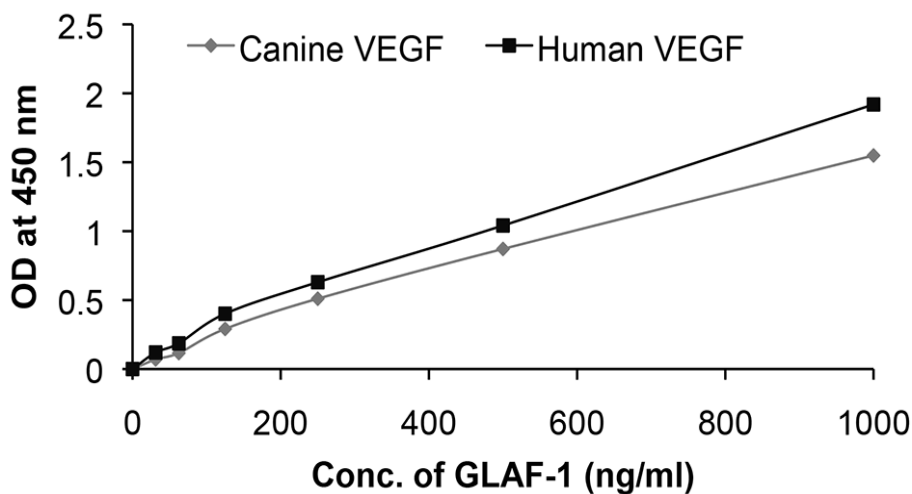


Fig. 12. Interaction of purified GLAF-1 antibody with human and dog VEGF

ELISA demonstrated affinity and cross reactivity of GLAF-1 to canine VEGF. ELISA was repeated three times in an independent experiment. The data presented is from one experiment.

4.2.5 Canine cancer cells express VEGF under cell culture conditions

VEGF is a potent mediator of both angiogenesis and vasculogenesis in dogs and has been proposed as a prognostic indicator in several types of canine cancers [107, 108]. As GLV-1h109 encodes anti-VEGF single-chain antibody, the level of VEGF expression by canine cancer cells might affect oncolytic efficiency of GLV-1h109. Therefore, we analyzed the level of VEGF expression from the two tested canine cancer cell lines under cell culture conditions (Fig. 13). Canine VEGF concentrations were determined using a Quantikine ELISA kit (R&D Systems, Minneapolis, MN, USA) developed for detection of canine VEGF, in accordance with the manufacturer's directions. STSA-1 and DT08/40 cells were plated in six-well culture plate and supernatants were collected at 24 and 48h respectively. Concentration of

VEGF in supernatant was represented as pg/10⁶ cells. As seen in Fig 13, mean VEGF levels in the supernatant of STSA-1 cells were 1556.9 pg/10⁶ cells (24h) and 2962.2 pg/10⁶ cells (48h), while that of DT08/40 cells were 170.8 pg/10⁶ cells (24h) and 183.3 pg/10⁶ cells (48h). STSA-1 cells produced about 9- to 16-fold more canine VEGF compared to the DT08/40 cells at the two different time points, respectively.

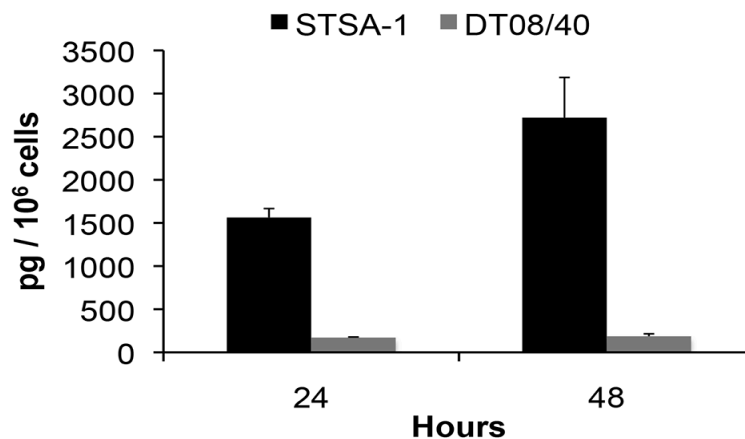


Fig. 13. VEGF expression in STSA-1 and DT08/40 canine cancer cells in cell culture

VEGF levels in STSA-1 and DT08/40 cell supernatants were determined by canine VEGF Quantikine ELISA kit (R&D Systems, Minneapolis, MN, USA). Each value represents the mean + standard deviation (SD) (n=3).

4.2.6 Systemic administration of GLV-1h109 virus significantly regresses growth of STSA-1 and DT08/40 derived tumors in nude mice

After characterization of GLV-1h109 in cell culture conditions, it was important to analyze the effect of virus treatment on tumor growth. Therefore, to test efficacy of GLV-1h109 in canine cancer xenografts, female nude mice (n=6/group) at an age of 6–8 weeks were implanted subcutaneously with 1x10⁶ STSA-1 cells. Four weeks post-implantation, all mice developed tumors with volumes of 600 to 1000 mm³. Animals were separated into two groups (n=6) and were injected with a single dose of GLV-1h109 (5x10⁶ pfu) or PBS (100µl) into the tail vein. The virus treatment resulted in a significant tumor regression in all GLV-1h109 treated mice (Fig. 14A). In contrast, due to excessive tumor burden (>3000 mm³), all animals of the PBS control group were euthanized after 14 dpi. The therapeutic effect of GLV-1h109 was also evaluated in canine prostate carcinoma DT08/40 tumor xenografts in nude mice. Tumors were generated by implanting 5 x 10⁶ canine prostate carcinoma cells subcutaneously into the right hind leg of 6- to 8-week-old nude mice. When tumors reached to an average volume of 200-300mm³, groups of mice (n = 6/group) were

injected (i/v) either with 5×10^6 pfu of GLV-1h109 virus or PBS (control). Tumor volume was measured subsequently after every 7 days. Data demonstrated that a single injection with GLV-1h109 vaccinia virus led to significant inhibition of the tumor growth (*p <0.05) of all virus-treated mice compared to PBS treated mice (Fig. 14B). Statistical significance between untreated mice and GLV-1h109-treated mice was first observed after 35 days. Finally, the toxicity of the GLV-1h109 virus was determined by monitoring the relative net body weight change of mice over time (Fig. 14C, D). All GLV-1h109-treated mice showed stable mean body weight over the course of the study. There were no signs of virus-mediated toxicity.

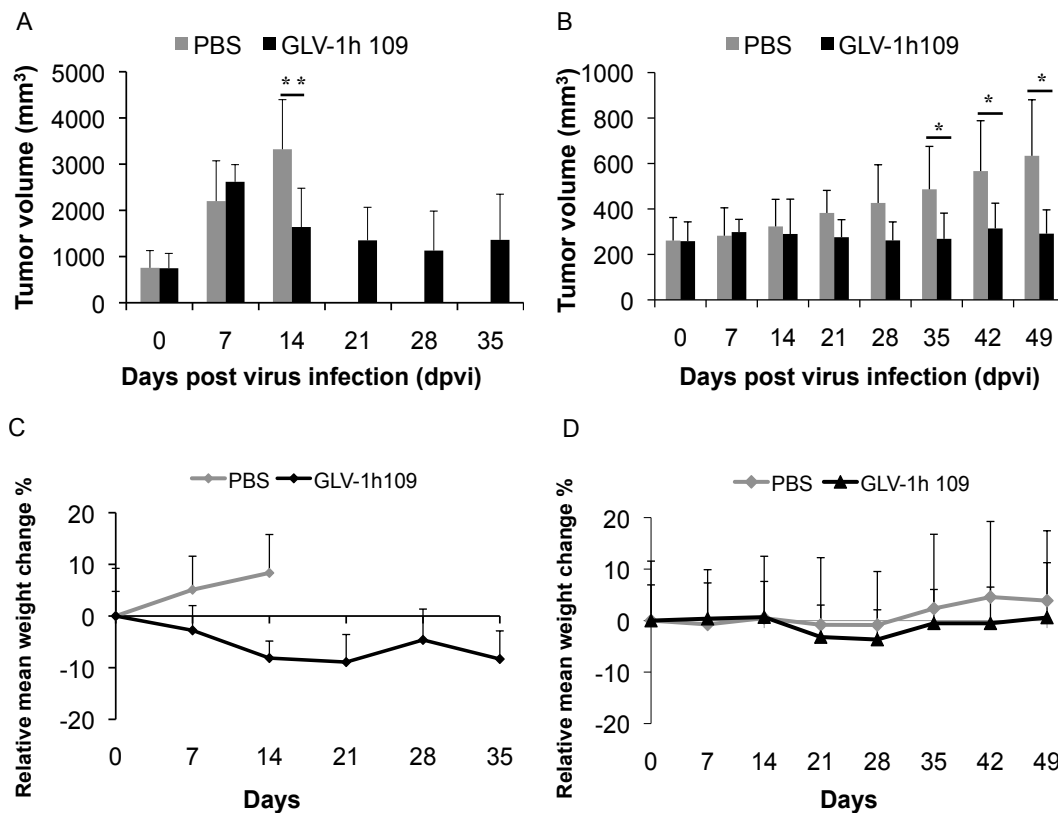


Fig. 14. Effects of systemic GLV-1h109 virus injection on tumor growth (A, B) and the body weights (C, D) of mice with STSA-1 or DT08/40 xenografts
 STSA-1 tumor-bearing mice (n = 6) (A, C) and DT08/40 tumor bearing mice (n = 6) (B, D) were either treated with a single dose of 5×10^6 pfu GLV-1h109 intravenously (i/v) or with PBS (negative control). Tumor growth and relative net body weight was monitored subsequently. The statistical significance was determined by Student's t-test where * and ** indicate P <0.05 and <0.01, respectively.

4.2.7 Bio-distribution of the virus and presence of GLAF-1 in tumor-bearing nude mice

The GLV-1h109 distribution in STSA-1 and DT08/40 xenografts was analyzed at the last time points after virus treatment. Table 5 summarizes the virus distribution data in both xenograft models. The highest viral titers were identified in the primary tumors of virus-treated mice (table 5).

Table 5: Bio-distribution of GLV-1h109 in DT08/40 and STSA-1 xenografts at 49 or 35 days post virus injection (dpi), respectively.

pfu / g	DT08/40 xenografts			STSA-1 xenografts		
Mouse	424 /	429 /	433/	329/	343/	335/
# / dpi	49 dpi	49 dpi	49 dpi	35 dpi	35 dpi	35 dpi
Tumor	2.7E+02	4.5E+03	1.3E+04	1.9E+07	4.9E+07	2.7E+07
Liver	n.d	n.d	n.d	5.4E+01	1.2E+02	4.9E+01
Lung	n.d	n.d	n.d	2.7E+02	9.6E+01	1.1E+02
Heart	n.d	n.d	n.d	n.d	n.d	n.d
Kidney	n.d	n.d	n.d	5.6E+01	n.d	n.d
Spleen	n.d	n.d	n.d	4.7E+01	7.2E+01	3.5E+01

The virus titres were determined by standard plaque assays on CV-1 cells using aliquots of the homogenized organs and were displayed as mean pfu/g of organ or tissue. For each organ, two aliquots of 0.1 ml were measured in triplicates. n. d.: not detected (estimate of assay sensitivity >10 pfu/organ).

Interestingly, the mean GLV-1h109 titers in primary solid tumors of STSA-1 xenografts at 35 dpi were about 10^4 fold higher than that of DT08/40 xenografts at 49 dpi. In addition, we observed the presence of plaque forming units in some organs of virus-injected STSA-1 mice, but not in the virus-treated DT08/40 xenografts. However, the numbers of GLV-1h109 virus particles in the healthy tissues were substantially reduced; e.g. in whole organs: livers (mean weight 1.2 g) about 89 pfu; lungs (mean weight 0.142 g) about 19 pfu and spleens (mean weight 0.2 g) about 10 pfu at 35 dpi (Table 5, here the pfu were given per gram of organ). In contrast, we found about 10^4 – 10^5 fold more GLV-1h109 pfu in solid tumors at this time point, which clearly shows that GLV-1h109 virus displays an enhanced tumor specific replication.

4.2.8 Use of GLV-1h109 as a diagnostic tool for canine cancers

GLV-1h109 expressed *Renilla-luciferase* GFP and β -glucuronidase when replicated in human tumor tissue [72]. GFP protein expressed by recombinant VACV strains enabled non-invasive optical imaging as well as allowed to monitor virus colonization in tumor tissue [8, 79]. In addition, we have recently shown that the detection of virus encoded β -glucuronidase (*GusA*) in the serum could be used to evaluate tumor colonization and/or transgene expression of oncolytic vaccinia virus in tumor-bearing mice [109]. Furthermore, GLV-1h109 was encoded with single-chain antibody GLAF-1 that was regulated by secretory promoter. Therefore, in this study we tested the presence and persistence of the *GusA* marker protein in combination with the GLAF-1 antibody. As seen in Fig. 15, the level of *GusA* marker protein was increased initially on day 7 (STSA-1) and day 21 (DT08/40) after virus injection. However, the level decreased over time. The maximum level of GLAF-1 in the serum of GLV-1h109-injected mice with STSA-1 xenografts was about nine-fold higher than in corresponding DT08/40 xenografts at 7 dpi. Interestingly, the maximal GLAF-1 protein in serum occurred a week earlier than the maximal *GusA*-signal in both the xenograft models (Fig. 15A, B).

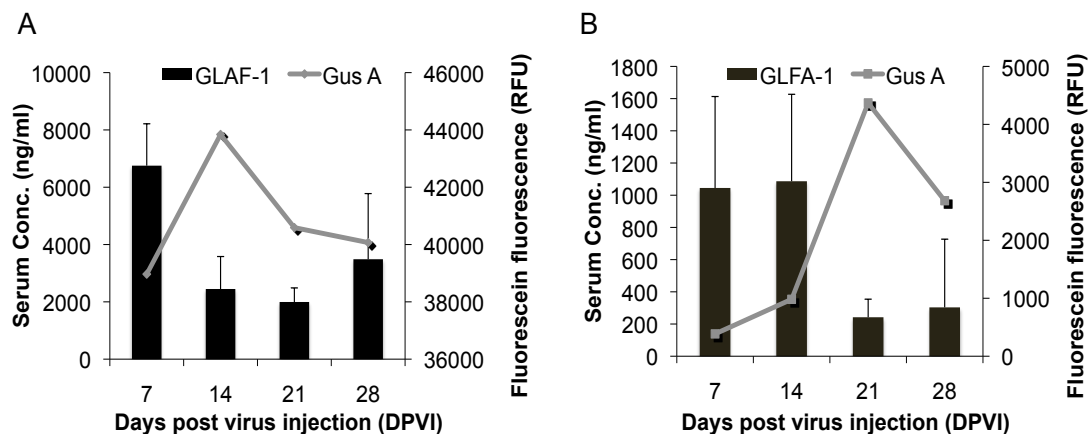


Fig. 15. Presence and persistence of GLAF-1 and *GusA* in serum of GLV-1h109-injected mice with tumor xenografts

A, B: Blood samples were collected at day 7, 14, 21 and 28 respectively from (A) STSA-1 and (B) DT08/40 tumor bearing mice (n = 6). Expression of GLAF-1 in sera was quantitatively determined using ELISA. GLAF-1 values shown (bars) are mean + SD. *GusA* activity (represented by lines) was measured by detecting the activation of the fluorogenic compound FDGlcU.

The different kinetics could be due to the fact that virus-infected cancer cells secrete GLAF-1 while *GusA* is only released to the blood stream via cell lysis. The results

demonstrated that analysis of GLAF-1 in the serum could also be used as a pharmacokinetic marker for virus colonization and persistence of GLV-1h109-tumor injection and virus activity.

4.2.9 GLV-1h109 replication resulted in GLAF-1 protein expression in tumor

In previous section (4.2.8), it was demonstrated that anti-VEGF single-chain antibody GLAF-1 was secreted into the circulatory system of tumor bearing mice injected with GLV-1h109. However, the expression of GLAF-1 protein in the tumor tissue may be crucial to inhibit tumor angiogenesis. Therefore, the expression of GLAF-1 in GLV-1h109, GLV-1h68 and PBS treated STSA-1 tumor sections was analyzed. The tumors were harvested at an early time point, 7 days after virus treatment. As the GLAF-1 protein had the DDDDK tag, tumor sections were stained with anti-DDDDK antibody. As seen in Fig. 16A, GLV-1h109-treated tumor sections showed expression of the GLAF-1 protein. GLV-1h68 and PBS-treated tumor sections did not stain for the GLAF-1 protein. Additionally, the presence of GLAF-1 protein was also analyzed in tumor tissue of STSA-1 and DT08/40 xenografts on day 35 and 49, respectively. GLAF-1 protein of approximately 30 kDa was detected by Western blot (Fig. 16B).

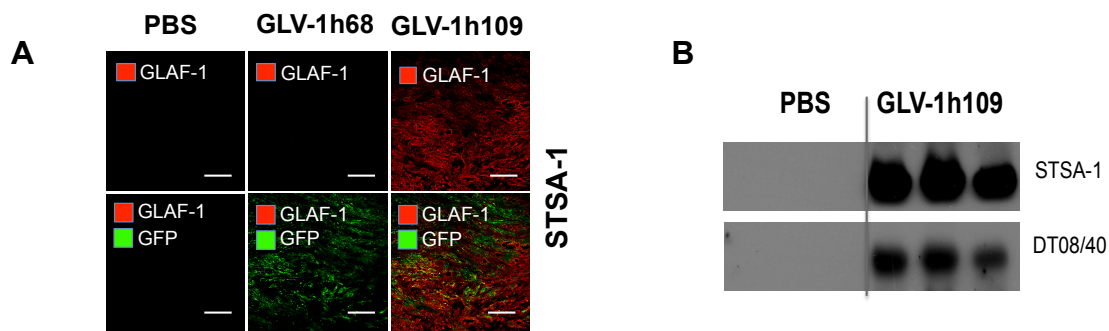


Fig 16. Expression of GLAF-1 in GLV-1h109-infected tumor tissue

A: Localization of GLAF-1 protein in virus-infected STSA-1 tumors. Overlays represent the virus infection GFP fluorescence (green) and the presence of GLAF-1 (red). Scale bars, 500 μ m. (200 \times magnification).

B: STSA-1 and DT08/40 tumor-bearing mice injected with GLV-1h109 and PBS were sacrificed on day 35 and day 49, respectively (end point of study). Tumors were collected, and proteins from tumor lysate were separated by SDS/PAGE. Western blot analysis was performed using anti-DDDK antibody.

Thus expression of GLAF-1 protein in tumor tissue was detected both at the initial stage as well as at the late stage of the tumor treatment.

4.2.10 GLV-1h109 colonization in tumor xenografts significantly inhibited development of tumor vasculature

Previously we have seen that STSA-1 cells express 9-16 times more VEGF than DT08/40 cells as well as expression of GLAF-1 was higher in STSA-1 xenografts than DT08/40 xenografts. In addition, an anti-VEGF strategy was successfully evaluated in dogs with canine soft tissue sarcomas [110]. Considering all these factors, the effects of GLV-1h109 on tumor vasculature and tumor microenvironment were tested in the STSA-1 xenograft model. The possible anti-VEGF effect of the GLAF-1 antibody on tumor angiogenesis and vasculogenesis was analyzed using the CD31 staining to visualize the vascular network in tissue sections of GLV-1h109, GLV-1h68 (VACV not encoding anti-VEGF antibody) and PBS-treated STSA-1 tumors by fluorescence microscopy. CD31-labeled cross-sections of tumors from PBS-, GLV-1h68- and GLV-1h109-treated mice were used for determination of the vascular density at the day 7 after treatment (Fig. 17). The vascular density of GLV-1h109-infected tumors was significantly decreased compared to GLV-1h68- and PBS- injected control tumors (GLV-1h109 vs GLV-1h68 ***P <0.0001; GLV-1h109 vs. PBS ***P <0.0003) (Fig. 17A, B). Interestingly, a significant reduction of the vascular density was observed in areas positive for virus infection detected by colonization of GFP fluorescence (Fig. 17A, B; inf+). However, the reduction in vascular density was not seen in the corresponding GFP negative areas of tumor sections (Fig. 17C; inf-), indicating that the reduction in vascular density is mediated not only by the expression of GLAF-1, but also by virus colonization in tumors. The vascular density between infected (inf+) areas of the GLV-1h109 tumor was also significantly lower than in non-infected (inf-) areas. [inf+ GLV-1h109 (Fig. 17B) vs. inf- GLV-1h109 (Fig. 14C); ***P < 0.0006].

In addition, the fluorescence intensity of the CD31 signal was measured in immunohistochemically stained (inf+) sections of STSA-1 tumors (Fig. 17D). The fluorescence intensity (blood vessel-related pixels) of GLV-1h109 virus-infected tumors was significantly decreased compared to GLV-1h68 or PBS-injected control tumors (GLV-1h109 vs. PBS **P=0.0051; GLV-1h109 vs. GLV-1h68 ***P=0.00001). This means that only the GLV-1h68 virus colonization up-regulated expression of the CD31 protein. The significant decrease of fluorescence intensity in GLV-1h109-infected tumors might be due to the reduction in the vascular density. Therefore, this study clearly demonstrated that the virus colonization and expression of GLAF-1 led

to a local inhibition of tumor angiogenesis in the GLV-1h109 virus-infected tumor tissue.

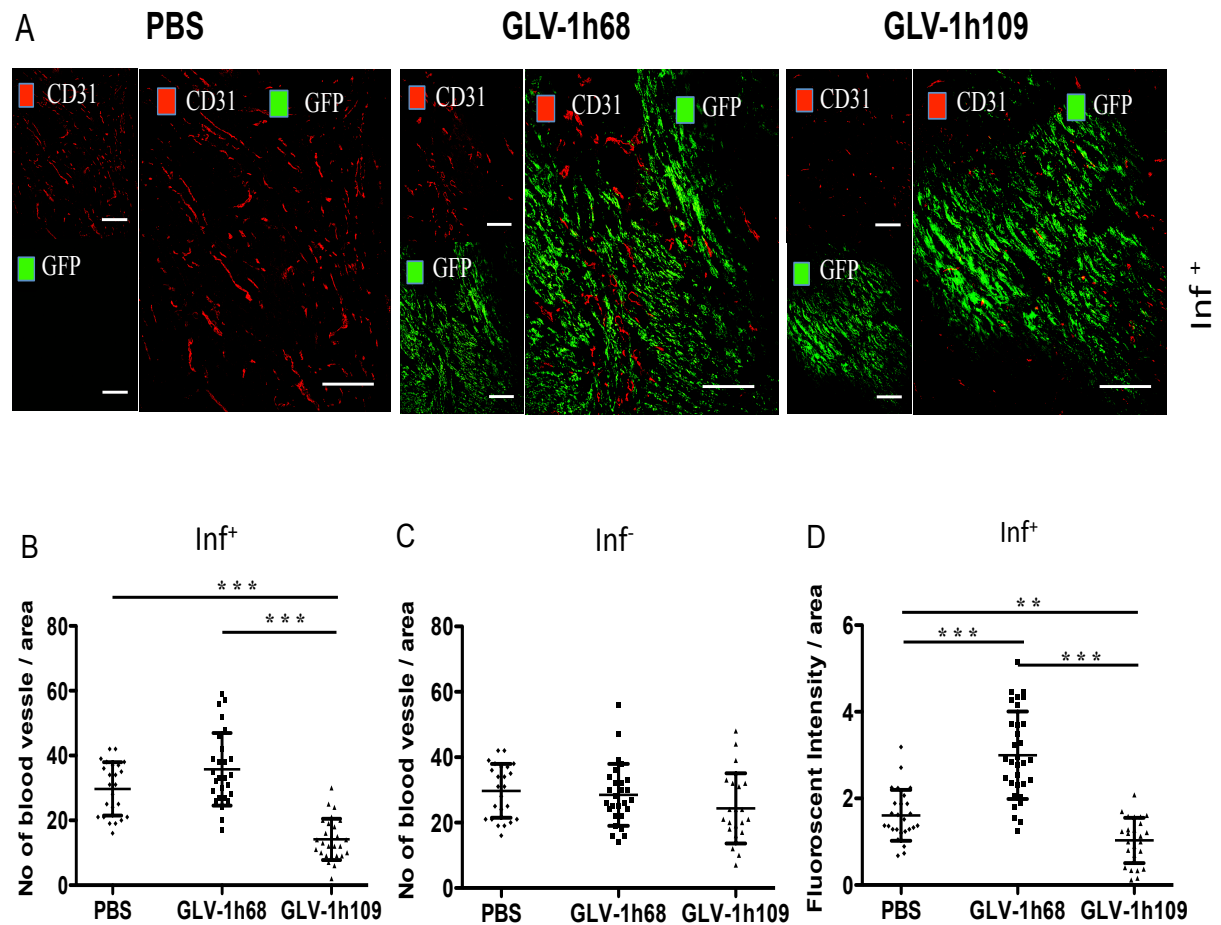


Fig. 17. Vascular densities in virus-treated (GLV-1h68 or GLV-1h109) and non-treated (PBS) tumors at 7 dpi

A-C: Blood vessel density in virus-infected (A, B; inf^+) and virus non-infected (C; inf^-) STSA-1 tumor areas

The vascular density was measured in CD31-labeled tumor cross-sections (n=3 mice per group, 18 images per mice) and presented as mean values +/- SD. (***) P < 0.001, (**P < 0.01, Student's t-test)

D: Fluorescence intensity of the CD31 signal in virus-infected (inf^+) STSA-1 tumor areas

The fluorescence intensity of the CD31-labeling represented the average brightness of all vessel-related pixels (VRP). The fluorescence signal representing the amount of CD31 expression in the blood vessels was measured in 18 images of each tumor (n = 3 mice per group). Mean values are shown as mean +/- SD. (***) P < 0.001, (**P < 0.01, Student's t-test).

4.2.11 Anti-angiogenesis therapy improved virus replication and distribution in STSA-1 tumor xenografts

In initial cell culture experiments, GLV-1h109 and its prototype virus GLV-1h68 had similar replication efficiency in STSA-1 cells. Additionally, anti-VEGF encoding virus significantly inhibited tumor angiogenesis. Recently, R. Jain *et al.* demonstrated that inhibition of tumor angiogenesis improved drug delivery to the tumor tissue [111]. Thus, whether inhibition of angiogenesis increased the replication and spread of this oncolytic VACV in STSA-1 xenografts was examined. As stated earlier, GLV-1h68 and GLV-1h109 encode a *Renilla* luciferase-GFP fusion protein enabling the visualization of viral colonization in tumors. Viral GFP expression in GLV-1h109-treated tumors was monitored by FACS analysis. In this experiment, three tumors from each treatment group were excised, single cell suspensions were prepared and cells were analyzed for GFP-positive signals by flow cytometry. As expected, STSA-1 xenografts from PBS control mice did not show GFP-positive signals (Fig. 18). However, GLV-1h109-infected tumors showed significantly increased number of GFP positive cells ($14.27 \pm 1.8\%$) compared to GLV-1h68 infected tumors ($8.67\% \pm 2.4\%$) (GLV-1h109 vs GLV-1h68 *P=0.036).

The number of infectious viral particles in STSA-1 tumor xenografts was then determined. Tumor-bearing mice were sacrificed at day 7 after GLV-1h68 or GLV-1h109 injection. Tumors were harvested, homogenized and analyzed for virus content with standard plaque assay. STSA-1 tumor xenografts injected with GLV-1h68 had a mean of 1.55×10^7 pfu/g tumor and GLV-1h109 infected STSA-1 xenografts had a mean of 3.17×10^7 pfu/g tumor. GLV-1h109 infection yielded a statistically significant (2 fold) increase in infectious viral particle compared to GLV-1h68 (p=0.024) (Fig. 18)

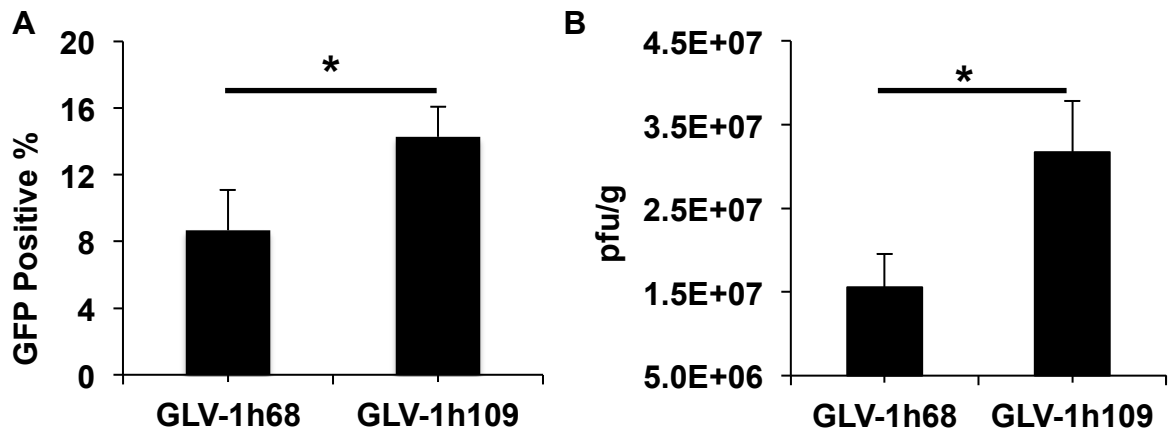


Fig. 18 Replication and distribution of virus in STSA-1 tumor xenografts

- A:** GFP-positive cells from STSA-1 tumor xenografts infected with VACV strains. GFP-positive cells were examined by FACS analysis and displayed as mean + SD (n=3).
- B:** Virus titres from STSA-1 tumor xenografts infected with VACV strains. The virus titres were determined by standard plaque assays on CV-1 cells using aliquots of the homogenized tumor tissue and were displayed as mean pfu/g of tissue (n=3).

4.2.12 Combination of VACV with anti-angiogenic therapy improves infiltration of innate immune cells in STSA-1 xenografts

Since oncolytic VACV GLV-1h109 displayed higher replication in tumors compared to GLV-1h68, the effect of anti-angiogenic therapy on the modulation of the host immune response was of interest. Therefore, the effect of GLV-1h109 and GLV-1h68 virus infection on host immune cells in tumors of STSA1-tumor-bearing mice was analyzed. Single cell suspensions prepared from STSA-1 tumors, resected 7 days after treatment with virus were analyzed by flow cytometry for the presence of host immune cells (Fig. 19). The presence of various innate immune cells was assessed using cellular antigen-specific markers. CD45 (leukocyte common antigen), Gr-1 antigen (Ly6C/Ly6G) of MDSCs, CD11b (Mac-1, mainly myeloid cells), F4/80 (macrophages) and MHCII (B cells, monocytes, macrophages and dendritic cells) were used to visualize the respective cell types in STSA-1 tumors. The tumor-derived Gr-1⁺CD11b⁺ cells consisted of 2 major subfractions based on differential Gr-1 expression, high (Gr-1^{high}) and intermediate (Gr-1^{int}). Gr-1^{high} represents immature and mature granulocytes, and a Gr-1^{int}, represents monocytes and other immature myeloid cells [42]. A significant increase of Gr-1^{high}CD11b⁺ (granulocytes), Gr-1^{int}CD11b⁺ (monocytes) and F4/80⁺CD45⁺ (macrophages) cells was observed in both GLV-1h109- and GLV-1h68-treated tumors compared to PBS-treated tumors (Fig. 19A, B, C). However, within the two virus-treated groups, GLV-1h109-treated

tumors showed significantly higher increase in infiltration of these immune cells compared to GLV-1h68-treated tumors. However, no significant differences were seen in the percentage of MHCII⁺CD45⁺ cells within GLV-1h109 and GLV-1h68 treated tumors (Fig. 19D). Thus, anti-angiogenic therapy increased the infiltration of the innate immune cells in tumor tissue treated with virus.

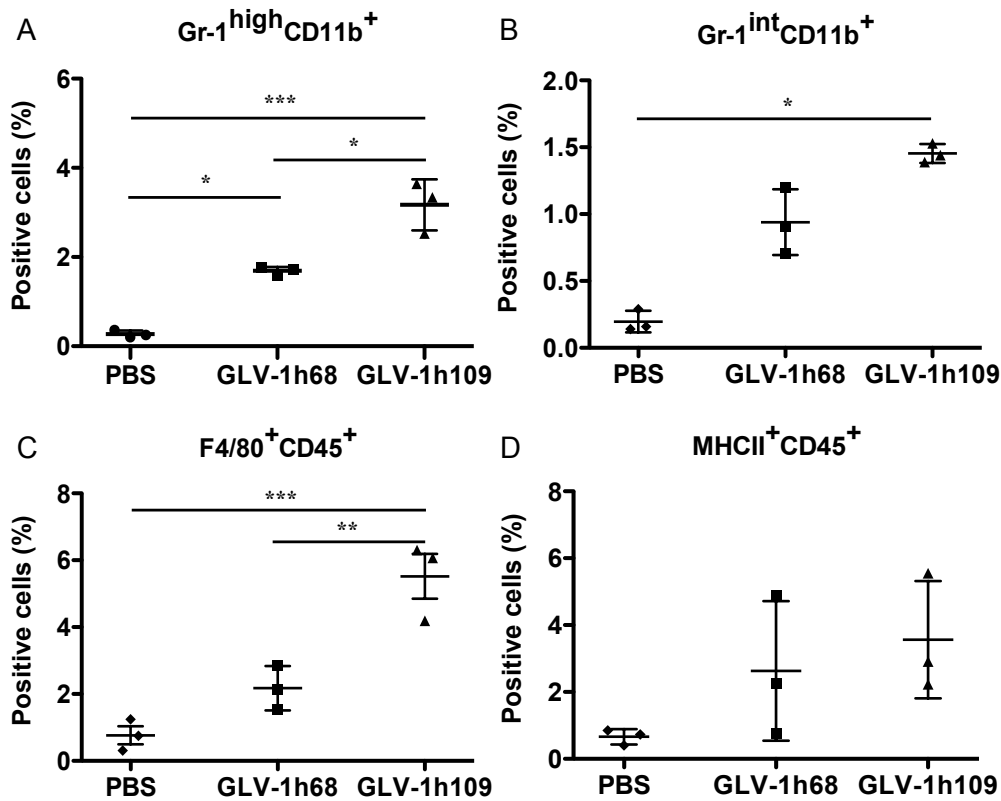


Fig. 19 Presence of immune cells in tumor bearing mice with STSA-1 xenografts at 7 days after GLV-1h68, GLV-1h109 or PBS treatment
 Percentage of (A) Gr-1^{high}CD11b⁺ (granulocytes), (B) Gr-1^{int}CD11b⁺ (monocytes), (C) F4/80⁺CD45⁺ (macrophages) or (D) MHCII⁺CD45⁺ (mainly B cells, macrophages and dendritic cells) cells in STSA-1 xenografts. Experiments were done twice with at least 3 animals per group. The data presented as mean values +/- SD. The statistical significance was analyzed using one-way ANOVA followed Bonferroni's multiple comparison test (***) P < 0.001, ** P < 0.01, *P < 0.05).

The direct virus interaction with cells of the host immune system was also analyzed at 7 dpi. At this time, 0.11% and 0.37% of Gr-1^{high} CD11b⁺ (granulocytes), 0.06% and 0.15% of Gr-1^{int}CD11b⁺ (monocytes) and 0.24% and 0.81% of F4/80⁺CD45⁺(macrophages) were GFP-positive in GLV-1h68- and GLV-1h109-infected tumors, respectively (table 6). This indicates that either these immune cells

were infected with vaccinia virus or that they had phagocytized virus-infected tumor cells.

Table 6. Percentage of GFP-positive immune cells in virus-treated STSA-1 tumor

Cell Markers	GLV-1h68	GLV-1h109	P value	Cell type
GFP ⁺ / Gr-1 ^{high} CD11b ⁺	0.11% ±	0.37% ±	** (P = 0.006)	GFP+ tumor associated granulocytes
GFP ⁺ / Gr-1 ^{int} CD11b ⁺	0.06% ±	0.15% ±	* (P = 0.042)	GFP+ tumor associated monocytes
GFP ⁺ / F4/80 ⁺	0.24% ±	0.81% ±	* (P = 0.028)	GFP+ tumor associated macrophages

Percentage GFP-positive cells in tumors from mice with STSA-1 xenografts at 7 days after GLV-1h109- or GLV-1h68-treatments. The data are presented as mean values +/- standard deviations. The statistical significance was analyzed using two-tailed unpaired Student's test (**P <0.01, *P <0.05).

The distribution of granulocytes and macrophages in tumors was also examined by staining of histological sections from STSA-1 tumor xenografts. As expected, the increased accumulation of granulocytes and macrophages was observed in GLV-1h109-infected tumors compared to PBS treated or GLV-1h68-infected tumors (Fig. 20A, B). Interestingly, the Gr-1⁺ cells (granulocytes) were mostly co-localized with virus in infected tumor regions (Fig. 20A), whereas the macrophages were diffusely distributed throughout the tumor (Fig. 20B).

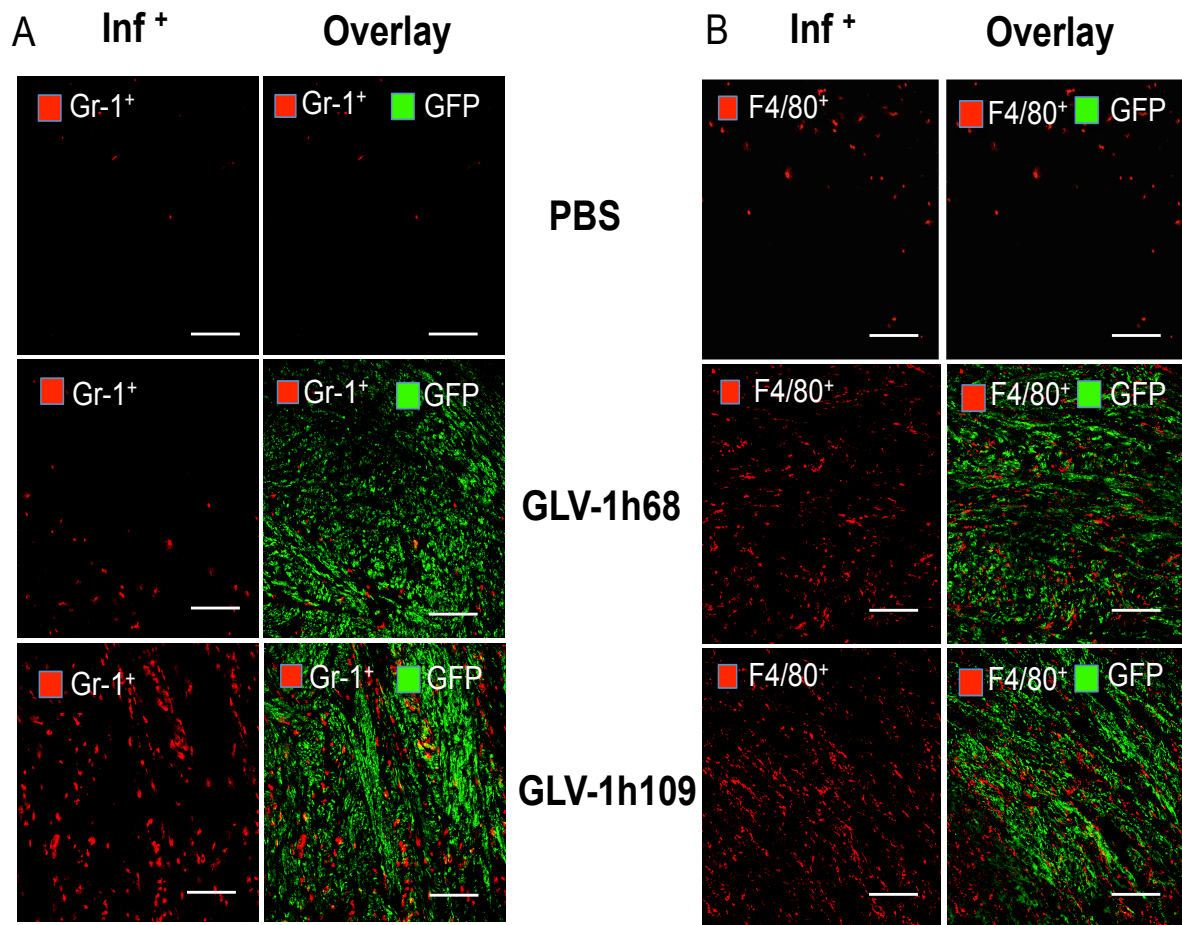


Fig. 20. Immunohistochemical staining of infected and uninfected STSA-1 tumors at 7 dpi for granulocytes (A) or macrophages (B)

Tumor bearing mice were either infected with GLV-1h109 or GLV-1h68 or mock treated (PBS). Cryosections (10 μm -thick) from STSA-1 tumors were labeled with either anti-Gr-1 (Ly-6G) antibody (A) for granulocytes or anti-F4/80⁺ antibody (B) for macrophages; both red. Virus infection and/or phagocytosis were indicated by GFP fluorescence (green). Overlays represented Gr-1⁺ and GFP (A) or F4/80⁺ and GFP (B). Scale bars: 500 μm (200X magnification).

4.3 Aim 3: Modulation of immune response by VACV therapy in canine cancer patients

Three way interactions between the administered oncolytic virus, the tumor and the host immune system are paramount in determining the therapeutic outcome of oncolytic virotherapy. In previous sections we have seen that oncolytic VACV strain LIVP6.1.1 induced infiltration of innate immune cells in tumor tissue. In addition, VACV treatment combined with inhibition of tumor angiogenesis significantly increased infiltration of innate immune cells in tumor compared to only VACV therapy. However, both these studies were carried out in nude mice that were deficient in immune system functional. Dogs with cancer were more ideal experimental models in that they could mimic human cancer patients [43]. Genelux Corporation San Diego, USA had started a phase I safety and dose escalation study with oncolytic VACV LIVP6.1.1 (V-VET1) in dogs with measurable malignancies. To elucidate the effect of VACV on modulation of the immune response, innate and adaptive immune response to V-VET1 therapy in canine cancer patients enrolled in this phase I clinical trial were analyzed.

4.3.1 Details of canine cancer patients and dose escalation scheme

The clinical trial was designed as an open-label, dose-escalating, non-randomized, single-center phase I study of V-VET1 administered intravenously in four 7-day cycles in dogs with measurable malignancies. In each cohort three dogs were enrolled and they were individually assessed for safety and dose-limiting toxicity (DLT). The dose escalation scheme was as shown in Table 7

Table 7: V-VET1 dosing schedule

Cohort	Dose per treatment ^a	Number of treatment / cycle	Number of Cycles	Total Volume of Each Injection
1	1×10^8	1	4	Final volume of preparation will be 1:1 (ml:kg) ratio with patient's weight to be infused within 15 minutes
2	3×10^8	1	4	
3	1×10^9	1	4	
4	3×10^9	1	4	

a. Listed dose was per 25 kg dog. Actual dose was adjusted based on body weight of individual dog.

To date, a total of eleven canine cancer patients were enrolled into a phase I dose escalation study. Three patients were recruited in each cohort. However, cohort 2 had four patients as one of the patients had only one cycle of treatment. As the study is not yet completed, only one patient from the last cohort has been analyzed for immune response. Each patient was treated with four cycles of V-VET1 at 7 days interval. The dose of V-VET1 was per 25 kg body weight of dog (table 7), however the final dosing was adjusted according to the body weight of each dog. The majority of patients had advanced stage cancers. Details of the tumor diagnoses, and the number of cycles of V-VET1 received by individual patients are presented in table 8.

Table 8: Patient details enrolled in phase I clinical trial

Cohort	Dose	Patient ID	Tumor type	Cycles of V-VET1
Cohort 1	1 x 10 ⁸ /25kg	V-VET-1-101	Adenocarcinoma	4
		V-VET-1-102	Soft tissue sarcoma	4
		V-VET-1-103	Osteosarcoma	4
Cohort 2	3 x 10 ⁸ /25kg	V-VET-1-104	T cell Lymphoma	2
		V-VET-1-106	Multiple mast cell tumors	7
		V-VET-1-107	Multiple mast cell tumors	4
		V-VET-1-108	Osteosarcoma	4
Cohort 3	1 x 10 ⁹ /25kg	V-VET-1-109	Soft tissue sarcoma	4
		V-VET-1-110	Sarcoma	4
		V-VET-1-111	Adenosarcoma	4
Cohort 4	3 x 10 ⁹ /25kg	V-VET-1-113	Soft tissue sarcoma	4

Blood samples were collected from each patient at pretreatment and at multiple time points during the first week and then weekly thereafter. Precise timings of samples for PBMC subset and cytokine analysis were as follows

PBMC analysis: Baseline (Week 0), Week 2, Week 4 and Week 8

Cytokine analysis: Baseline (Week 0), Week 1 Day 3, Week 2, Week 4 and Week 8

4.3.2 Optimization of canine PBMC staining for flowcytometry analysis

Peripheral blood from four healthy dogs was obtained in heparinized tubes from CVS Angel Care Cancer Center, Carlsbad, CA, USA. Control dogs were determined to be healthy by a veterinarian based on owner observations, physical examinations and complete blood count examination. PBMCs, isolated and aliquots prepared in freezing medium were stored in LN₂ according to mimic the clinical trial protocol. The presence of various immune cells was assessed using cellular antigen-specific markers. CD3, CD4, CD8, CD25 and Foxp3 were used for staining of subsets of T lymphocytes and CD11b, MHCII, CD14 and CD11c for staining of innate immune cells. In addition, cocktails of antibodies were used to stain activated T cells and B cells. Various cell types of canine PBMCs were defined as shown in table 9.

Table 9: Staining of canine immune cell types

Cell Markers	Cell type	Reference
CD3+CD4+	T helper Cell	[112]
CD3+CD8+	Cytotoxic T Cell	[112]
CD25+	Activated T cells	[113]
CD21+	B Cell	[114]
CD4+CD25+Foxp3+	Regulatory T cell (T _{reg})	[113]
CD11b+MHCII-CD14-	Myeloid derived suppressor cells (MDSCs)	[115]
CD14+	Macrophages	[116]
CD11c+	Dendritic cells	[117]

Flow cytometric analysis of all the immune cell subsets was in line with other published series. Among living cells immune cells were gated based on their forward and side scattering properties. After exclusion of cellular doublets in a FSC-A vs. FSC-H plot, gating of each immune cell type was performed as shown in Fig. 21. All the canine immune cell populations were within normal range for the respective dog breed (table 10). Thus, we confirmed that our methodology yielded results that were in line with other published series by measuring all subsets in PBMCs from four healthy dogs that had no active medical problems.

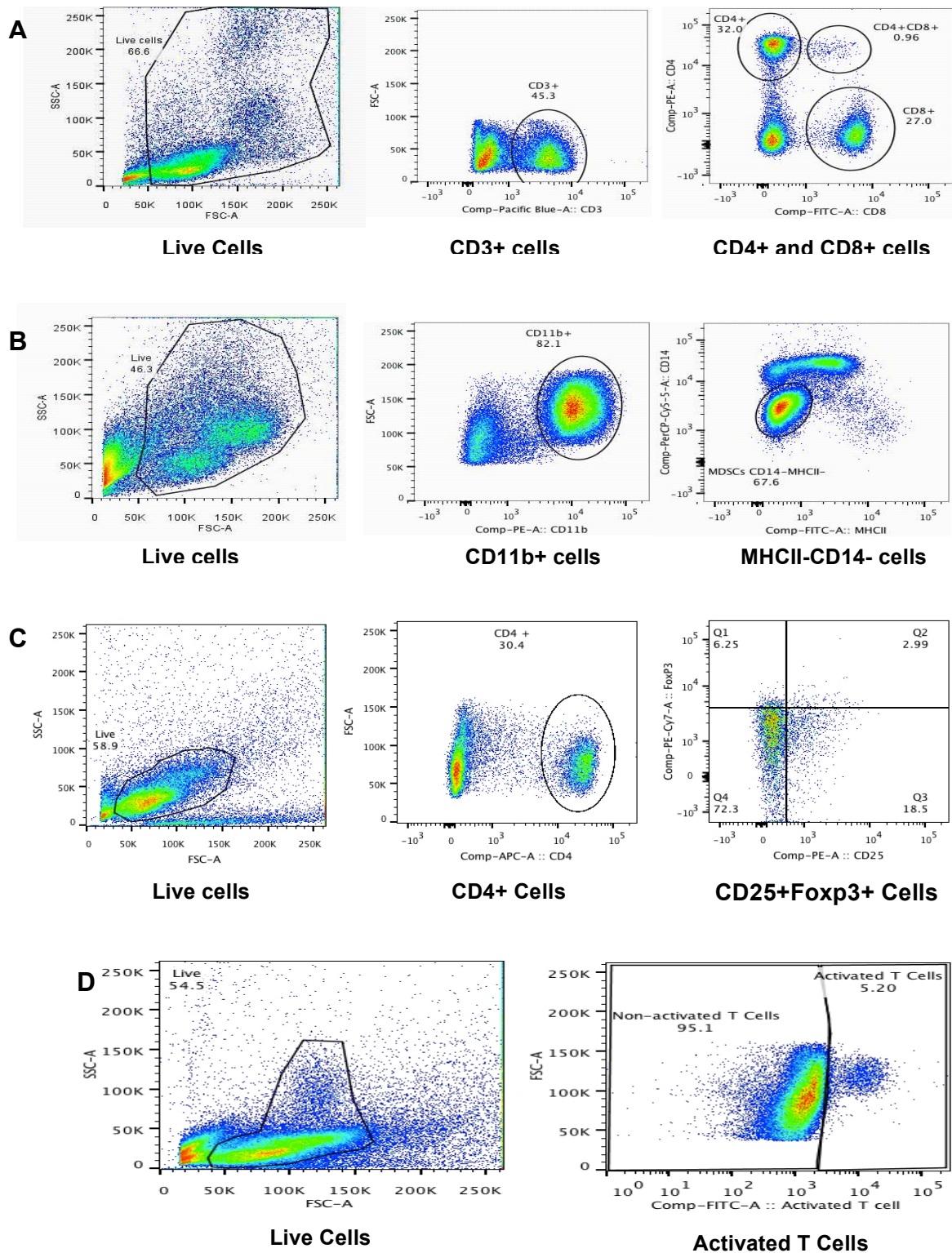


Fig. 21. Gating strategies to determine subpopulations of canine immune cells

All PBMCs were evaluated using the P1 gate (live cells) and subsequently gated based on relative expression levels of **A**: CD4+ (T helper) & CD8+ (Cytotoxic T lymphocyte) cells **B**: CD11b+MHCII-CD14- cells (MDSCs) **C**: CD4+CD25+Foxp3+ (T_{reg}) cells and **D**: Activated T cells.

4.3.3 V-VET1 treatment induced circulating cytotoxic T cell response in canine cancer patients

After standardization of canine immune cell staining, the components of the adaptive immune system in peripheral blood of canine cancer patients treated with V-VET1 in phase I clinical trial was analyzed by flow cytometry. Components of the adaptive immune system that mainly included for analysis were CD3+CD4+ (T-helper cells), CD3+CD8+ (Cytotoxic T cells) and activated T cells. PBMC subsets were analyzed pre and post viral therapy in 11 canine cancer patients from cohorts 1-4. Cell types were expressed as a proportion of total PBMC. Normal values of the immune cell populations in dogs vary extensively with age, breed, gender and disease status. Therefore, it was not appropriate to compare the immune cells in different dogs, therefore, the percentages of immune cells before V-VET1 treatment as baseline value and relative fold changes after virus treatment were reported.

Following injection of V-VET1, PBMC subset analysis from individual canine cancer patient showed a marked heterogeneity, but certain trends were observed and in some patients a correlation between specific subsets and therapeutic cycles was apparent. There was a non-significant increase in the concentration of CD3+CD4+ T cells one week after the first cycle of V-VET1 treatment compared to baseline (Fig. 22A). However, subsequently in a majority of patients, CD3+CD4+ T cell level decreased. As a result of VACV treatment, CD3+CD4+ T-cell numbers increased in eight (72.7%) patients one week after the first treatment, while three (27.3%) patients showed decreases in CD3+CD4+ T cells (table 10). The level of CD3+CD4+ was reduced to its initial levels subsequently (Fig. 22A). In contrast, VACV treatment increased CD3+CD8+ T cells in circulation in the majority of canine cancer patients. V-VET1 treatment showed incremental increase in CD3+CD8+ T cell levels in ten (90.9%) patients while in one (9.1%) patient the level decreased (table 10). A significant increase in CD3+CD8+ T cells was observed 21 days after initiation of V-VET1 treatment (Fig. 22B). However, eight weeks after initiation of V-VET1 treatment (four weeks after last cycle of virus treatment), the level of CD3+CD8+ T cells reached again the baseline level indicating that level of CD3+CD8+ T cells were influenced by VACV.

Similarly, VACV treatment increased the levels of activated T cells after completion of four cycles. Activated T cell levels were increased with virus treatment in nine (81.8%) canine cancer patients, while, two (18.2%) patients showed decreased

levels (table 10). Although increased levels of activated T cells were associated with V-VET1 treatment, the cell concentrations were not significantly higher compared to the baseline level before virus treatments (Fig. 22C).

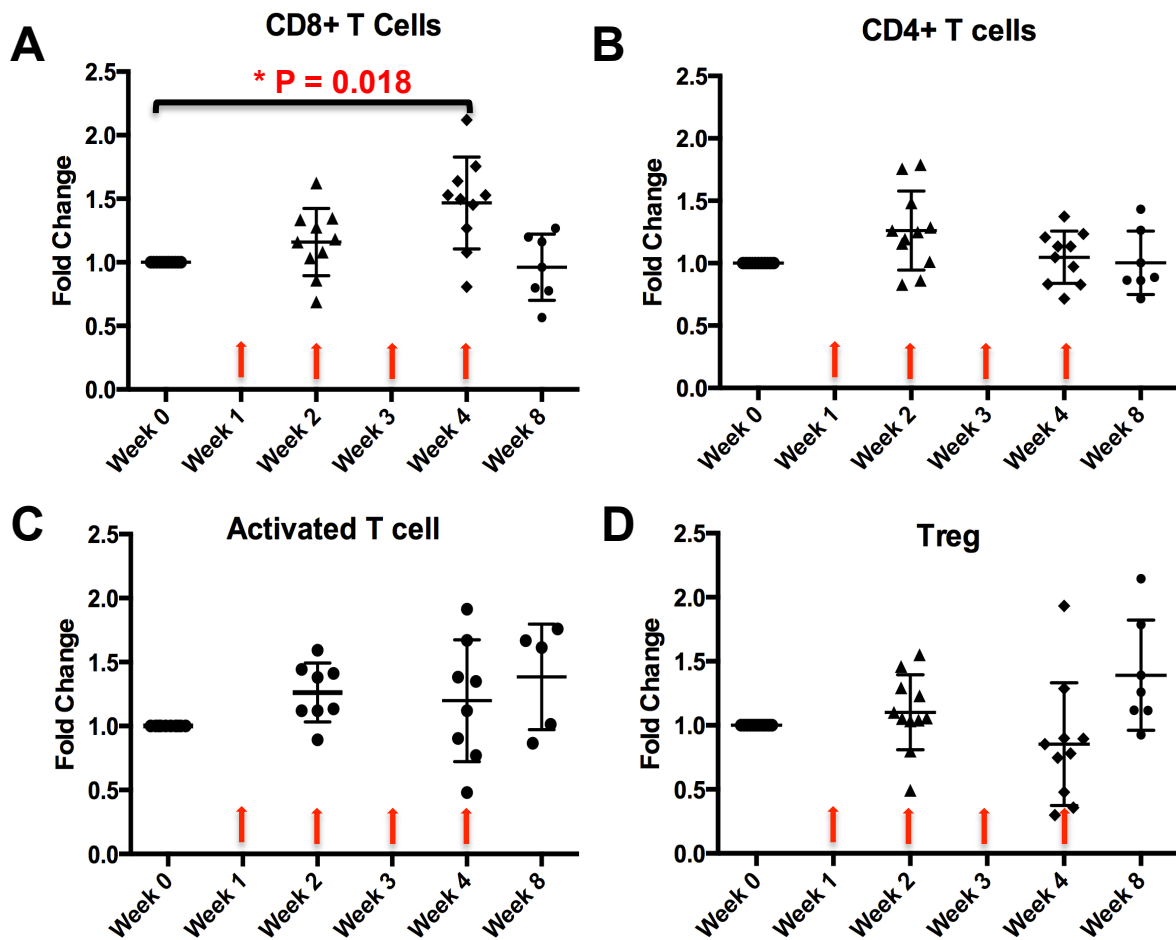


Fig. 22. V-VET1 treatment significantly increased in circulating CD8+ T cells in canine cancer patients.

Patients treated with V-VET1 (week 1, week 2, week 3 and week 4) were monitored for subsets of circulating T lymphocytes. Peripheral blood mononuclear cells from patients were isolated before and after the treatment and stained for CD4, CD8, T_{reg} and activated T cells. Percentage of CD8+ T cells (A), CD4+ T cells (B), activated T cells (C) and T_{reg} cells (D) in the total PBMC was represented here. V-VET1 treatment led to significant increase in CD8+ T cells 21 days after initiation of virus treatment. Red arrows indicate time of V-VET1 treatment.

The level of regulatory T (T_{reg}) cells in circulation of canine cancer patients enrolled in phase I clinical trial was analyzed. The frequency of T_{reg} (defined by CD4⁺CD25⁺FoxP3⁺ expression) cells was determined using antibodies against cell surface molecules CD4 and CD25, and intracellular staining of FoxP3 expression.

T_{reg} are immunosuppressive cells that inhibit functions of CD8+ cytotoxic T cells. Although T_{reg} cells were seen to increase in response to treatment in two patients (18.2%), in all other patients (81.8%), the levels of T_{reg} cells were either decreased or unaffected by the V-VET1 treatment (table 10). However, overall analysis of T_{reg} percentage did not show any significant change after V-VET1 treatment (Fig. 22D).

4.3.4 V-VET1 treatment reduces circulatory MDSCs in canine cancer patients

MDSCs are a recently described population of innate immune cells that accumulate in established tumors, exhibit immune suppressive functions, and block activation of T cells. Therefore, the effect of V-VET1 treatment on these inhibitory cells was of great interest. We defined the MDSC population in dogs as cells with CD11b⁺MHCII⁻CD14⁻ expression [115]. The percentages of MDSCs in dogs with cancer were evaluated by flow cytometry. Circulatory MDSCs in all canine cancer patients (100%) before treatment were found at high levels but decreased after treatment with V-VET1 (table 11). A gradual decrease in circulatory MDSCs started after first treatment, however, a significant decrease was observed 21 days (week 4) after initiation of virus treatment (Fig. 23). When treatment was stopped the frequency of MDSCs was reduced again to pretreatment levels indicating that circulatory MDSC frequency was affected by V-VET1 treatment in canine cancer patients.

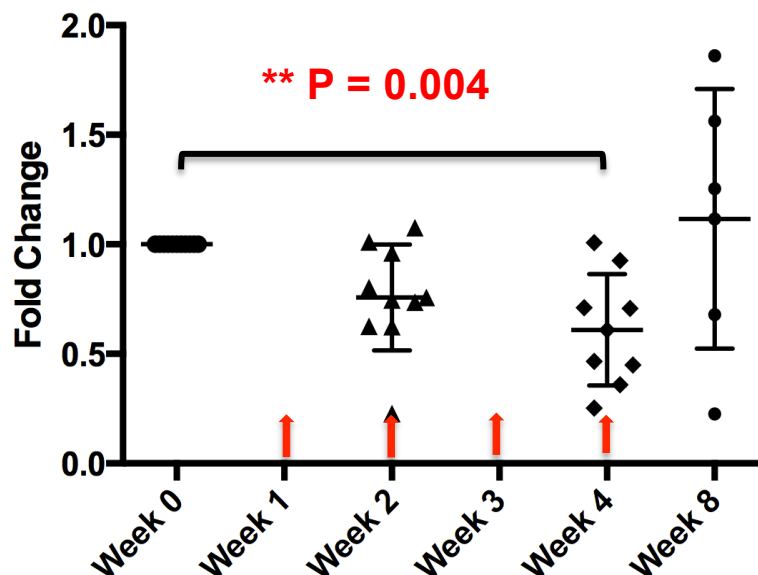


Fig. 23. Circulating MDSCs (CD11b⁺CD14⁻MHCII⁻) in canine cancer patients

Circulatory MDSC (CD11⁺CD14⁻MHCII⁻) population frequency was monitored over the time in canine cancer patients treated with V-VET1. (** Indicates P<0.01). Red arrows indicate time of V-VET1 treatment.

Additionally, the frequency of other subtypes of innate immune cells like dendritic cells and monocytes was also analyzed by flow cytometry. V-VET1 treatment did not change the level of either monocytes or dendritic cells in canine cancer patients. The percentage of subsets of adaptive and innate immune cells in each patient is presented in table 10 and 11.

Table 10: Percentages of T lymphocyte subsets in canine cancer patients treated with V-VET1

Cell type	Time after treatment	V-VET1-101	V-VET1-102	V-VET1-103	V-VET1-104	V-VET1-106	V-VET1-107	V-VET1-108	V-VET1-109	V-VET1-110	V-VET1-111	V-VET1-113
CD4	Week 0	15.20	18.69	26.53	32.10	15.76	24.06	20.31	49.59	16.07	41.84	14.55
	Week 2	18.13	32.86	33.14	47.56	20.26	27.82	17.51	50.16	28.76	34.61	12.28
	Week 4	14.78	23.07	30.08	NA	11.29	27.27	24.53	41.04	22.07	34.83	11.74
	Week 8	19.22	NA	NA	NA	11.28	21.32	NA	42.71	23.00	36.09	18.38
CD8	Week 0	18.87	15.72	11.60	12.80	8.69	20.82	25.64	21.36	25.21	24.61	24.41
	Week 2	20.37	25.55	7.69	16.35	11.71	24.62	17.67	18.35	26.09	32.82	39.21
	Week 4	30.93	42.75	NA	19.56	9.37	36.56	20.70	31.97	36.62	31.21	48.13
	Week 8	10.65	NA	NA	NA	6.74	16.64	NA	27.09	30.21	28.60	33.32
T _{reg}	Week 0	22.63	10.23	6.78	1.52	5.83	7.84	2.93	4.39	12.43	3.80	4.83
	Week 2	25.22	9.36	5.57	0.55	8.15	8.12	3.53	4.38	8.05	7.22	7.31
	Week 4	20.08	9.63	6.42	NA	8.66	12.86	2.97	4.45	5.01	6.17	7.66
	Week 8	24.18	NA	NA	NA	7.29	6.78	NA	3.15	5.49	6.11	6.29
Activated T	Week 0	3.12	2.84	6.84	3.05	1.28	3.15	6.37	7.60	3.96	1.10	1.28

Table 11: Percentages of subsets of innate immune cells in canine cancer patients treated with V-VET1

Cell type	Time after treatment	V-VET1-101	V-VET1-102	V-VET1-103	V-VET1-104	V-VET1-106	V-VET1-107	V-VET1-108	V-VET1-109	V-VET1-110	V-VET1-111	V-VET1-113
MDSC	Week 0	1.24	2.31	2.64	90.83	33.83	25.59	47.41	20.14	1.89	50.90	34.15
	Week 2	1.00	0.53	1.65	56.86	24.89	27.55	47.93	15.01	21.42	48.91	27.03
	Week 4	0.88	0.58	1.88	NA	34.11	9.19	21.33	18.66	39.94	23.67	20.19
	Week 8	0.84	NA	NA	NA	52.85	47.62	NA	25.28	49.47	11.47	37.93
CD14	Week 0	26.93	45.30	6.49	32.22	56.51	28.85	42.25	30.90	56.59	24.84	29.87
	Week 2	32.36	51.53	13.15	10.87	54.51	26.19	39.47	27.36	39.39	14.16	27.01
	Week 4	17.03	20.04	NA	31.98	48.74	8.76	62.06	21.58	23.70	NA	31.54
	Week 8	28.72	NA	NA	NA	40.99	20.17	NA	13.39	24.57	34.81	29.43
DC	Week 0	27.87	49.28	30.71	56.05	82.86	52.96	82.54	47.65	56.06	54.96	43.76
	Week 2	33.36	53.19	38.10	16.66	80.32	94.71	76.84	45.67	50.18	31.11	38.74
	Week 4	18.12	22.10	30.44	NA	77.99	78.52	81.55	28.09	57.42	47.56	42.46
	Week 8	30.02	NA	NA	NA	90.31	74.63	NA	66.37	65.33	49.17	48.39

4.3.5 Tumor type and viral dose did not affect modulation of immune response

Our study demonstrated that V-VET1 therapy modulated immune response especially frequency of circulatory CD8+ T cells and MDSCs in canine cancer patients. However, one of the main purposes of the phase I trial was to find maximum tolerable dose (MTD). Therefore, V-VET1 dose given to each patient varied based on the cohort in which the dog was enrolled. Other objective of the study was to analyze the effects of V-VET1 in canine patients with solid tumors. Tumors from the patients were categorized based on the clinical diagnosis as soft tissue sarcoma (3 patients), mast cell tumors (2 patients), osteosarcoma (2 patients) and adenocarcinoma (2 patients). Thus we hypothesized that viral dose and tumor type were one of the confounding factors that affect modulation of immune response after V-VET1 therapy. Therefore, we analyzed the frequency of circulatory CD3+CD8+ T cells and MDSCs (percentages of both immune cell types were changed after VACV therapy) as markers to compare effects of viral dose and tumor type on modulation of immune response.

Although frequency of CD3+CD8+ T cells increased as the dose of virus increased, however the increased frequency was not statistically significant (Fig. 24A). Likewise, frequency of CD3+CD8+ T cells did not differ significantly based on types of tumors (Fig. 24B). In addition, we compared the population of MDSC based on virus dose and tumor type. MDSC cells significantly decreased after V-VET1 treatment however there was no significant difference in frequency of these cells when compared based on different virus doses and tumor types (Fig. 24 C, D). Canine cancer patients were grouped according to the dose of virus injection in four cohorts. PBMCs from patients from first three cohorts given respective virus dose i.e. cohort 1 (1×10^8), cohort 2 (3×10^8) and cohort 3 (1×10^9) were analyzed for frequency of CD3+CD8+ T cells and MDSCs. Cohort 4 was not included for comparative analysis as only one patient was enrolled in this group till the end of study.

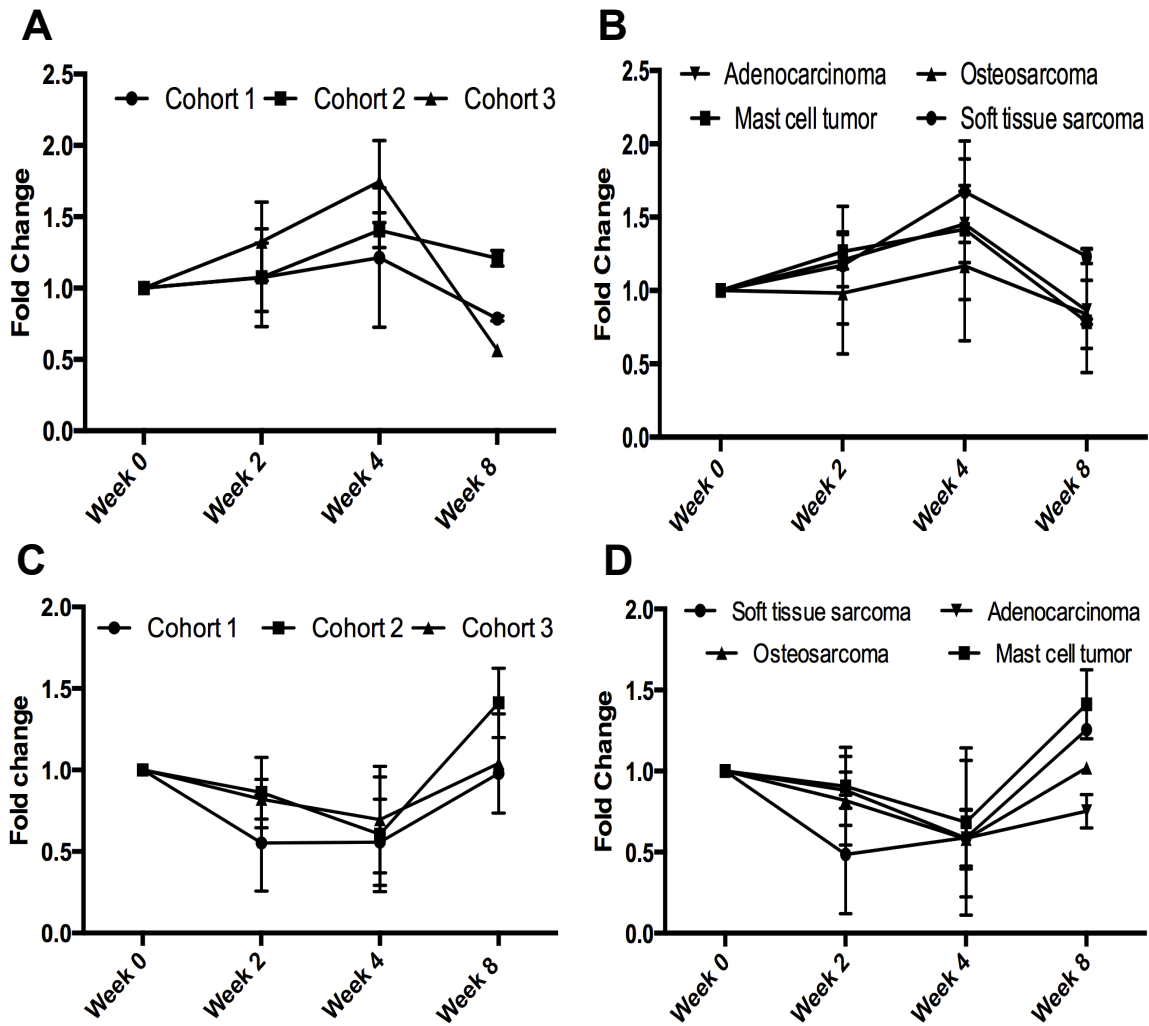


Fig. 24 Virus dose and tumor type did not influence the modulation of immune response after V-VET1 injection in canine cancer patients

Canine patients treated with V-VET1 were monitored for frequency of CD3+CD8+ T cells (A, B) and MDSC (C, D). Peripheral blood mononuclear cells from patients were collected before and after the treatment and stained for CD8+ T cell and MDSC cells. Change in frequency of CD3+CD8+ T cell (A) and MDSC (C) depending on virus dose was observed. Similarly changes in population of CD3+CD8+ T cells (B) and MDSC (D) based on tumor type was analyzed. Both virus dose and tumor type did not influence the frequency of circulatory CD3+CD8+ T cells and MDSC after virus treatment.

Our studies analyzing effect of LIP6.1.1 (V-VET1) in canine cancer patients have shown that VACV indeed modulated immune response. We could show that canine cancer patients treated with V-VET1 significantly increased CD8+ cytotoxic T cells after 21 days of initiation of virus treatment. In addition, V-VET1 treatment inhibited circulatory MDSCs, which are immunosuppressive in nature. Moreover, the changes in frequency of these immune cells did not depend on the dose of virus as well as

tumor type. We conclude that VACV positively influence the immune response in canine cancer patients, which will ultimately help to improve efficacy of oncolytic VACV therapy.

CHAPTER 5: DISCUSSION

Cancer is the leading cause of disease-related death in both human and dogs worldwide. Cancer in mankind accounts for about 7.6 million deaths annually [1]. By 2030, it is projected that there will be ~26 million new cancer cases and 17 million cancer deaths per year [2]. Likewise, cancer is the most common cause of natural death in dogs. The incidence of cancer is 1 to 2% in the canine population and accounts for about half of the deaths in dogs older than 10 years [3]. The major treatment options available for human cancers include surgery, radiation therapy, chemotherapy, immunotherapy or combinations of either of them. Veterinarians use more or less similar therapeutic protocol for the treatment of canine cancers as those used for treatment of human cancers. However, the overall prognosis for both human and canine patients diagnosed with cancer has not significantly improved. Till today, canine cancers are considered incurable with ineffective treatment options. Therefore, there is an urgent need for development of new treatment options against canine cancers. Furthermore, dogs with natural cancer are considered as one of the best animal models to develop new drugs for cancer therapy. Traditionally, rodent cancer models have been used for analyzing the biology of cancer initiation, promotion, and progression as well as development of cancer therapeutics. However, they do not adequately represent several important features that define cancer in humans, including biology of initiation of tumor, the complexity of cancer recurrence and metastasis and outcomes to novel therapies. To the contrary, dogs develop cancers naturally and share many characteristics with human malignancies. Tumor microenvironment, histopathology, molecular and genomics data from dog tumors has significant similarities with the corresponding human tumors [118]. These advantages of dog cancers provide a unique opportunity to integrate canine cancer patients in the studies designed for the development of new cancer drugs targeted against both human and canine cancers.

The need for effective therapies for human and canine cancers has led to extensive research in the cancer field, which has resulted in the testing of oncolytic viruses as a novel therapy to control tumor growth. Oncolytic viral therapies have made their mark on the cancer research world as another potential therapeutic option, with the possible advantages of lessening side effects as well as strengthening treatment efficacy due to higher tumor selectivity. Results have been so promising that

oncolytic viral treatments have now been approved for clinical trials in human cancer patients, and the first oncolytic viral therapy has now been marketed as a treatment for head and neck cancers in China [6]. Currently, a variety of oncolytic viruses are being evaluated for their ability to be used in anti-cancer therapy for human and canine cancers. One of the viruses being studied as an oncolytic virus is vaccinia virus.

Vaccinia virus belongs to the family of orthopox viruses and gained worldwide fame for its role as a vaccine for smallpox. One of the vaccinia virus strain used to study its oncolytic potential was GLV-1h68. The recombinant VACV strain GLV-1h68 was engineered with three gene insertions, *Ruc*-GFP fusion, β -galactosidase and β -glucuronidase, and has been successfully used for therapy of human and canine tumor xenografts with minimal toxicity to normal tissue [8, 42, 119]. Recently, a phase I trial was completed at the Royal Marsden Hospital in London, England, which demonstrated that administration of GL-ONC1, clinical grade GLV-1h68, is well tolerated with minimal toxicity with preliminary evidence of anticancer activity. In patients treated with GL-ONC1, no dose limiting toxicities were observed [79].

Like for other targeted therapies, a number of challenges remain for oncolytic virotherapy. These challenges mainly include replication of oncolytic viruses in non-tumor tissue, poor delivery of oncolytic viruses to the tumor site, relatively poor virus spread throughout solid tumor tissue, inefficient viral replication in immune-competent hosts and disadvantageous ratio between anti-viral and anti-tumoral immunity [120]. The limited delivery of oncolytic virus to tumor site is mainly attributed to virus neutralization by blood components [121, 122]. However, the components of the tumor microenvironment that include heterogeneous tumor vasculature and an army of innate immune cells, affect the spread and replication of oncolytic viruses in tumor tissue [120]. Despite this limitation, it has been shown that oncolytic viruses are also able to take advantage of certain features of the tumor microenvironment. Oncolytic viruses are modified or armed to inhibit the heterogeneous tumor vasculature density, which further improves tumor response [72]. Manipulation of the innate response helps the oncolytic virus infect and kill the tumor tissue and thereby enhanced the anti-tumor efficacy [120]. Thus, to analyze the oncolytic potential of VACV in canine cancer xenografts and to understand the

effects of modulation the tumor microenvironment using VACV the studies in this thesis were designed in following parts.

5.1 Therapeutic efficacy of the oncolytic VACV LIVP6.1.1 in canine cancer xenografts

The first part of the study was focused on the potential of oncolytic VACV in the treatment of canine cancer xenografts in nude mice. The efficacy of the wild-type VACV strain LIVP6.1.1 was tested in two canine cancer xenografts models i.e. canine soft tissue sarcoma and canine prostate carcinoma. As the oncolytic potential of viruses depends on the ability of the virus to efficiently infect and replicate in cancer cells, in initial experiments, the new virus strain LIVP6.1.1 was characterized for its replication efficiency and oncolytic potential in STSA-1 and DT08/40 canine cancer cells in culture. Infection of canine cancer cells with LIVP6.1.1 demonstrated that the virus replicated efficiently in both STSA-1 and DT08/40 cells. The maximum virus titer was observed after 48 and 96 hours post infection in STSA-1 and DT08/40 cells respectively, indicating that the virus replicates more efficiently in STSA-1 cells compared to DT08/40 cells. The replication of the oncolytic vaccinia virus in cancer cells is influenced by many host factors including the type of cancer cell [123]. The canine cancer cells used in the current study were obtained from two different canine patients. STSA-1 cells were derived from a biopsy obtained from a dog with grade II soft tissue sarcoma [42], DT08/40 cells were derived from biopsy material obtained from a dog with prostate carcinoma [124]. Thus, the variation in the speed of LIVP6.1.1 replication in STSA-1 and DT08/40 cells may be attributed to different origin and tumor types of these cancer cells. Furthermore, the oncolytic potential of virus is linked to its replication efficiency. STSA-1 and DT08/40 cells when infected with LIVP6.1.1 demonstrated efficient cytotoxicity. However, the rate of killing was much faster in STSA-1 cells compared to DT08/40 cells, which was not surprising considering the fact that LIVP6.1.1 replicated faster in STSA-1 cells. Taken together, LIVP6.1.1 efficiently infected, replicated in and killed STSA-1 and DT08/40 cancer cells although at different rates.

Further, we analyzed the therapeutic efficacy and safety of LIVP6.1.1 in mouse xenografts produced by implanting STSA-1 and DT08/40 cells. STSA-1 and DT08/40 tumor-bearing athymic nude mice were injected with a single dose of LIVP6.1.1 or

PBS as a control. Treatment of STSA-1 tumors with LIVP6.1.1 led to tumor inhibition 14 days after treatment with subsequent tumor regression. The tumor growth occurred in three phases: growth (Phase I), inhibition (Phase II) and regression (Phase III) as established by Zhang et al. for mammary carcinoma xenografts [8]. Further, virus treatment resulted in more efficient tumor regression and in some cases almost complete tumor regression. In contrast, LIVP6.1.1-treated DT08/40 tumors did not show the typical three-phase growth pattern. Virus-treated tumors did not grow as large as in the untreated controls in the early course of treatment as would have been expected. However, significant tumor regression was observed in virus treated groups compared to animals injected with PBS. The onset of tumor regression was observed after 35 days of treatment. STSA-1 tumors showed tumor regression 21 days earlier compared to tumor regression in DT08/40 xenografts. Therefore, virus treatment demonstrated that the rate of tumor regression was faster in STSA-1 tumors compared to DT08/40 tumors. It was previously demonstrated that the rate of virus replication in tumor xenografts influences the therapeutic efficacy of various oncolytic viruses like oncolytic VACV, herpes virus and adenovirus [125-127]. Therefore, faster therapeutic efficacy in STSA-1 tumor xenografts compared to DT08/40 tumor xenografts is likely attributed to faster replication of LIVP6.1.1 in STSA-1 cells. Additionally, the treatment with LIVP6.1.1 was well tolerated by the animals as evidenced by no major change in relative body weight of mice and by the fact that the virus was mainly detected in the tumor tissues. The concentration of virus in the STSA-1 tumors was 10,000- to 100,000- fold higher compared to tested normal body organs indicating the tumor-specificity of virus infection. However, minimal numbers of virus particles were also detected in normal body organs (table 3), which might be explained by the leakiness of blood vessels in solid tumors which uptake the virus that is released from the tumor cells and transport it to normal organs via blood circulation. Additionally, circulating virus-infected tumor cells or cell particles escaping from leaky tumor blood vessels may end up in healthy tissues such as the lung, liver, spleen and kidney. In summary, the data demonstrated that the replication of virus was (mostly) tumor-specific. Additionally, tumor-colonization of LIVP6.1.1 and viral oncolysis was analyzed by immunohistochemistry and it was demonstrated that the virus efficiently colonized tumor tissues. Staining of tumor sections with fluorescent-labeled anti-VACV antibody identified virus-colonized patches in tumors. Increased viral patches were correlated with decreased nuclear

staining in STSA-1 tumors, indicating an increase in virus-mediated cell death *in vivo*.

Analysis of tumor associated innate immune cells in tumor-bearing mice was performed 7 days after initial treatment. Upon virus treatment, an enhanced concentration of (infiltrating) granulocytes and macrophages in tumors was observed. Moreover, it was reported that virotherapy induces massive tumoral infiltration of MDSCs resembling neutrophils and macrophages, which may be part of a virotherapy-mediated antitumor mechanism [42]. The initiation of the innate responses and recruitment of immune cells might lead to tumor regression in cooperation with oncolysis [42, 128]. Thus, anti-tumor mechanism in STSA-1 xenografts could be a combination of the direct viral oncolysis of tumor cells and the virus-dependent infiltration of tumor-associated host immune cells.

5.2 The recombinant VACV strain GLV-1h109 encoding the anti-VEGF single-chain antibody was equally efficient in canine cancer xenografts

In the first part of the study, the effective oncolytic potential of the wild-type VACV strain LIVP6.1.1 in canine cancer xenografts was demonstrated. However, like other therapeutic modalities, oncolytic virotherapy encountered with several challenges. One of the major challenges faced by oncolytic virotherapy is the role of the tumor microenvironment in compromising the efficacy of the treatment. The components of the tumor microenvironment, especially heterogeneous tumor angiogenesis, have been shown to limit the spread and replication of oncolytic virus and thereby the efficacy of the therapy [120]. Therefore, the second part of the study was designed to understand the effects of modulation of tumor angiogenesis on the spread and replication of oncolytic VACV. The major strategy to inhibit tumor angiogenesis is blocking the growth factors required for the formation of new blood vessels. VEGF has shown to be one of the growth factors that play a key role in the signaling pathways that mediate tumor angiogenesis, tumor growth, and metastasis [87], and blocking of VEGF inhibited angiogenesis and restricted tumor growth [129, 130]. Therefore, VACV strain GLV-1h109 encoding the anti-VEGF single-chain antibody GLAF-1 was used to understand the effects of modulation of tumor angiogenesis on oncolytic virotherapy in canine cancer xenografts. The GLV-1h109 strain was derived from the prototype virus strain where the *lacZ* gene in GLV-168 was

replaced by a gene encoding the anti-VEGF single-chain antibody GLAF-1. In all the cell culture experiments GLV-1h68 was used as a control.

In initial experiments, the characterization of the new VACV strain GLV-1h109 was carried out in canine cancer cells. The replacement of the *lacZ* expression cassette with GLAF-1 at the J2R locus was confirmed by Western blot. The GLAF-1 insertion did not affect the expression and fluorescent protein function of the marker genes (*Ruc-GFP* and *gusA*) when compared to the parental virus GLV-1h68. GLAF-1 being a single-chain antibody with a secretory signal was expected to secrete into the cell supernatant. Western blot analysis of Infected STSA-1 and DT08/40 cells with GLV-1h109 indeed demonstrated the secretion of GLAF-1 in the cell supernatant (Fig. 8). The secretion of GLAF-1 by the infected cell might enable its quick delivery to the surrounding tumor tissue and more widespread binding to VEGF (Fig. 9). In addition, tumor infection by the virus was associated with GLAF-1 in peripheral blood (Fig. 12). The data clearly demonstrated that GLAF-1 could also be useful as a pharmacokinetic marker to monitor virus colonization and persistence in GLV-1h109-injected xenograft mice (Fig. 12). These findings have very well demonstrated the application of this virus-based system for efficient expression and distribution of recombinant single chain antibodies in the tumorigenic host. Furthermore, the new virus strain was characterized for replication efficiency and cytolytic potential in canine cancer cells in culture. GLV-1h109 was effective at infecting, replicating in, and killing STSA-1 and DT08/40 cells in cell culture as efficiently as the parental virus GLV-1h68. This indicated that insertion of the GLAF-1 gene did not negatively affect virus replication or the cytolytic activity in cell culture. The results were concomitant with the previous results where insertion of GLAF-1 did not influence the replication of GLV-1h109 in human cancer cell lines [72]. However, GLV-1h109 replicated better and faster in STSA-1 cells compared to replication in DT08/40 cells (**P= 0.0004). As described earlier for LVP6.1.1, this variation in the efficiency of GLV-1h109 replication can be attributed to different origin and types of cancer cells. Additionally, the replication efficiency of GLV-1h109 encoding the anti-VEGF single-chain antibody was shown to be better in the cells expressing higher level of VEGF [131]. Therefore, the higher level of VEGF expression in STSA-1 compared to DT08/40 cells (Fig. 10) could explain the better and faster replication of GLV-1h109 in STSA-1 cells.

The oncolytic effects of GLV-1h109 were tested in mice with STSA-1 and DT08/40 tumor xenografts. The results demonstrated that GLV-1h109 achieved a significant inhibition of tumor growth in both STSA-1 and DT08/40 canine xenograft models. However, the tumor regression was faster in STSA-1 tumor xenografts compared to that in DT08/40 xenografts. Virus-treated STSA-1 tumor xenografts demonstrated typical three-phase growth curve and tumor regression was observed as early as 14 days while DT08/40 tumor xenografts showed tumor regression only after 35 days. The faster therapeutic efficacy in STSA-1 tumor xenografts compared to DT08/40 tumor xenografts could be explained by faster replication of GLV-1h109 in STSA-1 cells. These findings were identical to the results obtained in previous studies where more efficient replication of LVP6.1.1 in STSA-1 tumor xenografts led to better tumor regression compared to DT08/40 xenografts.

Furthermore, effects of the anti-VEGF single-chain antibody GLAF-1 on tumor vasculature were tested in STSA-1 xenografts. There were two reasons to prefer STSA-1 tumor xenografts to DT08/40 tumor xenografts. The canine soft tissue sarcoma STSA-1 cells expressed higher levels of VEGF compared to DT08/40 cells (Fig. 10). Additionally, the serum of GLV-1h109-injected mice with STSA-1 xenografts contained a nine-fold greater level of GLAF-1 expression than in mice with DT08/40 xenografts on 7 dpi (Fig. 12). GLV-1h109-treated STSA-1 tumor xenografts demonstrated the intratumoral expression of GLAF-1 at 7 and 49 dpi (Fig. 13). In addition to intratumoral expression, it was important to examine the binding efficiency of GLAF-1 to canine VEGF. The GLAF-1 protein encoded by GLV-1h109 had binding affinity to human and mouse VEGF [72]. Cross-reactivity of GLAF-1 with VEGFs from other species other than human and mouse was not tested. It was demonstrated that GLAF-1 could specifically bind to canine VEGF (Fig 9). The GLAF-1 binding to VEGF from both canine and mouse origins is advantageous in canine xenograft models, as blocking of the both VEGF forms could be important for therapeutic efficacy [132].

STSA-1 tumors sections were tested for blood vessel staining at 7 days after virus treatment. Staining of STSA-1 tumor sections for CD31 (angiogenesis marker) showed a significant decrease in the number of blood vessels in GLV-1h109-infected tumors compared to GLV-1h68- and PBS-injected control tumors at 7 dpi (Fig. 14B). The drastic reduction of the vascular density of tumors might be due to the presence

of the GLAF-1 in GLV-1h109-treated STSA-1 tumors (Fig. 13). Interestingly, the significant reduction in vascular density was observed in virus-infected areas only (Fig. 14B, C). Localized effects of GLAF-1 on tumor vasculature might be due to the low concentration of GLAF-1 at the specific site in the tumor bed. It has been demonstrated that the inhibition of tumor vasculature requires complete blockade of VEGF [132] and blocking of VEGF is largely dependent on the concentration of anti-VEGF antibody [133, 134]. Highest concentrations of GLAF-1 in the virus-infected areas of STSA-1 xenografts compared to non-infected areas. Therefore, concentrations of GLAF-1 might not have been sufficient to completely block VEGF that might led to localized inhibition of vasculature in STSA-1 xenografts. Moreover, the effect of GLAF-1 showing decreased vascular density in STSA-1 tumor xenografts is well supported by the previous findings which demonstrated that the treatment with GLV-1h68 and another GLAF-1-negative oncolytic vaccinia virus strain, LIVP1.1.1, did not affect the blood vessel density of STSA-1 tumors [42]. In conclusion, systemic administration of oncolytic vaccinia virus GLV-1h109 encoding an anti-VEGF single-chain antibody led to significant decrease of tumor vasculature, which further inhibited tumor growth.

5.3 Anti-angiogenic therapy improved the spread and replication of VACV as well as infiltration of the innate immune response in canine cancer xenografts

Initial animal experiments have demonstrated that GLV-1h109 injection in mice with canine cancer xenografts was safe and significantly inhibited the tumor growth as well as decreased tumor blood vessel density. Further, virus-encoded single-chain anti-VEGF antibody GLAF-1 led to an enhanced therapeutic effects in different human tumor xenograft models compared to oncolytic viral therapy with the prototype strain GLV-1h68 alone [72]. The continuous production of the GLAF-1 in virus-colonized tumors led to an inhibition of tumor angiogenesis. This possible VEGF blockade and the proximate anti-angiogenesis effects would normalize the tumor vasculature that would enhance virus spread and ultimately virus replication in tumor tissue. In order to test this assumption, the replication and spread of GLV-1h109 was analyzed by counting the viral titers and viral-encoded GFP expression, respectively in STSA-1 xenografts at seven days after systemic viral injection. Flow

cytometry analysis demonstrated that the numbers of GFP-positive tumor cells were significantly higher in tumors treated with GLV-1h109 compared to GLV-1h68-treated tumors. Higher number of GFP-positive cells indicated a better spread and distribution of virus. The extent of virus replication was analyzed by viral titer determination in GLV-1h109- and GLV-1h68-treated tumor xenografts at 7 days post injection. A statistically significant (nearly 2-fold) increase in infectious viral particles was observed in GLV-1h109-treated STSA-1 xenografts compared to GLV-1h68-treated tumor xenografts. Inhibition of tumor angiogenesis has demonstrated an enhanced spread and replication of several oncolytic viruses (HSV, VACV and adenovirus) in tumor xenografts and thereby improved tumor regression [131, 135, 136]. A possible reason for these findings may be explained by the phenomenon called “vascular normalization” [137]. Vascular normalization is the process where blockade of VEGF can reverse many of the structural and functional abnormalities seen in tumor vessels [138]. An anti-VEGF therapy can improve tumor vessel perfusion, reduce tumor hypoxia, and in turn can enhance delivery of systemically administered therapeutic agent [139] in this case VACV. The “changed” vasculature seemed to allow an increased virus spread and thereby replication of GLV-1h109 in STSA-1 tumor xenografts. Therefore we conclude that modulation of tumor angiogenesis by the anti-VEGF single-chain antibody indeed influenced the spread and replication of VACV.

Furthermore, modulation of tumor angiogenesis and increased replication of oncolytic virus has shown to influence the infiltration of immune cells in tumor xenografts [120]. To investigate the GLV-1h109 virus interactions with the host immune cells, we analyzed the innate immune response in the early phase of virus infection by flow cytometry. Significantly increased accumulation of host immune cells especially granulocytes and macrophages was observed in GLV-1h109-infected tumors as compared to PBS or GLV-1h68-infected tumors (Fig. 15). Several recent studies have described that intratumoral replication of VACV induces massive tumoral infiltration of granulocytes, mainly neutrophils, that may be exerting antitumor effects *in vivo* through a number of different mechanisms [30, 42, 99, 140]. As the replication of VACV was higher in GLV-1h109 treated tumor xenografts, a significant increase in accumulation of these innate immune cells was not surprising. Furthermore, Breitbach and colleagues have postulated that neutrophils (Gr-1⁺ cells)

could mediate antitumor effects by the induction of vascular collapse in tumors [30]. In addition, a recent study has identified a cytotoxic population (N1) of tumor-associated neutrophils expressing CD11b⁺Ly6G⁺, capable of killing tumor cells [141]. In the current work, we found evidence of direct interactions of vaccinia virus or virus-infected cells with granulocytes and macrophages in the STSA-1 tumor tissue (Table 6; GFP-positive cells). Others and we in previous study have reported that these interactions may increase the activation and strength of host antitumor immune responses [42, 99, 141, 142]. This indicates that inhibition of tumor angiogenesis increases virus spread and replication, which further induces infiltration of innate immune cells in tumor bed. Consequently, the interactions of granulocytes and macrophages with vaccinia virus in the tumor bed may be crucial for the success of the virotherapy.

5.4 VACV injection induced circulatory immune response in canine patients recruited in phase I clinical trial

Anti-tumoural immune responses dictate the long-term therapeutic success of cancer treatment. Previous sections of this study have demonstrated that VACV replication in canine tumor xenografts induced infiltration of innate immune cells in the tumor xenografts and modulation of tumor angiogenesis significantly improved the frequency of the innate immune cells in the tumor bed. Similarly, recent reports in animal models [143-145] as well as in human clinical trials [146] support the hypothesis that virus-induced anti-tumoural immune responses significantly contribute to the outcome of the therapy. However, antitumor immune response has seldom been translated into clinical benefits. Given the lack of success of existing cancer immunotherapeutics, it is necessary to examine the immune response to VACV in canine cancer patients. Therefore, we have analyzed the immunomodulatory effects of V-VET1 (clinical grade LIVP6.1.1) treatment in canine cancer patients recruited in phase I clinical trial. This is the first reported clinical trial with an oncolytic VACV designed to study its safety and dose escalation in dogs with malignancies. Ideally, immune responses should be monitored within the tumor, but the tumor biopsy is not always accessible for analysis. In our study the amount of tumor biopsies obtained from individual canine patients were not sufficient to analyze the immune response. However an alternative method to monitor adaptive and innate immune response is

the characterization of circulating immune cells in the peripheral blood [147, 148]. This method has several advantages e.g. enough material is available and pretreatment immune monitoring can be performed without additional invasive interventions. Furthermore, in advanced cancer patients, tumors are located at different anatomical locations, it is of great importance that immune cells have the capacity to migrate to and eradicate tumor cells at different tissue sites. In preclinical and clinical studies, it has been shown that anti-cancer treatment results in increased population of anti-tumor immune cells in peripheral blood, highlighting the capacity of these cells to migrate to different body sites [149, 150]. Therefore, peripheral responses are of great relevance and can be considered as indirect analysis of the effects taking place in the tumor microenvironment.

In the present study, we performed evaluation pre- and post-V-VET1 treatment levels of circulatory T lymphocyte subsets in canine cancer patients. The frequency of circulatory CD3+CD4+ T lymphocytes and activated T lymphocytes was non-significantly increased in 72.7% and 81.8% patients, respectively, post-virus treatment compared to pre-treatment levels. CD3+CD8+ T lymphocyte was the only subtype that showed significantly increased levels at 21 days after initiation of treatment compared to pretreatment levels. The increased frequency of circulatory CD3+CD8+ T cells was observed in almost all patients (90.9%), irrespective of virus dose and tumor type. Since CD3+CD8+ lymphocytes are generally regarded as the major cytolytic cells, their increased frequency in circulation would suggest an increased population in the tumor microenvironment that would potentially allow the killing of infected cells [151]. The presence of cytotoxic T cells has been shown to be a favorable prognostic indicator in a number of human cancers, and gene expression profiling demonstrated that patients with high baseline tumor expression of genes related to both innate and adaptive immune response were more likely to favorably respond to immunotherapy [152]. Furthermore, tumor-associated CD8+ T cells in several canine cancers have shown to improve the prognosis of the disease [153, 154]. Therefore, increased circulatory CD3+CD8+ T cells from baseline in canine cancer patients treated with V-VET1, suggest that the cytotoxic T lymphocytes may have anti-tumor activity, and that changes in the immune microenvironment of the tumor may slow disease progression.

Further, the outcomes of the peripheral monitoring of T_{reg} (CD4+CD25+Foxp3+) and MDSCs (CD11b+MHCII-CD14-) in V-VET1-treated canine cancer patients were also encouraging. The significant decrease in circulating MDSCs after 21 days paralleled an increase in the overall CD3+CD8⁺ T cell population (Fig. 19). MDSCs generated in large numbers in cancer patients are able to directly inhibit Ag-specific T cell responses [155]. Increased MDSC level in both canine and human cancer patients represents a mechanism of immune suppression in cancer and therapeutic options that reduced the level of MDSCs have improved the prognosis of disease [156, 157]. Here, a similar regulatory impact of V-VET1 treatment upon MDSCs in canine cancer patients was documented. While there is substantial variation in identification of human MDSC and canine MDSC, the CD11b+MHCII-CD14- subset was defined as a key MDSCs subset in the recent study [115]. Similarly, another subtype of immune cells that play an important role in negatively regulating the development of anti-tumor immune response are regulatory T cells (T_{reg}) [158]. T_{reg} have been shown to directly suppress immune responses to tumors in mouse tumor models [159]. T_{reg}-induced immune suppression also appears to occur in humans as evidenced by clinical studies that correlate high T_{reg} numbers with impaired immune function [160]. In this study, the levels of T_{reg} cells were either decreased or unaffected by the V-VET1 therapy in almost all canine cancer patients (81.8 %) (Fig. 18D). However, the overall analysis of T_{reg} population did not show any significant change in the percentages of the circulatory T_{reg} after V-VET1 treatment. Interestingly, ratio of CD8/T_{reg} is a useful prognostic marker for canine cancers [158]. Decreased CD8/T_{reg} ratio in peripheral blood of canine osteosarcoma patients was associated with decreased survival [158]. In the current study, the percentages of CD8⁺ T cells increased over the time after V-VET1 treatment and consecutively increasing the ratio of CD8/T_{reg} post V-VET1 treatment. Therefore, it was encouraging that immune inhibitory cell population (concentration of MDSCs and relative concentrations of T_{reg} as described by CD8/T_{reg} ratio) in circulation has been significantly decreased after V-VET1 treatment.

Furthermore, type of tumor or dose of virus in canine patients did not affect the changes in frequencies of immune cells. Canine patients diagnosed for cancers were categorized in four different tumor types mainly, soft tissue sarcoma, mast cell tumor, adenocarcinoma and osteosarcoma. However, the frequencies of both CD3+CD8⁺ T

cells and MDSCs did not significantly change according to the type of tumor. Similarly, canine patients were given different virus doses to test maximum tolerable dose. Although, increase in virus dose showed increased CD3+CD8+ T cells post treatment; the change was not statistically significant. Therefore, it was concluded that the dose of virus and tumor type did not affect the changes in the frequencies of immune cells.

Lastly, the changes in percentages of the immune cells were observed only during the course of V-VET1 treatment. Total four cycles of V-VET1 were given (1 cycle every week) in individual patients and PBMCs were analyzed from pre-treatment till eight weeks after initiation of treatment at regular interval. Surprisingly, the positive change in the percentages of immune cells (increased CD3+CD8+ T cells and decreased MDSCs) was observed only during the course of V-VET1 treatment. However, when V-VET1 treatment was terminated the CD3+CD8+ T cell and MDSCs percentages were returned to the baseline level (Fig. 19 and Fig. 20). This phenomenon suggests that the modulation of immune cells were driven by the V-VET1 and VACV induced the changes in the frequencies of circulatory immune cells in canine cancer patients. The association between clinical activity of V-VET1 and change from baseline in CD3+CD8+ T cells and MDSCs that was studied in the current trial needs to be explored further.

In conclusion, systemic administration of oncolytic VACV strains led to significant inhibition of tumor growths in the treated canine tumors. Consequently, VACV showed capability to modulate the tumor microenvironment. Therefore, modulation of immune responses during treatment is of great importance to investigate the immunogenicity of the oncolytic viruses and the potential correlation between the immune response and the clinical outcome of the patients and also for future treatment design.

REFERENCES

1. Siegel, R., Ma, J., Zou, Z. and Jemal, A., *Cancer Statistics, 2014*. CA: A Cancer Journal for Clinicians, 2014. **64**(1): p. 9-29.
2. Thun, M.J., et al., *The global burden of cancer: priorities for prevention*. Carcinogenesis, 2010. **31**(1): p. 100-10.
3. Merlo, D.F., et al., *Cancer incidence in pet dogs: findings of the Animal Tumor Registry of Genoa, Italy*. J Vet Intern Med, 2008. **22**(4): p. 976-84.
4. Kelsey, J.L., A.S. Moore, and L.T. Glickman, *Epidemiologic studies of risk factors for cancer in pet dogs*. Epidemiol Rev, 1998. **20**(2): p. 204-17.
5. Baek, S.J., M.F. McEntee, and A.M. Legendre, *Review paper: Cancer chemopreventive compounds and canine cancer*. Vet Pathol, 2009. **46**(4): p. 576-88.
6. Garber, K., *China approves world's first oncolytic virus therapy for cancer treatment*. J Natl Cancer Inst, 2006. **98**(5): p. 298-300.
7. Sinha, G., *Companion therapeutics*. Nat Biotechnol, 2014. **32**(1): p. 12-4.
8. Zhang, Q., et al., *Eradication of solid human breast tumors in nude mice with an intravenously injected light-emitting oncolytic vaccinia virus*. Cancer Res, 2007. **67**(20): p. 10038-46.
9. Phuangsab, A., et al., *Newcastle disease virus therapy of human tumor xenografts: antitumor effects of local or systemic administration*. Cancer Lett, 2001. **172**(1): p. 27-36.
10. Hirasawa, K., et al., *Systemic reovirus therapy of metastatic cancer in immune-competent mice*. Cancer Res, 2003. **63**(2): p. 348-53.
11. De Palma, M., M.A. Veneri, and L. Naldini, *In vivo targeting of tumor endothelial cells by systemic delivery of lentiviral vectors*. Hum Gene Ther, 2003. **14**(12): p. 1193-206.
12. Fu, X. and X. Zhang, *Delivery of herpes simplex virus vectors through liposome formulation*. Mol Ther, 2001. **4**(5): p. 447-53.
13. Shafren, D.R., et al., *Systemic therapy of malignant human melanoma tumors by a common cold-producing enterovirus, coxsackievirus a21*. Clin Cancer Res, 2004. **10**(1 Pt 1): p. 53-60.
14. Tseng, J.C., et al., *Systemic tumor targeting and killing by Sindbis viral vectors*. Nat Biotechnol, 2004. **22**(1): p. 70-7.

15. Reddy, P.S., et al., *Seneca Valley virus, a systemically deliverable oncolytic picornavirus, and the treatment of neuroendocrine cancers*. J Natl Cancer Inst, 2007. **99**(21): p. 1623-33.
16. Dobbelstein, M., *Replicating adenoviruses in cancer therapy*. Curr Top Microbiol Immunol, 2004. **273**: p. 291-334.
17. Evgin, L., et al., *Potent oncolytic activity of raccoonpox virus in the absence of natural pathogenicity*. Mol Ther, 2010. **18**(5): p. 896-902.
18. G, D., *The influence of complicating diseases upon leukemia*. J Med Sci, 1904(127): p. 563-592.
19. Bierman, H.R., et al., *Remissions in leukemia of childhood following acute infectious disease: staphylococcus and streptococcus, varicella, and feline panleukopenia*. Cancer, 1953. **6**(3): p. 591-605.
20. Moore, A.E., *Effects of viruses on tumors*. Annu Rev Microbiol, 1954. **8**: p. 393-410.
21. Southam, C.M. and A.E. Moore, *Clinical studies of viruses as antineoplastic agents with particular reference to Egypt 101 virus*. Cancer, 1952. **5**(5): p. 1025-34.
22. Zielinski, T. and E. Jordan, *[Remote results of clinical observation of the oncolytic action of adenoviruses on cervix cancer]*. Nowotwory, 1969. **19**(3): p. 217-21.
23. Kelly, E. and S.J. Russell, *History of oncolytic viruses: genesis to genetic engineering*. Mol Ther, 2007. **15**(4): p. 651-9.
24. Alemany, R., C. Balague, and D.T. Curiel, *Replicative adenoviruses for cancer therapy*. Nat Biotechnol, 2000. **18**(7): p. 723-7.
25. Nakamura, T. and S.J. Russell, *Oncolytic measles viruses for cancer therapy*. Expert Opin Biol Ther, 2004. **4**(10): p. 1685-92.
26. Latchman, D.S., *Herpes simplex virus-based vectors for the treatment of cancer and neurodegenerative disease*. Curr Opin Mol Ther, 2005. **7**(5): p. 415-8.
27. Shen, Y. and J. Nemunaitis, *Fighting cancer with vaccinia virus: teaching new tricks to an old dog*. Mol Ther, 2005. **11**(2): p. 180-95.
28. Suskind, R.G., et al., *Viral agents oncolytic for human tumors in heterologous host; oncolytic effect of Coxsackie B viruses*. Proc Soc Exp Biol Med, 1957. **94**(2): p. 309-18.

29. Marcellus, R.C., et al., *Induction of p53-independent apoptosis by the adenovirus E4orf4 protein requires binding to the Balpha subunit of protein phosphatase 2A*. J Virol, 2000. **74**(17): p. 7869-77.
30. Breitbach, C.J., et al., *Targeted inflammation during oncolytic virus therapy severely compromises tumor blood flow*. Mol Ther, 2007. **15**(9): p. 1686-93.
31. Kirn, D.H. and S.H. Thorne, *Targeted and armed oncolytic poxviruses: a novel multi-mechanistic therapeutic class for cancer*. Nat Rev Cancer, 2009. **9**(1): p. 64-71.
32. Patil, S.S., et al., *Oncolytic virotherapy in veterinary medicine: current status and future prospects for canine patients*. J Transl Med, 2012. **10**: p. 3.
33. Kirn, D., *Clinical research results with dl1520 (Onyx-015), a replication-selective adenovirus for the treatment of cancer: what have we learned?* Gene Ther, 2001. **8**(2): p. 89-98.
34. clinicaltrial.gov. Available from: clinicaltrial.gov.
35. Galanis, E., et al., *Phase II trial of intravenous administration of Reolysin((R)) (Reovirus Serotype-3-dearing Strain) in patients with metastatic melanoma*. Mol Ther, 2012. **20**(10): p. 1998-2003.
36. Heo, J., et al., *Randomized dose-finding clinical trial of oncolytic immunotherapeutic vaccinia JX-594 in liver cancer*. Nat Med, 2013. **19**(3): p. 329-36.
37. Aghi, M.K. and E.A. Chiocca, *Phase Ib trial of oncolytic herpes virus G207 shows safety of multiple injections and documents viral replication*. Mol Ther, 2009. **17**(1): p. 8-9.
38. Kaufman, H.L. and S.D. Bines, *OPTIM trial: a Phase III trial of an oncolytic herpes virus encoding GM-CSF for unresectable stage III or IV melanoma*. Future Oncol, 2010. **6**(6): p. 941-9.
39. Kanaya, N., et al., *Anti-tumor effect of adenoviral vector-mediated p53 gene transfer on the growth of canine osteosarcoma xenografts in nude mice*. J Vet Med Sci, 2011. **73**(7): p. 877-83.
40. Thacker, E.E., et al., *A genetically engineered adenovirus vector targeted to CD40 mediates transduction of canine dendritic cells and promotes antigen-specific immune responses in vivo*. Vaccine, 2009. **27**(50): p. 7116-24.
41. Hwang, C.C., et al., *Oncolytic reovirus in canine mast cell tumor*. PLoS One, 2013. **8**(9): p. e73555.

42. Gentschev, I., et al., *Preclinical evaluation of oncolytic vaccinia virus for therapy of canine soft tissue sarcoma*. PLoS One, 2012. **7**(5): p. e37239.
43. Paoloni, M. and C. Khanna, *Translation of new cancer treatments from pet dogs to humans*. Nat Rev Cancer, 2008. **8**(2): p. 147-56.
44. Vail, D.M. and E.G. MacEwen, *Spontaneously occurring tumors of companion animals as models for human cancer*. Cancer Invest, 2000. **18**(8): p. 781-92.
45. Genelhu, M.C., et al., *A comparative study between mixed-type tumours from human salivary and canine mammary glands*. BMC Cancer, 2007. **7**: p. 218.
46. Paoloni, M.C. and C. Khanna, *Comparative oncology today*. Vet Clin North Am Small Anim Pract, 2007. **37**(6): p. 1023-32; v.
47. Lindblad-Toh, K., et al., *Genome sequence, comparative analysis and haplotype structure of the domestic dog*. Nature, 2005. **438**(7069): p. 803-19.
48. Bukowski, J.A., D. Wartenberg, and M. Goldschmidt, *Environmental causes for sinonasal cancers in pet dogs, and their usefulness as sentinels of indoor cancer risk*. J Toxicol Environ Health A, 1998. **54**(7): p. 579-91.
49. Rivera, P. and H. von Euler, *Molecular biological aspects on canine and human mammary tumors*. Vet Pathol, 2011. **48**(1): p. 132-46.
50. Le, L.P., et al., *Infectivity enhancement for adenoviral transduction of canine osteosarcoma cells*. Gene Ther, 2006. **13**(5): p. 389-99.
51. Nanhai Chen, A.S., *Oncolytic vaccinia virus: a theranostic agent for cancer*. Future Virology, 2010. **5**(6): p. 763-784.
52. Stritzker, J., et al., *Vaccinia virus-mediated melanin production allows MR and optoacoustic deep tissue imaging and laser-induced thermotherapy of cancer*. Proc Natl Acad Sci U S A, 2013. **110**(9): p. 3316-20.
53. Jenner, E., *An inquiry into the causes and effects of the variolae vaccinae, a disease discovered in some of the western counties of England, particularly near Gloucestershire, and known by the name of the Cow Pox*. New York, 1798. **Dover**.
54. Henderson, D.A., *Edward Jenner's vaccine*. Public Health Rep, 1997. **112**(2): p. 116-21.
55. Roenigk, H.H., Jr., et al., *Immunotherapy of malignant melanoma with vaccinia virus*. Arch Dermatol, 1974. **109**(5): p. 668-73.

56. Arakawa, S., Jr., et al., *Clinical trial of attenuated vaccinia virus AS strain in the treatment of advanced adenocarcinoma. Report on two cases.* J Cancer Res Clin Oncol, 1987. **113**(1): p. 95-8.
57. Moss, B., *Genetically engineered poxviruses for recombinant gene expression, vaccination, and safety.* Proc Natl Acad Sci U S A, 1996. **93**(21): p. 11341-8.
58. Doms, R.W., R. Blumenthal, and B. Moss, *Fusion of intra- and extracellular forms of vaccinia virus with the cell membrane.* J Virol, 1990. **64**(10): p. 4884-92.
59. Vanderplasschen, A., M. Hollinshead, and G.L. Smith, *Intracellular and extracellular vaccinia virions enter cells by different mechanisms.* J Gen Virol, 1998. **79 (Pt 4)**: p. 877-87.
60. Moss, B., *Poxviridae: the viruses and their replication.* Fields Virology. Vol. 2. 2007: Philadelphia: Lippincott Williams & Wilkins. 2905-2946.
61. Davison, A.J. and B. Moss, *Structure of vaccinia virus early promoters.* J Mol Biol, 1989. **210**(4): p. 749-69.
62. Sodeik, B. and J. Krijnse-Locker, *Assembly of vaccinia virus revisited: de novo membrane synthesis or acquisition from the host?* Trends Microbiol, 2002. **10**(1): p. 15-24.
63. Smith, G.L., A. Vanderplasschen, and M. Law, *The formation and function of extracellular enveloped vaccinia virus.* J Gen Virol, 2002. **83**(Pt 12): p. 2915-31.
64. Ward, B.M. and B. Moss, *Vaccinia virus intracellular movement is associated with microtubules and independent of actin tails.* J Virol, 2001. **75**(23): p. 11651-63.
65. Moss, B., *The viruses and their replication.* 4 ed. Fields Virology. Vol. 4. 2001, Philadelphia: Lippincott, Williams & Wilkins. 2849–2883.
66. Wong, H.H., N.R. Lemoine, and Y. Wang, *Oncolytic Viruses for Cancer Therapy: Overcoming the Obstacles.* Viruses, 2010. **2**(1): p. 78-106.
67. Chen, N.G., et al., *Replication efficiency of oncolytic vaccinia virus in cell cultures prognosticates the virulence and antitumor efficacy in mice.* J Transl Med, 2011. **9**: p. 164.
68. Breitbach, C.J., et al., *Oncolytic vaccinia virus disrupts tumor-associated vasculature in humans.* Cancer Res, 2013. **73**(4): p. 1265-75.

69. Aarts, W.M., J. Schlom, and J.W. Hodge, *Vector-based vaccine/cytokine combination therapy to enhance induction of immune responses to a self-antigen and antitumor activity*. *Cancer Res*, 2002. **62**(20): p. 5770-7.
70. Berinstein, N.L., *Carcinoembryonic antigen as a target for therapeutic anticancer vaccines: a review*. *J Clin Oncol*, 2002. **20**(8): p. 2197-207.
71. Greiner, J.W., et al., *Vaccine-based therapy directed against carcinoembryonic antigen demonstrates antitumor activity on spontaneous intestinal tumors in the absence of autoimmunity*. *Cancer Res*, 2002. **62**(23): p. 6944-51.
72. Frentzen, A., et al., *Anti-VEGF single-chain antibody GLAF-1 encoded by oncolytic vaccinia virus significantly enhances antitumor therapy*. *Proc Natl Acad Sci U S A*, 2009. **106**(31): p. 12915-20.
73. Sturm, J.B., et al., *Functional hyper-IL-6 from vaccinia virus-colonized tumors triggers platelet formation and helps to alleviate toxicity of mitomycin C enhanced virus therapy*. *J Transl Med*, 2012. **10**: p. 9.
74. Yu, Y.A., et al., *Regression of human pancreatic tumor xenografts in mice after a single systemic injection of recombinant vaccinia virus GLV-1h68*. *Mol Cancer Ther*, 2009. **8**(1): p. 141-51.
75. Advani, S.J., et al., *Preferential replication of systemically delivered oncolytic vaccinia virus in focally irradiated glioma xenografts*. *Clin Cancer Res*, 2012. **18**(9): p. 2579-90.
76. Buckel, L., et al., *Combination of fractionated irradiation with anti-VEGF expressing vaccinia virus therapy enhances tumor control by simultaneous radiosensitization of tumor associated endothelium*. *Int J Cancer*, 2013. **133**(12): p. 2989-99.
77. Robinson, B.W., et al., *Cytokine gene therapy or infusion as treatment for solid human cancer*. *J Immunother*, 1998. **21**(3): p. 211-7.
78. Marchesi, V., *Immunotherapy: Oncolytic vaccinia virus shows promise in liver cancer*. *Nat Rev Clin Oncol*, 2013. **10**(4): p. 182.
79. Khan KH, Y.A., Mateo J, Tunariu N, Yap T, Tan D, Harrington K, Bono J. *Phase I clinical trial of a genetically modified and oncolytic vaccinia virus GL-ONC1 with green fluorescent protein imaging*. in *ASCO Annual meeting proceedings errata*. 2013. USA: Journal of clinical oncology.

80. Netti, P.A., et al., *Role of extracellular matrix assembly in interstitial transport in solid tumors*. *Cancer Res*, 2000. **60**(9): p. 2497-503.
81. Sauthoff, H., et al., *Intratumoral spread of wild-type adenovirus is limited after local injection of human xenograft tumors: virus persists and spreads systemically at late time points*. *Hum Gene Ther*, 2003. **14**(5): p. 425-33.
82. Markert, J.M., et al., *Phase Ib trial of mutant herpes simplex virus G207 inoculated pre-and post-tumor resection for recurrent GBM*. *Mol Ther*, 2009. **17**(1): p. 199-207.
83. Kim, D.H., et al., *Enhancing poxvirus oncolytic effects through increased spread and immune evasion*. *Cancer Res*, 2008. **68**(7): p. 2071-5.
84. Schafer, S., et al., *Vaccinia virus-mediated intra-tumoral expression of matrix metalloproteinase 9 enhances oncolysis of PC-3 xenograft tumors*. *BMC Cancer*, 2012. **12**: p. 366.
85. Folkman, J., *Tumor angiogenesis: therapeutic implications*. *N Engl J Med*, 1971. **285**(21): p. 1182-6.
86. Jain, R.K., *Normalizing tumor microenvironment to treat cancer: bench to bedside to biomarkers*. *J Clin Oncol*, 2013. **31**(17): p. 2205-18.
87. De Falco, S., *Antiangiogenesis therapy: an update after the first decade*. *Korean J Intern Med*, 2014. **29**(1): p. 1-11.
88. Guse, K., et al., *Antiangiogenic arming of an oncolytic vaccinia virus enhances antitumor efficacy in renal cell cancer models*. *J Virol*, 2010. **84**(2): p. 856-66.
89. Tysome, J.R., et al., *Lister vaccine strain of vaccinia virus armed with the endostatin-angiostatin fusion gene: an oncolytic virus superior to dl1520 (ONYX-015) for human head and neck cancer*. *Hum Gene Ther*, 2011. **22**(9): p. 1101-8.
90. Fulci, G., et al., *Cyclophosphamide enhances glioma virotherapy by inhibiting innate immune responses*. *Proc Natl Acad Sci U S A*, 2006. **103**(34): p. 12873-8.
91. Chiocca, E.A., et al., *A phase I open-label, dose-escalation, multi-institutional trial of injection with an E1B-Attenuated adenovirus, ONYX-015, into the peritumoral region of recurrent malignant gliomas, in the adjuvant setting*. *Mol Ther*, 2004. **10**(5): p. 958-66.

92. Prestwich, R.J., et al., *The case of oncolytic viruses versus the immune system: waiting on the judgment of Solomon*. Hum Gene Ther, 2009. **20**(10): p. 1119-32.
93. Waldhauer, I. and A. Steinle, *NK cells and cancer immunosurveillance*. Oncogene, 2008. **27**(45): p. 5932-43.
94. Reschner, A., et al., *Innate lymphocyte and dendritic cell cross-talk: a key factor in the regulation of the immune response*. Clin Exp Immunol, 2008. **152**(2): p. 219-26.
95. Long, K.B. and G.L. Beatty, *Harnessing the antitumor potential of macrophages for cancer immunotherapy*. Oncoimmunology, 2013. **2**(12): p. e26860.
96. Mantovani, A., C. Garlanda, and P. Allavena, *Molecular pathways and targets in cancer-related inflammation*. Ann Med, 2010. **42**(3): p. 161-70.
97. Wesolowski, R., J. Markowitz, and W.E. Carson, 3rd, *Myeloid derived suppressor cells - a new therapeutic target in the treatment of cancer*. J Immunother Cancer, 2013. **1**: p. 10.
98. Kirn, D.H., et al., *Targeting of interferon- β to produce a specific, multi-mechanistic oncolytic vaccinia virus*. PLoS Med, 2007. **4**(12): p. e353.
99. John, L.B., et al., *Oncolytic virus and anti-4-1BB combination therapy elicits strong antitumor immunity against established cancer*. Cancer Res, 2012. **72**(7): p. 1651-60.
100. Walker, J.D., I. Sehgal, and K.G. Kousoulas, *Oncolytic herpes simplex virus 1 encoding 15-prostaglandin dehydrogenase mitigates immune suppression and reduces ectopic primary and metastatic breast cancer in mice*. J Virol, 2011. **85**(14): p. 7363-71.
101. Carvalho, M.I., et al., *A role for T-lymphocytes in human breast cancer and in canine mammary tumors*. Biomed Res Int, 2014. **2014**: p. 130894.
102. Sakaguchi, S., et al., *Regulatory T cells: how do they suppress immune responses?* Int Immunol, 2009. **21**(10): p. 1105-11.
103. Tysome, J.R., et al., *A novel therapeutic regimen to eradicate established solid tumors with an effective induction of tumor-specific immunity*. Clin Cancer Res, 2012. **18**(24): p. 6679-89.

104. Thorne, S.H. and C.H. Contag, *Integrating the biological characteristics of oncolytic viruses and immune cells can optimize therapeutic benefits of cell-based delivery*. Gene Ther, 2008. **15**(10): p. 753-8.
105. Lapteva, N., et al., *Targeting the intratumoral dendritic cells by the oncolytic adenoviral vaccine expressing RANTES elicits potent antitumor immunity*. J Immunother, 2009. **32**(2): p. 145-56.
106. London, C.A., et al., *Phase I dose-escalating study of SU11654, a small molecule receptor tyrosine kinase inhibitor, in dogs with spontaneous malignancies*. Clin Cancer Res, 2003. **9**(7): p. 2755-68.
107. Patrino, R., et al., *VEGF concentration from plasma-activated platelets rich correlates with microvascular density and grading in canine mast cell tumour spontaneous model*. J Cell Mol Med, 2009. **13**(3): p. 555-61.
108. de Queiroz, G.F., et al., *Vascular endothelial growth factor expression and microvascular density in soft tissue sarcomas in dogs*. J Vet Diagn Invest, 2010. **22**(1): p. 105-8.
109. Hess, M., et al., *Bacterial glucuronidase as general marker for oncolytic virotherapy or other biological therapies*. J Transl Med, 2011. **9**: p. 172.
110. Kamstock, D., et al., *Evaluation of a xenogeneic VEGF vaccine in dogs with soft tissue sarcoma*. Cancer Immunol Immunother, 2007. **56**(8): p. 1299-309.
111. Stylianopoulos, T. and R.K. Jain, *Combining two strategies to improve perfusion and drug delivery in solid tumors*. Proc Natl Acad Sci U S A, 2013. **110**(46): p. 18632-7.
112. Avery, P.R., et al., *Flow cytometric characterization and clinical outcome of CD4+ T-cell lymphoma in dogs: 67 cases*. J Vet Intern Med, 2014. **28**(2): p. 538-46.
113. Pinheiro, D., et al., *Phenotypic and functional characterization of a CD4(+) CD25(high) FOXP3(high) regulatory T-cell population in the dog*. Immunology, 2011. **132**(1): p. 111-22.
114. Marconato, L., et al., *Assessment of bone marrow infiltration diagnosed by flow cytometry in canine large B cell lymphoma: prognostic significance and proposal of a cut-off value*. Vet J, 2013. **197**(3): p. 776-81.
115. Goulart, M.R., G.E. Pluhar, and J.R. Ohlfest, *Identification of myeloid derived suppressor cells in dogs with naturally occurring cancer*. PLoS One, 2012. **7**(3): p. e33274.

116. Sherger, M., et al., *Identification of myeloid derived suppressor cells in the peripheral blood of tumor bearing dogs*. BMC Vet Res, 2012. **8**: p. 209.
117. Mielcarek, M., et al., *Identification and characterization of canine dendritic cells generated in vivo*. Biol Blood Marrow Transplant, 2007. **13**(11): p. 1286-93.
118. Ranieri, G., et al., *A model of study for human cancer: Spontaneous occurring tumors in dogs. Biological features and translation for new anticancer therapies*. Crit Rev Oncol Hematol, 2013. **88**(1): p. 187-97.
119. Ehrig, K., et al., *Growth inhibition of different human colorectal cancer xenografts after a single intravenous injection of oncolytic vaccinia virus GLV-1h68*. J Transl Med, 2013. **11**: p. 79.
120. Tysome, J.R., N.R. Lemoine, and Y. Wang, *Update on oncolytic viral therapy - targeting angiogenesis*. Onco Targets Ther, 2013. **6**: p. 1031-40.
121. Tsai, V., et al., *Impact of human neutralizing antibodies on antitumor efficacy of an oncolytic adenovirus in a murine model*. Clin Cancer Res, 2004. **10**(21): p. 7199-206.
122. Chen, Y., et al., *Pre-existent adenovirus antibody inhibits systemic toxicity and antitumor activity of CN706 in the nude mouse LNCaP xenograft model: implications and proposals for human therapy*. Hum Gene Ther, 2000. **11**(11): p. 1553-67.
123. Ascierto, M.L., et al., *Permissivity of the NCI-60 cancer cell lines to oncolytic Vaccinia Virus GLV-1h68*. BMC Cancer, 2011. **11**: p. 451.
124. Reimann-Berg, N., et al., *Two new cases of polysomy 13 in canine prostate cancer*. Cytogenet Genome Res, 2011. **132**(1-2): p. 16-21.
125. Kuruppu, D. and K.K. Tanabe, *Viral oncolysis by herpes simplex virus and other viruses*. Cancer Biol Ther, 2005. **4**(5): p. 524-31.
126. Weibel, S., et al., *Viral-mediated oncolysis is the most critical factor in the late-phase of the tumor regression process upon vaccinia virus infection*. BMC Cancer, 2011. **11**: p. 68.
127. Thomas, M.A., et al., *Immunosuppression enhances oncolytic adenovirus replication and antitumor efficacy in the Syrian hamster model*. Mol Ther, 2008. **16**(10): p. 1665-73.
128. Worschech, A., et al., *The immunologic aspects of poxvirus oncolytic therapy*. Cancer Immunol Immunother, 2009. **58**(9): p. 1355-62.

129. Carmeliet, P. and R.K. Jain, *Principles and mechanisms of vessel normalization for cancer and other angiogenic diseases*. Nat Rev Drug Discov, 2011. **10**(6): p. 417-27.
130. Pavlidis, E.T. and T.E. Pavlidis, *Role of bevacizumab in colorectal cancer growth and its adverse effects: a review*. World J Gastroenterol, 2013. **19**(31): p. 5051-60.
131. Weibel, S., et al., *Treatment of malignant effusion by oncolytic virotherapy in an experimental subcutaneous xenograft model of lung cancer*. J Transl Med, 2013. **11**: p. 106.
132. Gerber, H.P., et al., *Complete inhibition of rhabdomyosarcoma xenograft growth and neovascularization requires blockade of both tumor and host vascular endothelial growth factor*. Cancer Res, 2000. **60**(22): p. 6253-8.
133. Yu, Y., et al., *A humanized anti-VEGF rabbit monoclonal antibody inhibits angiogenesis and blocks tumor growth in xenograft models*. PLoS One, 2010. **5**(2): p. e9072.
134. Sullivan, L.A. and R.A. Brekken, *The VEGF family in cancer and antibody-based strategies for their inhibition*. MAbs, 2010. **2**(2): p. 165-75.
135. Su, C., et al., *Gene-viral cancer therapy using dual-regulated oncolytic adenovirus with antiangiogenesis gene for increased efficacy*. Mol Cancer Res, 2008. **6**(4): p. 568-75.
136. Mahller, Y.Y., et al., *Oncolytic HSV and erlotinib inhibit tumor growth and angiogenesis in a novel malignant peripheral nerve sheath tumor xenograft model*. Mol Ther, 2007. **15**(2): p. 279-86.
137. Winkler, F., et al., *Kinetics of vascular normalization by VEGFR2 blockade governs brain tumor response to radiation: role of oxygenation, angiopoietin-1, and matrix metalloproteinases*. Cancer Cell, 2004. **6**(6): p. 553-63.
138. Jain, R.K., *Normalization of tumor vasculature: an emerging concept in antiangiogenic therapy*. Science, 2005. **307**(5706): p. 58-62.
139. Goel, S., et al., *Normalization of the vasculature for treatment of cancer and other diseases*. Physiol Rev, 2011. **91**(3): p. 1071-121.
140. Gil, M., et al., *Photodynamic therapy augments the efficacy of oncolytic vaccinia virus against primary and metastatic tumours in mice*. Br J Cancer, 2011. **105**(10): p. 1512-21.

141. Fridlender, Z.G., et al., *Polarization of tumor-associated neutrophil phenotype by TGF-beta: "N1" versus "N2" TAN*. *Cancer Cell*, 2009. **16**(3): p. 183-94.
142. Gentschev, I., et al., *Regression of human prostate tumors and metastases in nude mice following treatment with the recombinant oncolytic vaccinia virus GLV-1h68*. *J Biomed Biotechnol*, 2010. **2010**: p. 489759.
143. Bernt, K.M., et al., *Assessment of a combined, adenovirus-mediated oncolytic and immunostimulatory tumor therapy*. *Cancer Res*, 2005. **65**(10): p. 4343-52.
144. Choi, K.J., et al., *Concurrent delivery of GM-CSF and B7-1 using an oncolytic adenovirus elicits potent antitumor effect*. *Gene Ther*, 2006. **13**(13): p. 1010-20.
145. Lee, Y.S., et al., *Enhanced antitumor effect of oncolytic adenovirus expressing interleukin-12 and B7-1 in an immunocompetent murine model*. *Clin Cancer Res*, 2006. **12**(19): p. 5859-68.
146. Senzer, N.N., et al., *Phase II clinical trial of a granulocyte-macrophage colony-stimulating factor-encoding, second-generation oncolytic herpesvirus in patients with unresectable metastatic melanoma*. *J Clin Oncol*, 2009. **27**(34): p. 5763-71.
147. Bonehill, A., et al., *Single-step antigen loading and activation of dendritic cells by mRNA electroporation for the purpose of therapeutic vaccination in melanoma patients*. *Clin Cancer Res*, 2009. **15**(10): p. 3366-75.
148. Tjin, E.P., et al., *T-cell immune function in tumor, skin, and peripheral blood of advanced stage melanoma patients: implications for immunotherapy*. *Clin Cancer Res*, 2011. **17**(17): p. 5736-47.
149. Van Lint, S., et al., *Preclinical evaluation of TriMix and antigen mRNA-based antitumor therapy*. *Cancer Res*, 2012. **72**(7): p. 1661-71.
150. Li, H., et al., *Induction of strong antitumor immunity by an HSV-2-based oncolytic virus in a murine mammary tumor model*. *J Gene Med*, 2007. **9**(3): p. 161-9.
151. Sato, E., et al., *Intraepithelial CD8+ tumor-infiltrating lymphocytes and a high CD8+/regulatory T cell ratio are associated with favorable prognosis in ovarian cancer*. *Proc Natl Acad Sci U S A*, 2005. **102**(51): p. 18538-43.
152. Zamarin, D., et al., *Localized oncolytic virotherapy overcomes systemic tumor resistance to immune checkpoint blockade immunotherapy*. *Sci Transl Med*, 2014. **6**(226): p. 226ra32.

153. Saeki, K., et al., *Significance of tumor-infiltrating immune cells in spontaneous canine mammary gland tumor: 140 cases*. J Vet Med Sci, 2012. **74**(2): p. 227-30.
154. Carvalho, M.I., et al., *T-lymphocytic infiltrate in canine mammary tumours: clinic and prognostic implications*. In Vivo, 2011. **25**(6): p. 963-9.
155. Almand, B., et al., *Increased production of immature myeloid cells in cancer patients: a mechanism of immunosuppression in cancer*. J Immunol, 2001. **166**(1): p. 678-89.
156. Poschke, I., et al., *Immature immunosuppressive CD14+HLA-DR-/low cells in melanoma patients are Stat3hi and overexpress CD80, CD83, and DC-sign*. Cancer Res, 2010. **70**(11): p. 4335-45.
157. Gabitass, R.F., et al., *Elevated myeloid-derived suppressor cells in pancreatic, esophageal and gastric cancer are an independent prognostic factor and are associated with significant elevation of the Th2 cytokine interleukin-13*. Cancer Immunol Immunother, 2011. **60**(10): p. 1419-30.
158. Biller, B.J., et al., *Decreased ratio of CD8+ T cells to regulatory T cells associated with decreased survival in dogs with osteosarcoma*. J Vet Intern Med, 2010. **24**(5): p. 1118-23.
159. Liu, Z., et al., *Tumor regulatory T cells potently abrogate antitumor immunity*. J Immunol, 2009. **182**(10): p. 6160-7.
160. Dannull, J., et al., *Enhancement of vaccine-mediated antitumor immunity in cancer patients after depletion of regulatory T cells*. J Clin Invest, 2005. **115**(12): p. 3623-33.

APPENDIX

%	Percent
°C	Degree Celsius
α	Anti
μ	Micro
μg	Microgram
μL	Microliter
μm	Micrometer
BSA	bovine serum albumine
CCD	Charge-coupled device
CEV	Cell-associated enveloped virus
cm ²	Centimeter square
CMC	Carboxymethylcellulose
CO ₂	Carbon dioxide
CPE	cytopathic effect
dH ₂ O	Double-distilled H ₂ O
DMEM	Dulbecco's modified Eagle's medium
DMSO	Dimethyl sulfoxid
DNA	Deoxyribonucleic acid
dpi	days post injection
ds	Double-stranded
EDTA	diaminoethanetetraacetic acid
EEV	Extracellular enveloped virus
ELISA	Enzyme-linked immunosorbent assay
ER	Endoplasmatic reticulum
FACS	Fluorescence-activated cell sorting
FBS	Fetal bovine serum
Fig.	Figure

g	grams
GFP	green fluorescent protein
h	hours
H ₂ O ₂	Hydrogen peroxide
HCl	Hydrochloric acid
hpi	Hours post infection
HRP	Horseradish peroxidase
IEV	Intracellular enveloped virion
IMV	Intracellular mature virus
IV	Immature virion
i./v.	Intravenous
kDa	kilo Dalton
mA	milli Ampere
mg	Milligram
min	Minute
ml	Milliliter
mm	Millimeter
mM	Millimolar
mm ³	Cubic millimeter
mRNA	messenger RNA
MOI	Multiplicity of infection
MVA	Modified vaccinia virus Ankara
N	Normal
N ₂	Nitrogen
NaOH	Sodium hydroxide
n.d.	Not detectable
NEAA	Non-essential amino acids
neg	Negative
NK	Natural killer

PBS	Phosphate buffered saline
PFA	Paraformaldehyde
pfu	Plaque forming units
pg	Picogram
pH	Potential hydrogenii
PI	Propidium iodide
PMSF	Phenylmethylsulfonyl fluoride
pos	Positive
PVDF	Polyvinylidene difluoride
RNA	Ribonucleic acid
RPMI	Roswell Park Memorial Institute medium
RT	Room temperature
Ruc	<i>Renilla</i> luciferase
SDS-PAGE	Sodiumdodecylsulfate polyacrylamide gel electrophoresis

ACKNOWLEDGMENTS

This work was carried out at the Department of Biochemistry, University of Wuerzburg, Bavaria, Germany and Genelux Corporation at San Diego Science Center, San Diego, California, USA, between May 2011 and April 2014. This study was supported by a grant from Genelux Corporation and doctoral fellowship from the German Excellence Initiative to the Graduate School of Life Sciences, University of Wuerzburg. This work could not have been accomplished without the help of the people on the next few pages, to which I extend my sincerest thanks and gratitude.

I am indebted to Professor Aladar A Szalay, who gave me an opportunity to work under his guidance and to avail the excellent lab facilities required to complete my PhD studies successfully. I would like to thank him and Genelux Corp. for giving me the opportunity to live and work in the United States and to explore and experience a different culture and way of life to the full extend. His benevolent attitude and unending motivation have helped me immensely in not only completing the PhD but also developing in me a research attitude.

Sincerest appreciation to PD Dr. Ivaylo Gentshev for helping me in conducting animal experiments as well as his guidance and mentorship. I appreciate his continuous support for all administrative responsibilities at graduate school and thesis correction. Without his help this work would not be close to what it is now.

I wish to extend my gratitude to Professor Utz Fischer who agreed to be one of my supervisors and guided me throughout this project period. I will be failing in my duty if I do not acknowledge PD Dr. Jochen Stritzker for his guidance and mentorship as well as proof reading of my thesis.

Thanks to Professor Friedrich Grummt, for critical review of the thesis and his support of all AG Szalay's students.

Special mention to Dr. Tony Yu and Dr. Qian Zhang in San Diego for their guidance and having regular discussions that helped me in developing the immunological studies as well as understanding of the clinical trials. Appreciation is given to Dr. Nanhai Chen who helped me in designing the animal experiments and discussing the key aspects of preclinical studies. I would like to thank Dr. Joseph Cappello in

particular for his help with improving the thesis as well as for great discussions during my stay in San Diego.

Thanks also to Dr. Boris Minev and Dr. Mehmet Clinic for the help and guidance for developing immunological assays. I am very thankful to Alexa, Klass, Ulrike Geissinger and Dessi for the help with clinical trial sample processing. I would like to also thank Ulrike Donat for teaching me Microscopy, Marion for help with FACS analysis during preclinical study, Michael for help with β -glucuronidase assay, Johana for cryosections and Prisca for help with animal experiments. Thank you Terry Trevino and Jason Aguilar for all the technical assistance.

I am grateful to all members of the Wuerzburg group, especially Dr. Barbara Haertl, Dr. Steffi Wiebel, Dr. Elizabeth Hoffman, Dr. Susanne Rohn, Christina, Julian, Alex, Sascha, Tobias and Ivan. Lorenz thank you for being such a special friend to me during my time in Würzburg, your hospitality and friendship during this time meant very much.

I take this opportunity to express my gratitude to all members of Genelux Corporation including Dr. Rohit, Terry Chamberlin, Anu, Audrey, Eduardo, Huiang Wang, Ting, Britta, Mario, Johanas, Mayssam, Feng, Kim, Tom, Robin, Bill and Nadia. I would like to extend my special thanks to Erik, Prisca, Dessi and Bobby for being dear friends during my stay in San Diego. I am also thankful for Camha's assistance with all kinds of different problems and taking care of us foreign students.

To my friends Sanjay, Raji, Ankit, Mohit, Anindya, Kushal, Raj, Priti and Sheetal who have supported me through this journey, I am so very thankful.

The list of acknowledgments will be incomplete without thanking my parents and whole Patil family. To my late father, wherever you are, I know you are a part of me, supporting and encouraging me in every step of my life. Thank you, Mom and Sandesh for always being with me and for continuous encouragement. Lastly, very special thanks to my dear wife for sharing your life with me, a constant support and understanding as well as bearing a pain of staying away for such a long time.

CURRICULUM VITAE

Personal Information:

Name: SANDEEP SADASHIV PATIL
Date of Birth: 30 March 1985
Place of Birth: Nagaon Kavathe, Maharashtra, India
Nationality: Indian
Address: Versbacher straÙe, 40
Wuerzburg, 9070,
Germany

Education:

07/2002 – 07/2007 Bachelors of Veterinary Science
Bombay Veterinary College,
Parel, Mumbai, India

Higher Education

07/2007 – 07/2009 Masters in Virology
National Institute of Virology,
University of Pune, Pune, India

Doctoral Degree:

04/2011 – the present Doctoral studies supervised by Professor Aladar A.
Szalay, Julius-Maximilians-Universität, Würzburg,
Germany; Graduate school of life science, Germany; and
Genelux Corporation, San Diego, USA

LIST OF PUBLICATIONS

Manuscripts

Patil SS, Gentschev I, Nolte I, Ogilvie G, Szalay AA

Oncolytic virotherapy in veterinary medicine: current status and future prospects for canine patients.

J Transl Med. 2012 Jan 4; 10:3 Cited in PubMed; PMID: 22216938.

Patil SS, Gentschev I, Adelfinger M, Donat U, Hess M, Nolte, Frentzen A, Szalay AA

Virotherapy of canine tumors with oncolytic vaccinia virus GLV-1h109 expressing an anti-VEGF single-chain antibody

PLoS One. 2012; 7(10): e47472 Cited in PubMed; PMID: 23091626.

Gentschev I, **Patil SS**, Adelfinger M, Weibel S, Geissinger U, Frentzen A, Chen NG, Yu YA, Zhang Q, Ogilvie G, Szalay AA

Characterization and evaluation of a new oncolytic vaccinia virus strain LIVP6.1.1 for canine cancer therapy

Bioengineered. 2013 Mar-Apr; 4(2): 84-9 Cited in PubMed; PMID: 23093804.

Gentschev I, **Patil SS**, Petrov I, Cappello J, Adelfinger M, Szalay AA

Oncolytic virotherapy of canine and feline cancer

Viruses. 2014 May 16;6(5):2122-37 Cited in PubMed; PMID: 24841386

Poster presentations

Patil SS, Gentschev I, Adelfinger M, Frentzen A, Szalay AA (2012, June)

“Oncolytic virotherapy and modulation of tumor microenvironment with vaccinia virus strains”

Poster presentation at StratCan Summer School on Tumor Immunology organized by Karolinska institute, Stockholm, Sweden

Patil SS, Gentshev I, Adelfinger M, Frentzen A, Szalay AA (2012, October)
“Oncolytic virotherapy with vaccinia virus strains”

Poster presentation at 7th International Symposium organized by the students of the Graduate School of Life Sciences, University of Wuerzburg, Wuerzburg, Germany.

Patil SS, Gentshev I, Adelfinger M, Frentzen A, Chen N, Szalay AA (2014, January)

Virotherapy of canine tumor xenografts with oncolytic vaccinia virus GLV-1h109 encoding the anti-VEGF single-chain antibody

Poster presentation at AACR-Prostate Cancer Foundation Conference on Advances in Prostate Cancer Research held in San Diego, CA, USA.